Master's thesis

NTNU
Norwegian University of Science and Technology
Faculty of Natural Sciences
Department of Chemical Engineering

Quyen Lily Dinh

Investigating the Influence of Water Wash Design and Operating Conditions on MEA Emissions in Amine Scrubbing

Master's thesis in Sustainable Chemical and Biochemical Engineering
Supervisor: Hanna Knuutila
Co-supervisor: Andressa Nakao and Maxime François
June 2023

NTNU
Norwegian University of Science and Technology

Quyen Lily Dinh

Investigating the Influence of Water Wash Design and Operating Conditions on MEA Emissions in Amine Scrubbing

Master's thesis in Sustainable Chemical and Biochemical Engineering
Supervisor: Hanna Knuutila
Co-supervisor: Andressa Nakao and Maxime François
June 2023

Norwegian University of Science and Technology
Faculty of Natural Sciences
Department of Chemical Engineering

NTNU
Norwegian University of
Science and Technology

Declaration of Compliance

I, Quyen Lily Dinh, hereby declare that the work done in this thesis is independent and in accordance with the exam regulations of the Norwegian University of Science and Technology.

Place and Date: Trondheim, June 7th 2023

Signature:

Quyen Lily Dinh

Preface

This master thesis was written during the spring semester of 2023 at the Norwegian University of Science and Technology as the final part of the two-year master's program Sustainable Chemical and Biochemical Engineering. The thesis was written as a part of the course TKP4901 - Chemical Process Technology Master's Thesis at the Department of Chemical Engineering in the research group Environmental Engineering and Reactor Technology.

I would like to thank my supervisor, Prof. Hanna Knuutila, for her expertise and giving me the opportunity to work with carbon capture, as it has allowed me to contribute to an issue of such importance in today's society. I would also like to extend my sincere appreciation to my co-supervisors, Dr. Andressa Nakao and Maxime François, for their valuable inputs and insightful discussions. Lastly, I would like to acknowledge the support and encouragement from my family and friends, who have been a constant source of motivation throughout my academic journey.

Abstract

Carbon capture plays a crucial role in addressing the urgent challenge of climate change. As greenhouse gas emissions continue to rise, the need for effective strategies to reduce carbon dioxide (CO_2) levels in the atmosphere has become paramount. Among the various technologies available, absorption-based CO_2 capture processes such as amine scrubbing, stands out as a mature solution. However, a challenge related to this technology is the emissions of the solvent which can harm both the environment and human health. Therefore, it is essential to investigate technologies that reduce emissions in an amine scrubbing process, such as the water wash section, to minimize environmental impact. This thesis investigates the impact of water wash design and operating conditions on monoethanolamine (MEA) emissions in an amine scrubbing process with the objective of optimizing the water wash to minimize emissions. Through case studies and simulations using the CO2SIM tool, various parameters including water wash height, water temperature, lean amine temperature, flow rate, amine concentration, and the number of water wash stages were investigated. The aim of this thesis was to keep the volatile emissions under 1 ppm, as CO2SIM only provides information on vapor-phased emissions.

It was found that increasing the water wash height significantly reduced emissions, but cost considerations must be taken into account when determining the optimal height. Higher flow rates were found to reduce emissions, but also here the cost will increase with increasing flow rates. This emphasize the need to strike a balance between high and low flow rates for optimal emission reduction without compromising cost efficiency. Lean amine temperature and water temperature were identified as important factors influencing the emissions, with higher temperatures resulting in increased emissions. However, practical constraints such as climate and process efficiency should be considered when selecting temperature conditions. Low water temperature is feasible in colder countries such as Norway, but is less likely to work in countries with warmer climates, for instance in central Europe. Increasing amine concentration in the water entering the second water wash stage led to higher emissions. Although this was expected, it was interesting to confirm that the emissions are concentration dependent as well as temperature dependent. In the last case study performed, one water wash stage was removed to see the impact of using one versus two water wash stages. Removing one water wash stage resulted in a substantial increase in emissions, highlighting the effectiveness of employing two water wash stages.

In the final study, which was a study conducted with all the information gained throughout this thesis, optimizing the water wash height was found to have a more significant impact on emission reduction compared to lean amine temperature. It was decided to only change two parameters in the final study, keeping the rest of the parameters studied in this thesis the same as in the base case. This indicates that the base case demonstrated favorable emission levels, and that the initial water wash design and operating conditions were already working well. It is important to highlight that the adjustments made to the water wash section did not have any impact on the energy consumption. This suggests that the proposed optimizations can be implemented without compromising energy efficiency, thereby ensuring sustainable and cost-effective operations.

In conclusion, this thesis aimed to provide valuable insights into optimizing the water wash section of the amine scrubbing process to minimize amine emissions. The findings emphasize the significance of controlling parameters and provide practical guidance for achieving effective emission reduction in amine scrubbing systems. These insights contribute to the advancement of amine scrubbing processes and offer a basis for further research in this field.

Sammendrag

Karbonfangst spiller en avgjørende rolle i bekjempelsen av den presserende utfordringen med klimaendringer. Ettersom utslippene av drivhusgasser fortsetter å øke, har behovet for effektive strategier for å redusere karbondioksid (CO_2) nivåene i atmosfæren blitt helt avgjørende. Blant de ulike tilgjengelige teknologiene utmerker absorpsjonsbaserte CO_2-fangstprosesser seg som en etablert løsning, og da spesielt aminrensing. En utfordring relatert til denne teknologien er utslipp av aminer, da det kan skade både miljøet og menneskers helse. Derfor er det viktig å undersøke teknologier som reduserer utslipp i aminrensing, som for eksempel vannvask, da denne forskningen bidrar til å minimere miljøpåvirkningene. Denne avhandlingen undersøker effekten av vannvasksdesign og driftsforhold på aminutslipp i en aminrensingsprosess med mål om å optimalisere vannvasken for å minimere utslipp. Gjennom casestudier og simuleringer ved bruk av CO2SIM-verktøyet ble ulike parametere som vannvaskhøyde, vanntemperatur, regenerert amin-temperatur, strømningshastighet, aminkonsentrasjon og antall vannvaskseksjoner undersøkt. Målet var å holde de flyktige utslippene under 1 ppm, ettersom CO2SIM kun gir informasjon om utslipp i form av dampfase.

Det ble funnet at økning av vannvaskhøyde reduserte aminutslippene, men kostnadsaspekter må tas i betraktning ved valg av optimal høyde. Økt strømningshastighet bidro til reduserte utslipp, men på grunn av de økte kostnadene knyttet til høyere strømningshastighet, er det nødvendig å finne en balanse mellom høy og lav strømningshastighet for å oppnå optimal utslippsreduksjon. Regenerert amintemperatur og vanntemperatur ble identifisert som viktige faktorer som påvirket utslipp, der høyere temperaturer resulterte i økte utslipp. Imidlertid må praktiske begrensninger som klima og prosesseffektivitet vurderes ved valg av temperaturforhold. Lav vanntemperatur er gjennomførbart i kaldere land som Norge, men er mindre sannsynlig å fungere i land med varmere klima, som for eksempel i Sentral-Europa. Økning av aminkonsentrasjonen i vannet som kommer inn i det andre vannvasksstadiet førte til høyere utslipp. Selv om dette var forventet, var det interessant å få bekreftet at utslippene også er avhengig av konsentrasjonen og ikke bare av temperaturen. I den siste casestudien ble ett vannvaskssteg fjernet for å undersøke effekten av bruk av ett vannvaskssteg i forhold til to vannvaskssteg. Fjerning av ett vannvaskssteg resulterte i en betydelig økning i utslipp, noe som understreker effektiviteten av å bruke to vannvaskssteg.

I den siste studien, hvor all informasjon i denne avhandlingen ble samlet, ble det funnet at optimalisering av vannvaskhøyden hadde en større innvirkning på utslippsreduksjon sammenlignet med regenerert amintemperatur. I den siste studien ble det bestemt at kun to parametere skulle endres, mens resten av parametrene ble holdt konstante som i basecasen. Dette indikerer at basecasen viste gunstige utslippsnivåer og at den opprinnelige utformingen av vannvaksseksjonen og driftsforholdene allerede fungerte godt. Det er viktig å merke seg at justeringene som ble gjort i vannvaksseksjonen ikke hadde noen innvirkning på energiforbruket. Dette antyder at de foreslåtte optimaliseringene kan implementeres uten å gå på bekostning av energieffektiviteten, og dermed sikre bærekraftig og kostnadseffektiv drift.

Denne avhandlingen hadde som mål å gi verdifulle innsikter i optimaliseringen av vannvaksseksjonen i aminrensingsprosessen for å minimere aminutslipp. Funnene understreker betydningen av å kontrollere parametrene og gir praktisk veiledning for å oppnå effektiv reduksjon av utslipp i aminrensingssystemer. Disse innsiktene bidrar til utviklingen av aminrensingsprosesser og gir et grunnlag for videre forskning på dette området.

List of Figures

List of Tables

Abbreviations

GHG	Greenhouse gas
CO_2	Carbon dioxide
NOx	Nitrous oxides
SO_2	Sulfur dioxide
SOx	Sulfur oxides
CCS	Carbon capture and storage
CO	Carbon monoxide
PCC	Post-combustion carbon capture
MEA	Monoethanolamine
AD	Average deviation
AAD	Absolute Average Deviation
VLE	Vapor Liquid Equilibrium
ARD	Average Relative Deviation
AARD	Absolute Average Relative Deviation
AMP	2-amino-2-methyl-1-propanol
SRD	Specific Reboiler Duty

Table of Contents

1 Introduction

1.1 Motivation

Climate change and increasing global average temperature are major issues the world is currently facing, and immediate action is necessary to prevent severe consequences for humanity. Scientists are more certain than ever that increasing concentrations of greenhouse gases (GHG) in the atmosphere is the main cause of global warming and climate change [6]. The most significant contributor to these concentrations is carbon dioxide (CO_2), which has reached alarmingly high levels over the last century, resulting in irreversible changes to the global climate [7]. The high concentration of CO_2 in the atmosphere is strongly linked to human activities, with industrial activities being significant contributors to anthropogenic GHG emissions. [8]. In order to achieve a sustainable future, GHG emissions such as CO_2 need to be reduced. The Paris Agreement, a binding international agreement on climate change, has set the goal of limiting global warming to below 2 °C, and ideally, even less than 1.5 °C compared to pre-industrial times [9].

According to the Intergovernmental Panel on Climate Change, carbon capture and storage (CCS) is essential to achieve zero emissions and keep global average temperature below 2 °C by 2050 [10]. CCS allows for the continued use of fossil fuels while significantly reducing their CO_2 emissions. The process involves separating CO_2 from an energy conversion or industrial process, compressing it, transporting it, and storing it underground [11]. Carbon capture technologies are currently under extensive research, and several approaches have been developed. The most mature and well-established technology for carbon capture is considered to be post-combustion carbon capture (PCC) [12]. The most commonly used PCC method involves the removal of CO_2 through chemical absorption using an aqueous solvent. While this approach has undergone pilot plant and industrial testing, uncertainties remain about its scale-up to larger installations. Power plant flue gas volumes are high and contain low partial pressure of CO_2, which makes the CO_2 removal a highly energy-intensive and expensive process. Therefore, optimizing the process design is important to ensure low pressure drop and heat requirements while achieving the necessary separation target. Designing large-scale columns requires taking into account important factors such as column diameter, packing type and size, packed section height, pressure drop, physical properties of the chemical system, and hydrodynamic parameters to achieve the most effective design [13].

Implementation of PCC can also face environmental challenges due to potential solvent emissions. The choice of absorption solvent is highly important in PCC, and when using an amine solution, the process is referred to as amine scrubbing. Amines are ideal for separating CO_2 from many CO_2-containing flue gases due to their reversible reactions with CO_2. Not only can an amine scrubbing plant remove 85 to 90% of the CO_2, but the process can also remove a considerable amount of other polluting components such as ashes, nitrous oxides (NOx), and sulfur dioxide (SO_2), due to the required pre-treatment of the flue gas [14]. However, amines are known to be volatile, and small amounts of the solvent can vaporize into the gas phase and be carried out of the absorber column with the treated gas. Amine emissions from a PCC process can come from the absorbent itself or its degradation products, and can occur as gas-phase emissions, liquid droplets, or small aerosols [15]. Gas-phase emissions can typically be captured using a water wash system, while the liquid droplets can be removed from absorber columns using demisters. However, aerosol-based emissions have only recently been investigated for PCC, and little information is available in this area. Recent studies by Majeed and Svendsen have suggested that water wash sections in

a CO_2 capture column can effectively reduce gaseous and aerosol-born amine emissions, but the effectiveness of this approach for removing droplets or particles in the range of 0.1-3 μm is still unclear [15]. Thus, reducing emissions from PCC remains an important research topic, and this thesis focuses on investigating the potential of water wash sections to reduce emissions from the process.

1.2 Scope of Work

While many studies in the literature mention the addition of water wash sections to reduce emissions and manage water balance, information on optimal operating conditions for these sections and how to minimize emissions is limited. Therefore, it is considered valuable to understand the influence of different operating conditions and modifications on amine scrubbing processes and how they affect emissions. This thesis aims to provide insights into the design and operation of water wash sections to maintain volatile emissions below 1 ppm by investigating the key parameters affecting emissions. By identifying optimal operating conditions, this research can contribute to the sustainable implementation of water wash sections in an amine scrubbing process.

To perform various case studies, a base case was established by simulating a typical amine scrubbing process using flue gas from a coal plant. The process included an absorber column and a desorber column, with two identical water wash sections at the top of the absorber. The entire amine scrubbing process was simulated to provide an overview of the process. The focus will thereafter be on the absorber and the water wash section. The simulations were performed using CO2SIM, an in-house process simulator developed at SINTEF Materials and Chemistry.

To ensure the accuracy of the simulation tool, it was validated against experimental data. A validation of the equilibrium model was also performed to ensure reliable data for the water wash section. The validation of the equilibrium model verifies the model's accuracy in areas where the concentration of amine is low, which is the case for water wash sections.

The case studies involved varying several parameters and modifications on the system, including the height of the water wash sections, the temperature of the water entering the water wash sections, the temperature of the lean amine, the flow rate, and the amine concentration in the water. Another case was conducted with a single water wash section to compare it with the use of two water wash sections. The primary objective of this thesis is to determine the most effective operating conditions for the water wash sections in terms of emissions and present a final study based on the findings gathered in this research.

1.3 Outline of the Thesis

Chapter 1 introduces the motivation and scope of this thesis, while Chapter 2 describes the fundamental theory of post-combustion carbon capture and amine scrubbing. Chapter 2 also addresses the challenges associated with amine scrubbing, such as high energy consumption and amine emissions. Additionally, it covers some theory about flue gas. Chapter 3 presents a literature review that includes relevant studies and findings on 30 wt% MEA pilot campaigns that validate the absorber and desorber, as well as previous work related to water wash sections.

Chapter 4 outlines the methods utilized in this thesis. Firstly, a brief description about the simulation tool and the validation of the simulation tool was provided. Following is a section about the base case developed and the case studies conducted throughout this research. Chapter 5 discusses the validation process for the simulation tool, including its comparison against experimental campaigns and the equilibrium model in CO2SIM.

Chapter 6 presents the results and discussion of each case study in separate sections, as well as a final study conducted with all the information gathered throughout this thesis. Chapter 6 also contains a summary and comparison of the findings. Chapter 7 concludes the thesis with final conclusions and recommendations for future research.

2 Theory

2.1 Post-combustion Carbon Capture

Carbon capture and storage has become a crucial technique for meeting the goals of the Paris Agreement, as it covers a range of technologies designed to reduce CO_2 emissions from industrial processes [16]. The CCS process involves capturing CO_2 from fuel or flue gas, producing a pure stream of CO_2 that can be compressed for transportation, and storing it in geological formations onshore or offshore [17]. As of September 2022, there were 196 projects in the CCS facilities pipeline, representing a 44% increase in the number of facilities since the Global Status of CCS 2021 report. Of these facilities, 30 are currently operational, with a capture capacity of 42.58 millions of tonnes per annum (Mtpa) [18]. Carbon capture technologies are currently undergoing extensive research, with various methods being developed for capturing CO_2. The main methods developed are post-combustion, pre-combustion, and oxy-combustion capture [19], [20], [21]:

- Pre-combustion capture: Removes CO_2 from fossil fuels before the combustion is completed. Pre-combustion technologies captures CO_2 in a synthesis gas after conversion of carbon monoxide (CO) into CO_2.
- Post-combustion capture: Removes CO_2 and other gases from burning fossil fuels. Post-combustion technologies capture CO_2 in the exhaust gases once the fuel has been fully burned with air.
- Oxy-combustion capture: Burns fuel using pure oxygen instead of air, resulting in a flue gas with a high concentration of CO_2 that can be easily separated and sent directly to storage.

Out of the mentioned carbon capture methods, the most researched and widely preferred option is post-combustion carbon capture. PCC is capable of recovering CO_2 at a rate of up to 800 tonnes per day, and it can be conveniently retrofitted into both new and existing industrial facilities [22]. PCC is also effective for diluting CO_2 streams, such as flue gases from power plants where the pressure is low [23]. However, one significant drawback of PCC is its high regeneration energy demand, which can be a challenging and costly aspect of the process. Additionally, the PCC process can alter the composition of flue gas and generate new pollutants, which can lead to further environmental issues [24].

In Figure 1, a schematic diagram of a typical absorption-based PCC process is shown with two stages: an absorber and a desorber stage. The CO_2-containing flue gas is introduced at the bottom of the absorber, while the cold lean absorbent enters at the top. The flue gas typically consist of N_2, H_2O, O_2, CO_2 and small amounts of NOx and sulfur oxides (SOx) [25]. To separate CO_2 from the other components, the flue gas must be cooled down so that the absorber operates at a temperature of 40-60 °C [26] and 1 atmosphere pressure [27]. The flue gas and absorbent come into contact in a packed column, which is filled with porous packing material [28]. The packed column facilitates a countercurrent process between the fresh absorbent and upward flowing flue gas, providing a large surface area for contact between the two phases. As the fresh absorbent flows down the column, the absorbent continues to capture CO_2 at the bottom of the column where the concentration in the gas is very high, despite its already high CO_2 content. This happens due to a series of chemical reactions that release heat. The resulting CO_2-lean gas exits the top of the column and is released to the atmosphere.

If the absorbent used is volatile, a small amount of it can be released into the atmosphere during the carbon capture process. To minimize the emissions of solvent and other volatile compounds, a water wash section can be employed. A water wash section is typically a packed column located above the absorber and positioned before the lean amine inlet. In this section, the gas from the absorber enters the bottom of the column, while cold water is introduced at the top and flows countercurrent to the gas. The water is relatively cold and contains low concentrations of amines, which can condense the amine compounds. Due to the low amine concentration in the water, the amine equilibrium is shifted, causing the amine to dissolve in the liquid phase [29]. The process is particularly effective at reducing gas phase emissions [30]. Note that the schematic diagram presented in Figure 1 does not include a water wash section.

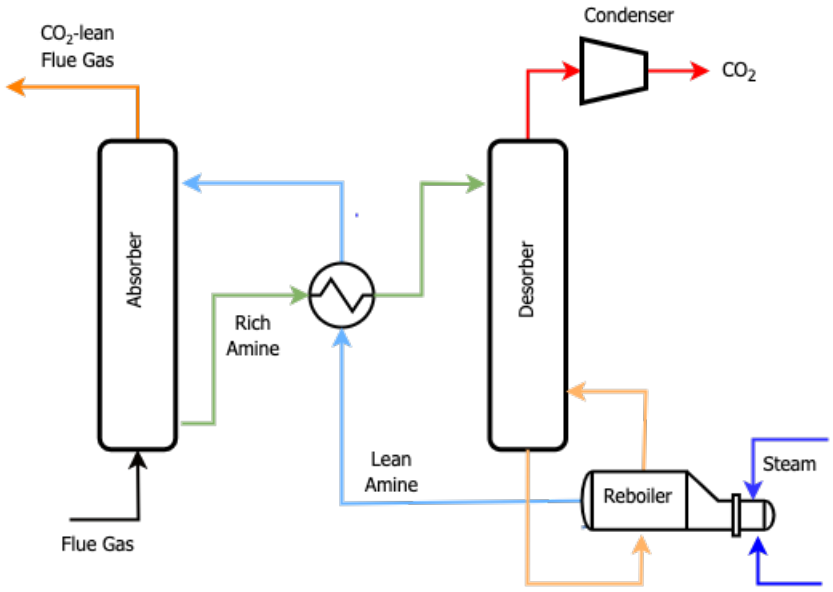

Figure 1: Schematic diagram of a typical post-combustion carbon capture process.

The rich absorbent is collected and pumped into a heat exchanger where it is heated by the lean solution. It is then introduced at the top of the desorber, which operates at a temperature of 100-140 °C [26] and 1 atmosphere pressure [27]. The desorber is heated by steam generated at the bottom of the reboiler. The steam is produced to transfer heat to the absorbent, to lower the CO_2 partial pressure in the gas phase which drives more CO_2 to be dissolved and dilute the CO_2 that is released. The stream carrying the CO_2 is led out of the column and sent to a condenser, while the water is recirculated back into the desorber. The gas stream which contains a high concentration of CO_2 is taken out at the top of the desorber. A reboiler is placed at the bottom of the desorber to regenerate the solvent. A fraction of the lean CO_2 is evaporated and re-enters the desorber, while the rest is sent back to the heat exchanger, where the solvent releases heat to the rich solvent before recirculating back to the absorber. [26], [31]

2.2 Amine Scrubbing

The choice of absorption solvent is highly important in an absorption-desorption process. Among the available options, amine solvent are the most widely used capture agents, leading to what is known as amine scrubbing [32]. This technology has been used effectively on a smaller scale for decades and is considered the most mature carbon capture technology available [33]. Amine scrubbing has high efficiency in absorbing CO_2 from flue gas produced by fossil-fuel power plants operating with high partial pressure of CO_2. Moreover, the amine-based aqueous solution can be regenerated and reintroduced into the process to capture additional CO_2 [34].

Amines are suitable in a PCC process because of its reversible reactions with CO_2, making them ideal for the separation from various CO_2-containing gases, including flue gas [35]. Desirable properties when selecting an amine solvent is high CO_2 loading capacity, fast absorption and desorption kinetics, low enthalpy of absorption, high solubility, high selectivity for CO_2 and low lifetime cost. It is also desired that the amine has favorable environmental properties such as low volatility, low viscosity and low degradation rate [36]. The performance of an amine scrubbing plant depends on three different factors: the energy performance, the environmental performance and the economic performance [37].

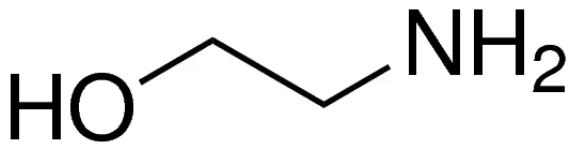

Figure 2: Molecule structure of monoethanolamine.

Figure 2 shows the molecule structure of monoethanolamine (MEA). MEA is a primary amine, meaning it has two hydrogen atoms directly attached to the nitrogen atom. MEA is widely recognized as the benchmark solvent for PCC technology due to the fast CO_2 absorption rate and established commercial application in the gas processing industry. MEA exhibits a high affinity for CO_2 at low temperatures, and low affinity at high temperatures, allowing for the use of smaller columns and reducing the need for longer residence time. Moreover, MEA has a high capacity due to its low molecular weight and is relatively inexpensive [4]. However, there are some limitations to its use, such as a maximum loading limit of 0.5 mole CO_2 per mole MEA and a high heat of reaction, which results in high energy requirements. In addition, MEA is degradable, corrosive, and sensitive to impurities. Therefore, MEA requires desulfurization and nitrification of the flue gas to function effectively [38]. These properties also require the use of more expensive construction materials due to corrosion concerns.

Although amine scrubbing is effective in reducing atmospheric CO_2 emissions, it can lead to changes in the flue gas composition and generate new pollutants, making it necessary to evaluate the sustainability of the absorbent used. MEA, for instance, can produce different compounds due to absorbent degradation and byproducts formed through reactions with flue gas impurities during the capture process. These compounds can exit the plant through air vents and potentially impact human health and the environment, especially if the compounds are toxic or carcinogenic [39]. Furthermore, MEA is a volatile amine, which means that it can vaporize into the gas phase and be carried out of the absorber column with the treated gas, resulting in amine emissions [40].

Table 1: Chemical reactions in the absorption of CO_2 by MEA. [4]

Reaction type	Reaction
Water dissociation	$2\,H_2O \longleftrightarrow H_3O^+ + OH^-$
CO_2 hydrolysis	$CO_2 + H_2O \longleftrightarrow H_3O^+ + HCO_3^-$
Bicarbamate dissociation	$HCO_3^- + H_2O \longleftrightarrow CO_3^{2-} + H_3O^+$
Carbamate hydrolysis	$MEACOO^- + H_2O \longleftrightarrow MEA + HCO_3^-$
Amine protonation	$MEA^+ + H_2O \longleftrightarrow MEA + H_3O^+$
Carbamate formation	$MEA + CO_2 + H_2O \longrightarrow MEACOO^- + H_3O^+$
Bicarbamate formation	$CO_2 + OH^- \longrightarrow HCO_3^-$

Table 1 shows the chemical reactions that occur during the absorption of CO_2 by MEA in an amine scrubbing system. The absorption process involves the diffusion of CO_2 from the gas phase into the solvent, where it reacts with the amine and undergoes a chemical change that allows more CO_2 to dissolve in the system. The amount of CO_2 that can be absorbed depends on the solubility of CO_2 in the liquid and the saturation point of the solution. While MEA may not directly participate in the water dissociation and hydrolysis reactions, it can influence their concentration through protonation equilibria. Protonation reactions occur rapidly, whereas the formation of carbamate and bicarbamate occurs slowly. Notably, the formation of carbamate is the primary mechanism by which CO_2 is absorbed.

The reaction between CO_2 and MEA is exothermic, and it is preferable to have low temperatures in the absorber and high temperatures in the desorber to reverse the reaction. Heat is released when CO_2 is absorbed which will increase the temperature in the absorber column. The temperature plays a crucial role as it has a direct influence on the reaction between CO_2 and MEA, as well as the volatility of the compounds. Higher temperatures increase the volatility of the reaction products, which can result in gas-phase emissions. Therefore, controlling the temperature is essential for effective CO_2 capture and to prevent unwanted emissions.

2.3 Energy Consumption in a Carbon Capture Process

In a carbon capture and storage process there are several expenses one has to take into consideration. The capture of CO_2 is the most costly aspect of the CCS process, accounting for 60-70% of the total expenses, followed by compression, which accounts for approximately 20%. The remaining costs are related to transport, injection, and monitoring. To reduce the cost of CCS, the focus should be on reducing the cost of CO_2 capture, which is energy-intensive and has the largest impact on the overall cost. Therefore, low-energy CO_2 capture methods are the most efficient way to lower the cost of CCS [41]. Given that CO_2 capture is highly energy-intensive, reducing the energy consumption is essential for achieving lower CCS cost.

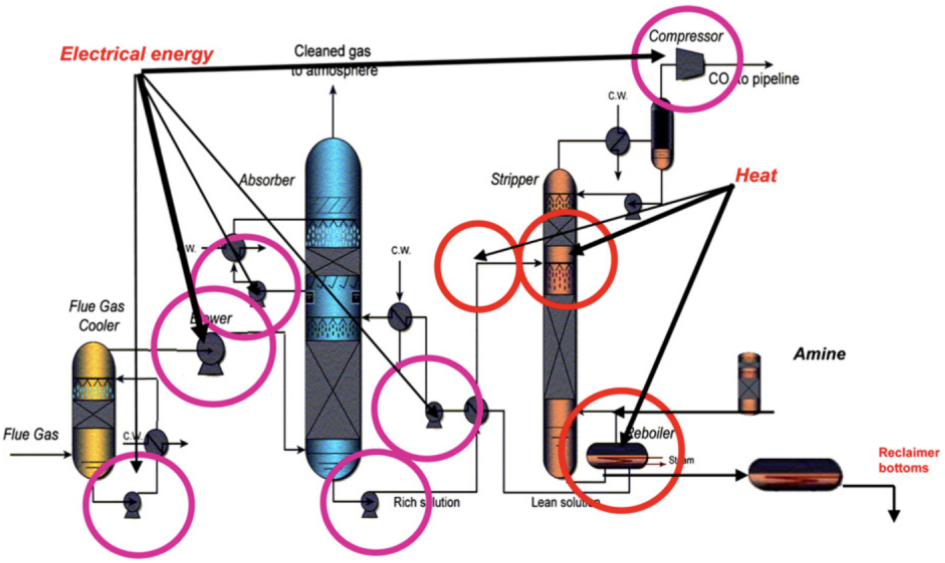

Figure 3: Energy sinks in a conventional post-combustion CO_2 capture process. [1]

Figure 3 shows the main energy sinks in a conventional post combustion absorption process. These include the heat required for the reboiler and desorber, the energy needed to power the liquid circulation pumps and drive the exhaust has through the absorber, and the compressor [1]. However, the most significant contributor to the overall energy demand is the regeneration of the solvent, which is highly energy intensive. The factors responsible for this high demand include the heat required to reverse the absorption reaction, the heat to overcome the sensible heat loss when the rich solvent and the leans solvent is heat exchanged, and the heat required to produce stream in the desorber to overcome the overhead pressure drop [42].

The desorber receives a CO_2-rich stream at the top section, which flows downwards and releases more CO_2 as it is stripped off by the presence of stripping steam. This heat is crucial to create vapors that remove the CO_2 from the liquid phase and into the gas phase. The driving force behind this desorption process is the difference between the partial pressure of CO_2 in the gas phase and the equilibrium partial pressure of CO_2. To achieve the necessary stripping temperature, heat is also required to raise the temperature of the rich stream. Although a heat exchanger can raise the temperature, it may not reach the reboiler temperature, creating a temperature gap known as the sensible heat [43].

2.4 Amine Emissions

From an amine scrubbing plant, environmental impacts can arise from direct emissions and chemical reactions with ambient air. The magnitude and nature of emissions are determined by the parent amine used in the process, as well as by the degradation products formed during the process, and the quantity of the release of emissions from the plant. In recent years, there has been a growing attention on amine emissions from carbon capture plants due to the potential of increase in operating costs associated with the injection of fresh solvent to compensate for the lost amine [44]. Moreover, amine losses can give rise to environmental concerns because the amines may react with nitrogen oxides in the atmosphere under certain conditions, leading to carcinogens such as nitrosamines and nitramines [45]. Amine loss is considered as one of the main concerns in the realization of the state-of-the-art PCC plants [15].

Amine emissions from CO_2 capture plants are a result of various mechanisms that release volatile solvents in gas form or solvent-carrying aerosols into the atmosphere. These emissions can originate from the absorption column or from upstream units that contaminate the solvent in the absorber [13]. Amine emissions are typically classified as gas-phase, droplet, or aerosol emissions, and are mainly caused by two mechanisms: amine volatility and aerosol emissions [46]. Amine volatility refers to how easily amines can turn into a gas. When amines are in a liquid state, it has the potential to evaporate and become a gas. This process of evaporation releases the amine into the atmosphere. The volatility of the amine depends on its structure, temperature, and CO_2 levels, with higher temperatures increasing the vapor pressure and volatility [47]. Gas-phase emissions follow Henry's law and are largely influenced by the temperature of the flue gas and the composition of the amine solvent [48]. To effectively reduce gas-phase emissions, a water wash section can be installed at the top of the absorber column.

Droplet emissions can occur when droplets of solvent are carried out of the system with the gas phase. These droplets are more likely to form and be carried out of the column by the gas phase at higher gas velocities in the absorber. Packed bed columns, which are commonly used in amine scrubbing, can contribute to this phenomenon when the liquid flows through the packing material in the opposite direction of the gas phase. To reduce these emissions, a demister unit is often employed. This unit is typically placed before a water wash section to prevent droplets with high amine concentration from entering and decreasing the efficiency of the water wash process [29].

Aerosol emissions can occur when certain gas phase components present in the absorber undergo a transformation. This transformation involves the condensation of these components, leading to the formation of wet aerosols. Once the components become part of the aerosols, they are carried out of the plant by the aerosols themselves. These emissions have received significant attention in recent years due to their difficulty in removal and their significant impact on the environment [49]. The mechanisms of aerosol formation and growth are related to the degree of supersaturation. Nucleation occurs when supersaturation exceeds a critical value, resulting in nuclei through the condensation of molecules of the condensing components (homogeneous nucleation) or on impurities in the flue gas (heterogeneous nucleation). Heterogeneous nucleation occurs at low supersaturation ($S \sim$ 1-1.03), while homogeneous nucleation occurs at higher supersaturation ($S >$ 2-5) [46]. MEA is known to promote fog formation and aerosol emissions. Once formed, aerosols can pass through the water wash system without being effectively controlled by conventional demisters, which may have limited efficiency in removing small aerosols. However, studies have shown that water wash systems can reduce both gaseous and aerosol emissions. In the water wash sections, aerosol droplets

grow extensively due to water condensation, making them easier to remove in a demister. [49, 15]

2.5 Flue Gas Emissions

Burning of fossil fuels is a significant contributor to global warming and climate change, leading to the release of CO_2 and other harmful pollutants. Despite this, fossil fuels will continue to be the primary source of energy for the foreseeable future. To address this issue, it is important to implement flue gas treatments that can minimize the amount of pollutants released during combustion. Flue gas is produced when fossil fuels like natural gas, coal, wood or oil are burned to generate power or heat. If left untreated, flue gas can significantly impact air quality at the local and regional levels, leading to strict clean-air regulations and treatment requirements for power plants and industrial facilities [50]. Typically, flue gases contain 3-15 vol% of CO_2. In this thesis, the flue gas from a coal-fired power plant is utilized in the study. To gain an understanding of coal flue gas in regards to emissions and CO_2 content, flue gas from coal fired flue gas and flue gas from a natural gas turbine will be compared. The typical compositions of these two types of flue gases are shown in Table 2 [5].

Table 2: Typical composition of [5]

Flue Gas	CO_2 [%]	O_2 [%]	N_2 [%]	Impurities
Natural Gas	4	14	82	Low SOx and NOx levels, 10-15% O_2
Coal Flue Gas	13	5	82	High SOx and NOx levels, 3-6% O_2

From Table 2, it can be observed that flue gas from a natural gas turbine is lower in CO_2 content, but higher in O_2 content compared to flue gas from a coal-fired power plant. The emissions that stem from the combustion of natural gas are much lower than those from coal. When combusted in a new, efficient natural gas power plant, natural gas will emit 50-60% less CO_2 compared to emissions from a typical new coal plant [51]. Coal-fired power plants do not only emit CO_2, but also other harmful toxins, including mercury, which can have an immediate and significant impact on human health. Implementing an amine scrubbing process for CO_2 capture in the exhaust gas of a power plant may encounter a potential issue due to the presence of small particles that can serve as sites for condensation. This can lead to the aerosol phase carrying a substantial amount of amine out of the CO_2 scrubber. The presence of fine particles in the flue gas, referred to as a "penetration window," is responsible for increased amine losses and environmental concerns [52]. These particles typically range in size around 100 nm and are capable of serving as nuclei for volatile amine species to condense on, resulting in significant amine emissions from CO_2 scrubbers [53]. In the presence of soot particles, which are mainly composed of carbon and are produced during incomplete coal combustion, amine emissions were found to be 2-4 times higher compared to flue gas without soot particles [53].

The combustion of natural gas can emit several pollutants, including CO_2, NOx, SO_2 and particulate matter. Nevertheless, natural gas is considered to be a cleaner-burning fuel compared to other fossil fuels like coal. Natural gas combustion typically emits about half the CO_2 emissions of coal combustion for the same amount of energy produced, while also producing negligible amounts of sulfur, mercury, and particulate matter. However, the process of extracting, transporting, and storing natural gas can result in methane emissions, which is a potent greenhouse gas. [51]

3 Literature Review

In recent years, extensive research has been done on CCS in response to global climate change and rising temperatures. With the construction of full-scale CO_2 capture plants on the horizon, attention has turned to the potential emissions and energy performance of these plants. This thesis focuses on simulating the amine scrubbing process using 30 wt% MEA as the amine solvent, which has been the most commonly used solvent due to its many desirable properties. This chapter investigates previous research on CO_2 capture using 30 wt% MEA, amine emissions associated with PCC, and the removal of emissions with a water wash section.

3.1 Pilot campaigns using 30 wt% MEA

For the amine scrubbing process in this thesis, a simulation model consisting of an absorber, a desorber, and two water wash sections, with 30 wt% MEA as the amine solvent was developed. To ensure the accuracy of the simulation tool, validation of the absorber and desorber against experimental campaigns was necessary, allowing for comparison of experimental data with simulated data. Several research papers on CO_2 capture using 30 wt% MEA have been published, and this section presents the papers that were used for validation purposes.

Tobiesen et al. (2007) [54] published *"Experimental validation of a rigorous absorber model for CO_2 post-combustion capture"* with the objective to develop a rigorous rate-based model and validate it against mass-transfer data. This work was a three-month campaign carried out in a laboratory pilot plant located at NTNU, with a total of 20 runs published for the campaign. The absorber column had a diameter of 0.15 m and was packed with 4.36 m of Sulzer Mellapak 250 packing. The experimental data obtained from the campaign was used to test the model, with gas and liquid side mass-transfer rated compared to the simulated rates. The results showed an absolute average deviation (AAD) of 6.26% and a total average deviation (AD) of 6.16%, which were considered satisfactory. In addition, the temperature profiles from the experiment were compared to the simulated profiles, and a satisfactory agreement was found.

Tobiesen et al. (2008) [55] published *"Experimental validation of a rigorous desorber model for CO_2 post-combustion capture"* with the objective to develop a rigorous rate-based model and validate it against mass-transfer data. The experimental campaign was conducted using a pilot plant located at NTNU, with a desorber packing of 3.89 m Sulzer Mellapak 250 and a diameter of 0.10 m, along with a reboiler and a condenser. A total of 19 runs were published for the campaign. The experimental and simulated CO_2 mass-transfer rates were found to be in good agreement, with AAD and AD values of 9.92% and 9.91%, respectively. Additionally, the comparison of simulated and measured reboiler temperatures showed good agreement.

Notz et al. (2012) [3] published *"Post-combustion CO_2 capture by reactive absorption: Pilot plant description and results of systematic studies with MEA"* which described a pilot plant developed as a part of the EU CASTOR project located at the University of Kaiserslautern. The paper provides detailed information about the pilot plant, including the absorber column, which is packed with Sulzer Mellapak and has a height of 4.2 m and diameter of 0.125 m, and the desorber column, which also has Sulzer Mellapak packing and measures 2.52 m in height and 0.125 m in diameter. The authors performed 47 experiments and evaluated the data to establish a baseline for comparing new solvents tested in pilot plants, making the results useful for validating models of the PCC

process with MEA.

Aronu et al. (2011) [2] published *"Solubility of CO_2 in 15, 30, 45 and 60 mass% MEA from 40 to 120 °C and model representation using the extended UNIQUAC framework"* with the objective to present a consistent VLE data set for MEA through experimental VLE measurements for 15, 30, 45 and 60 mass% MEA in the low and high CO_2 loading regions from 40 to 120 °C. The publication outlines a model that provides a good representation of the experimental VLE data for CO_2 partial pressures and total pressures for all MEA concentrations, with an absolute average relative deviation (AARD) of 24.3% and 11.7%, respectively.

3.2 Water Wash Section

The water wash section is a significant element in this thesis, as optimizing it is crucial for minimizing amine emissions. All case studies performed in this thesis feature two water wash sections located on top of the absorber. This section presents relevant existing data and findings concerning the water wash section.

Majeed and Svendsen (2017 and 2018) reported that water wash systems can effectively reduce aerosol emissions while increasing droplet size by a factor of 2-8 between the absorber section outlet and wash section outlet, making the demister unit more efficient in removing droplets. However, the effectiveness of the water wash is reduced as the CO_2 content in the flue gas increases. The study also showed that increasing the temperature of the lean amine can increase both the droplet size and emissions, while increasing the temperature in the final water wash section has a similar effect, but to a lesser degree. On the other hand, other parameters studied in this publication, such as increasing the water wash height, had little to no significant effect other than increasing residence time. [15], [56]

Both Stec et al. (2015) [57] and Notz et al. (2012) [3] reported that adding a small amount of fresh water to the water wash recycle stream can prevent excessive amine accumulation in the water wash section and compensate for water losses.

Kang. et al (2017) provided a study on modelling aerosol growth in an absorber and water wash. It was reported that the water wash section used the same L/G ratio as the absober, which was 5.3 mole/mole. The researchers observed rapid growth of aerosols at the beginning of the water wash section, before it entered into a stable growth stage. [58]

Fulk and Rochelle (2013) reported that by increasing the residence time in the water wash column to promote aerosol growth, the removal efficiency can be enhanced while reducing the partial pressure. The study used an L/G ratio of 5 mole/mole for the water wash section. [59]

Madeddu et al. (2019) reported that the solvent used in the water wash section was the same water recovered in the desorber condenser. The water wash sections were designed with the same diameter as the absorber. The packing height was the only design parameter to be determined, and it was determined through a sensitivity analysis that involved adjusting the packing height until the desired performance was achieved. [60]

4 Method

4.1 CO2SIM

The simulation tool used in this thesis was CO2SIM, an in-house process simulation program developed at SINTEF Materials and Chemistry. CO2SIM is a flexible simulation tool for solving a wide range of processes related to CO_2 capture. The simulator offers optimization procedures and methods for data acquisition from various sources, for example from pilot plants [61]. CO2SIM was used to simulate and define a base case of an amine scrubbing process consisting of an absorber, a desorber, and two identical water wash sections. The simulation tool was then employed to run several case studies, which are described in detail in the following sections. To ensure accuracy of the simulation tool, a validation of CO2SIM was carried out, and the results are presented in Chapter 5.

4.2 Validation of CO2SIM

Validation is necessary to assess the accuracy of simulation tools such as CO2SIM. In this regard, the vapor liquid equilibrium (VLE) of CO_2 in 30 wt% MEA was used to generate equilibrium curves for flash tank simulations, which were then compared against experimental data by Aronu et al. (2011) [2]. Additionally, the performance of CO2SIM was validated against experimental campaigns to evaluate if the simulation model gave an accurate prediction. In order to do so, the percentage deviation in absorption and desorption rates between simulation and experimental data was calculated. The temperature profiles in the columns were investigated, as well as the lean and rich loading and the composition in each streams. These parameters from the experimental campaign were compared with the simulated values. In this thesis, the simulation tool CO2SIM has been validated against the experimental campaigns by Tobiesen et al. (2007) [54], Tobiesen et al. (2008) [55], and Notz et al. (2012) [3] for both the absorber and desorber, each with 30 wt% MEA as the solvent. A detailed description of the validation procedure and performance is provided in Chapter 5.

4.3 Defining a Base Case

The base case of this study consisted of an absorber with two water wash stages at the top and a desorber. The simulations were carried out using version 7.1.0.5 of CO2SIM. The thermo package used for the simulations was the inbuilt template "Ordinary Electrolyte Non-Random Theory" model with the mixture "MEA_AMP_CC2_OeNRTL". The base case uses flue gas from a coal fire power plant. In order to achieve realistic results, the Tiller plant in Trondheim was used as a reference when building the base case. The data of the Tiller plant is in-house data and can be found in Table 38 in Appendix H.

The composition of the coal flue gas used was obtained by Svendsen et al. [62]. The coal flue gas contained 13 vol% CO_2 on a dry basis, and the wet vol% of CO_2 was calculated assuming that flue gas was saturated with water. The data for the lean solvent entering the absorber was not given by Svendsen et al. [62] and was therefore calculated based on 30 wt% MEA and a lean loading of 0.17 mole CO_2/mole MEA. To achieve 95% capture rate, the liquid-to-gas ratio (L/G) was adjusted

during the simulation of the base case, resulting in lean solvent flow rate and reboiler duty that differ slightly from the calculated values. Table 3 summarizes the inlet conditions and composition of the coal flue gas, as well as the calculated values of the lean solvent flow rate.

Table 3: The inlet conditions and composition of the coal flue gas and the lean solvent entering the absorber column.

	Coal Flue Gas	Lean Solvent
CO_2 [mole fraction]	0.1227	0.0196
H_2O [mole fraction]	0.0560	0.8615
MEA [mole fraction]	-	0.1153
N_2 [mole fraction]	0.8213	-
Loading [mole CO_2/mole MEA]	-	0.17
Flow Rate [kmol/h]	6.25	18.00
T [°C]	35.0	39.4
P [kPa]	100	100

The absorber had a packing height of 15 m and a diameter of 0.2 m. The desired capture rate of CO_2 was decided to be 95%. The process was simulated step by step, starting with the absorber and afterwards adding other elements one by one. This was to ensure that the simulation was working properly and to easily identify potential convergence issues. The inlets in the absorber was set to be a gas stream and a lean liquid stream. Once the absorber was simulated, the water wash sections were added to the system. Both water wash sections had an identical height of 2.4 m and diameter of 0.2 m. As there is limited information available regarding the typical L/G ratio used in the water wash sections, the same L/G ratio as in the absorber column was used. Following the water wash section, the desorber was simulated with a height of 12 m and a diameter of 0.12 m. In order to get the simulation to converge, a small trace amount of 2-amino-2-methyl-1-propanol (AMP) was added to the lean solvent. However, the amount of AMP was so small that it was not expected to affect the results. The packing type used for all of columns in the base case was Mellapak 250Y, which is the default packing in CO2SIM.

Figure 4 shows the flow sheet of the base case built in CO2SIM. The flue gas enters the absorber column from the bottom, while the lean solvent is introduced at the top of the column. The treated flue gas from the absorber, labeled "GasAbsTreat", is directed to the first water wash stage, labeled "WW1". To facilitate convergence of the column, the liquid stream introduced into the water wash contained water with small amounts of MEA and CO_2 along with trace amount of AMP. After exiting the water wash section, the liquid underwent a pressure change as it was pressurized to 400 kPa. The stream was then directed to a flash unit where temperature and pressure were set to equal the inlet conditions.

The second water wash, labeled "WW2", was modeled after the first water wash, and the process was carried out as previously described for WW1. The CO_2-enriched stream exits the bottom of the absorber and is directed through a pump with the pressure set at 400 kPa, before entering a heat exchanger. The heat exchanger is used to warm up the rich stream and cool down the lean one. The warm rich liquid flow enters the top of the desorber, while the vapor from the heat exchanger is mixed with the clean top stream of the desorber and sent to a condenser to

extract CO_2. The CO_2-depleted flow exits the bottom of the desorber. A portion of the stream is vaporized in the reboiler and recirculated back to the desorber, while the remaining portion is cooled in the heat exchanger before being redirected to the absorber. To maintain consistent flow rates, control blocks were installed before the liquid inlets for the absorber and water wash. The operating conditions for all the streams in the simulation is listed in Table 39 in Appendix I.

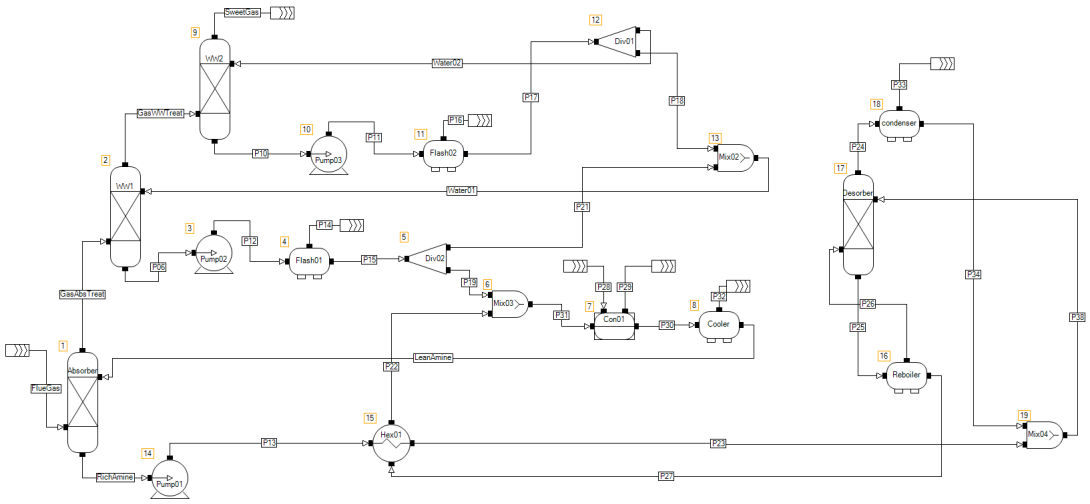

Figure 4: Flow sheet of the base case in CO2SIM.

4.4 Case Studies

The main focus of this thesis was to investigate the water wash sections and their impact on emissions. To gain a better understanding of the parameters affecting the emissions and energy consumption, modifications were made to the base case, and various system variables were adjusted. An important aspect of these case studies was to identify the parameters and operating conditions that keep volatile emissions below a certain level, which was set at 1 ppm for this study. The following sections provide a description of the conditions and modifications implemented in the study.

Each simulation was performed using CO2SIM, and the optimal conditions for each simulation were determined using Matlab. The optimization code was originally developed by senior researcher Finn Andrew Tobiesen from SINTEF and subsequently modified by postdoctoral researcher Andressa Nakao.

4.4.1 Case Study - Water Wash Height

Table 4: Case study - Water Wash Height.

Case 1	Total height of WW1 and WW2 decreased to 2 m
Case 2	Total height of WW1 and WW2 decreased to 4 m
Case 3	Total height of WW1 and WW2 increased to 6 m
Case 4	Total height of WW1 and WW2 increased to 8 m

The first modification implemented involved changing the water wash height. Four cases with varying water wash heights were simulated, and labeled as Cases 1, 2, 3, and 4 in Table 4. The base case had an initial water wash height of 2.4 m each, giving a total height of 4.8 m. For Case 1, the water wash sections were reduced to a height of 1 m each, giving a total height of 2 m. In Case 2, the water wash height was reduced to 2 m each, giving a total height of 4 m. For the remaining two cases, the height was increased. In Case 3, the height was increased to 3 m each, giving a total height of 6 m. Finally, in Case 4, the height was increased to 4 m each, giving a total height of 8 m. The diameter of the water wash sections was kept constant at 0.2 m for all cases. In the base case, the reboiler duty was 36.5 kJ/s, and the lean gas and flow rates were 6.2 kmol/h and 18 kmol/h, respectively. For cases 1-4, the reboiler duty and lean flow rate were adjusted to achieve a 95% CO_2 capture, with a reboiler duty of 45 kJ/s and a lean flow rate of 24.5 kmol/h. The gas flow was kept constant for all cases and the same as in the base case.

4.4.2 Case Study - Water Temperature in Water Wash Section

Table 5: Case Study - Water Temperature in Water Wash Section.

Case 5	Temperature of water in WW1 and WW2 decreased to 20 °C
Case 6	Temperature of water in WW1 and WW2 decreased to 25 °C
Case 7	Temperature of water in WW1 and WW2 increased to 35 °C
Case 8	Temperature of water in WW1 and WW2 increased to 40 °C
Case 9	Temperature of water in WW1 increased to 40 °C and constant at 30 °C in WW2
Case 10	Temperature of water in WW1 increased to 45 °C and constant at 30 °C in WW2

The geometry of the equipment for this case study was identical to the base case. The reboiler duty was set to 45 kJ/s and the lean flow was 24.5 kmol/h to achieve a 95% capture rate, while the gas flow rate was set to 6.2 kmol/h. A total of six case studies was performed, where the only parameter changed was the temperature of the water entering the water wash sections, labeled as "Water01" and "Water02" in Figure 4.

The temperature of the streams "Water01" and "Water02" was kept at 30 °C in the base case. To assess whether this temperature affects the emissions and energy consumption of the water wash sections, the temperature of these streams was varied in this case study. An overview of the cases performed for this study is given in Table 5. In Case 5 and 6, the temperature was reduced to 20 and 25 °C, respectively. In Case 7 and 8, the temperature was increased to 35 and 40 °C, respectively.

Two additional cases were performed in which the temperature of the water entering the first water wash stage (WW1) was increased while the temperature of the second water wash stage (WW2) remained constant. In Case 9, the temperature of WW1 was set to 40 °C while WW2 was maintained at 30 °C. In Case 10, WW2 was still held at 30 °C, while the temperature of WW1 was further increased to 45 °C.

4.4.3 Case Study - Lean Amine Temperature

Table 6: Case Study - Lean Amine Temperature

Case 11	Temperature of lean amine decreased to 20 °C
Case 12	Temperature of lean amine decreased to 25 °C
Case 13	Temperature of lean amine decreased to 30 °C
Case 14	Temperature of lean amine decreased to 35 °C

These case studies were performed with the same geometry and gas flow rate as the base case, with a water wash height of 4.8 m in total and a water wash diameter of 0.2 m. To achieve a 95% capture rate, the reboiler duty and the lean flow rate were adjusted to 45 kJ/s and 24 kmol/h, respectively.

In the base case, the lean amine liquid was set to a temperature of 40 °C. To investigate the effect of this temperature on emissions, the lean amine temperature was varied between 20 to 40 °C in this case study. The simulations performed for this case study are labeled as Case 11, 12, 13 and 14 in Table 6. Case 11 used a lean amine temperature of 20 °C, while Case 12 used 25 °C. For Case 13, the lean amine temperature was set at 30 °C, and Case 14 used a temperature of 35 °C.

4.4.4 Case Study - Flow Rate

Table 7: Case Study - Flow Rate

Case 15	Flow rate increased from 20 kmol/h to 40 kmol/h
Case 16	Flow rate decreased from 20 kmol/h to 10 kmol/h

The equipment geometry used in this case study was identical to the base case, and the reboiler duty and lean flow rate were adjusted to achieve a 95% capture rate. Specifically, the reboiler duty was set to 45 kJ/s and the lean flow rate was set to 24.5 kmol/h.

There is a lack of literature discussing the optimal flow rate for water wash sections, which is typically determined by finding the lowest possible rate that can still wet the packing. If the flow rate is too low, the column may not operate effectively. Increasing the flow rate is expected to reduce emissions, but finding a balance between low emissions and low flow rate is desirable. In this study, two cases were performed as shown in Table 7. The flow rate of the base case was set to be 20 kmol/h. In Case 15, the flow rate was doubled to 40 kmol/h. In Case 16, the flow rate was halved to 10 kmol/h.

4.4.5 Case Study - Amine Concentration in Water in Water Wash Section

Table 8: Case Study - Amine Concentration in Water in Water Wash Section

Case 17	0.5 wt% MEA in the water entering WW2
Case 18	1 wt% MEA in the water entering WW2

Two case studies were performed to investigate the effect of MEA concentration in the water entering the second water wash stage. These case studies are identified as Case 17 and Case 18 in Table 8. The geometry of the equipment and the operating conditions are the same as in the previous case studies, except that the water entering the second water wash section now contains a higher amount of MEA. In the base case, a small amount of MEA was added to the water stream entering the water wash stage to ensure system convergence. By increasing the MEA concentration in the water stream, one can determine if there are any concentration-dependent trends in the emissions. Case 17 involved a concentration of 0.5 wt% MEA in the water entering the upper water wash section, while Case 18 involved a concentration of 1 wt% MEA in the same water stream.

4.4.6 Case Study - Remove one Water Wash Stage

Table 9: Case Study - Remove one Water Wash Stage.

Case 19	Case with only one water wash section
Case 20	Water wash with height of 2 m
Case 21	Water wash with height of 4 m
Case 22	Water wash with height of 6 m
Case 23	Water wash with height of 8 m
Case 24	Amine concentration of 1 wt% entering the water wash
Case 25	Amine concentration of 0.5 wt% entering the water wash

For this case study, a new case was built in CO2SIM with an absorber and desorber geometry identical to the base case. In the base case, the packing height for the single water wash stage was 4.8 m, which was the total height of both water wash sections in the original base case that had two sections. The water wash section diameter was set at 0.2 m. Operating conditions for this case study were the same as those of the original base case, with identical reboiler duty, gas flow rate, and lean flow rate. Case 20-25 required adjustments in the reboiler duty and lean flow rate to achieve a 95% CO_2 capture rate. The same flue gas composition was used in both cases, which were in-house data of the Tiller plant located in Trondheim. The flow sheet for this case study in CO2SIM is illustrated in Figure 5. This study was performed to investigate the impact of using one versus two water wash sections.

Seven case studies were performed for the case with only one water wash section, as listed in Table 9. The first case, labeled as Case 19, used the same operational parameters as the base case for the scenario with two water wash sections, with a water wash stage height of 4.8 m. In Case

20, 21, 22 and 23, the water wash height was varied, set at 2 m, 4 m, 6 m, and 8 m, respectively. The last two cases examines the influence of amine concentration in the water stream entering the water wash stage. In Case 24, the amine concentration was set to 1 wt%, while Case 25 had a concentration of 0.5 wt%, both represented by the stream labeled as "Water" in Figure 5.

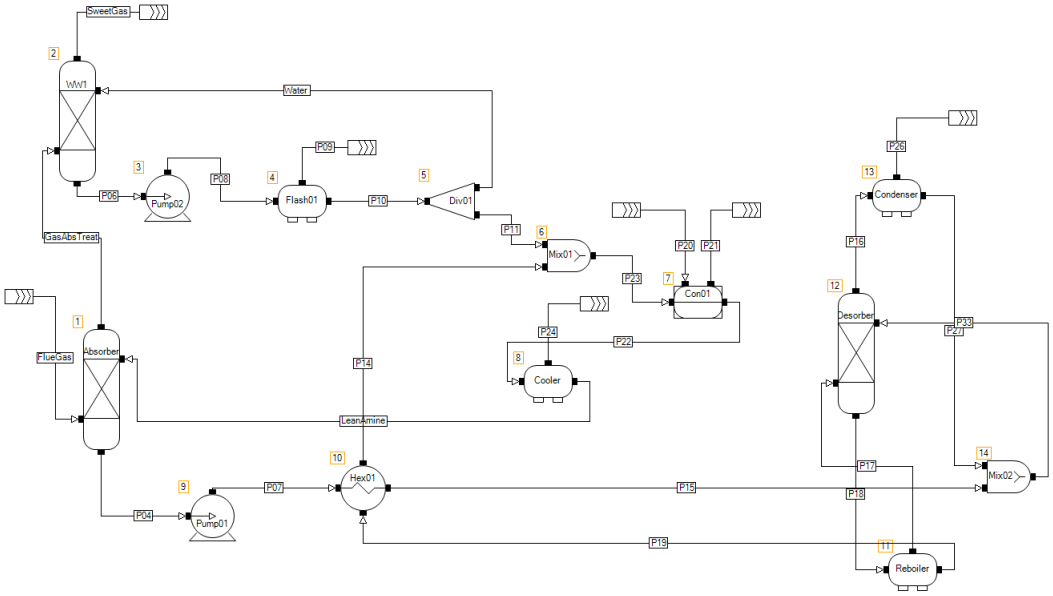

Figure 5: Flow sheet of the case with only one water wash section in CO2SIM.

5 Validation

This chapter presents a detailed description of the validation procedures carried out for the simulation tool, CO2SIM, along with the corresponding results.

5.1 Validation of Vapor-Liquid Equilibrium

Accurately predicting VLE is crucial for determining process operating characteristics and ensuring accurate simulations. Therefore, it is important to test the accuracy of CO2SIM in this regard. To validate the model, a flash unit was used to simulate an equilibrium stage. The input was a mixture of CO_2, 30 wt% MEA and water, which resulted in vapor and liquid streams as outputs. The curves obtained from the simulation results were compared against experimental data by Aronu et al. (2011) [2]. The average relative deviation (ARD) and AARD for the simulation results were calculated from the following equations:

$$ARD = \frac{|x_{sim} - x_{exp}|}{x_{exp}} \tag{1}$$

$$AARD = \frac{\sum_{i=1}^{n} ARD}{n} \cdot 100 \tag{2}$$

In the work of Aronu et al. (2011) [2], CO_2 partial pressures over loaded MEA solutions were measured using a low-temperature equilibrium apparatus, while total pressures were measured with a high-temperature equilibrium apparatus. Therefore, the experimental data is presented as CO_2 partial pressures as function of loading in solution for temperatures ranging from 40 to 80 °C, while for temperatures ranging from 60 to 120 °C, total pressures are given. In order for the flash unit to run in CO2SIM, total pressure is required. The experimental loading and the partial pressure of CO_2 in the gas phase given in the publication can be used to calculate an indicating total pressure by using Raoult's law. This was done for temperatures ranging from 40 to 80 °C as these experiments did not provide a total pressure. Raoult's law is given in Equation 3.

$$P = P_2^{SAT} + x_i(P_1^{SAT} - P_2^{SAT}) \tag{3}$$

To estimate the total pressure, Raoult's law can be used as a starting point, although it provides only an approximation. The calculated total pressure was then used as a starting point for simulating the flash unit. If the simulated CO_2 loading was significantly lower than the experimental CO_2 loading, the total pressure was increased. However, setting the total pressure too high would cause the vapor fraction in the gas outlet to approach zero, preventing the simulated partial pressure of CO_2 from being calculated. The key was therefore to determine the total pressure that would yield a vapor fraction in the gas outlet while providing the most similar values between the simulated and the experimental CO_2 loadings. The calculated total pressure for temperatures of 40, 60, and 80 °C, obtained using Raoult's law, as well as the total pressues used in the simulations, are presented in Table 31, Table 32, and Table 33 in Appendix A, respectively. To determine the corresponding gas and liquid loading from the flash unit, a TP flash was utilized, with the temperature set to match the equilibrium point temperature specified in the paper. The inlet stream was set to have

the same loading and temperature as given in the paper.

Figure 6 illustrates the partial pressure of CO_2 plotted as a function of CO_2 loading for temperatures 40, 60 and 80 °C, as well as experimental data from Aronu et al. (2011) [2]. The figure demonstrates that the model is reasonably well-matched to the experimental data from Aronu et al. Specifically, for α-values below 0.4, the simulated model accurately predicts the CO_2 partial pressure in comparison to the experimental data. However, for α-values exceeding 0.4, the simulated model tends to underestimate the CO_2 partial pressure, especially at temperatures of 40 and 60 °C.

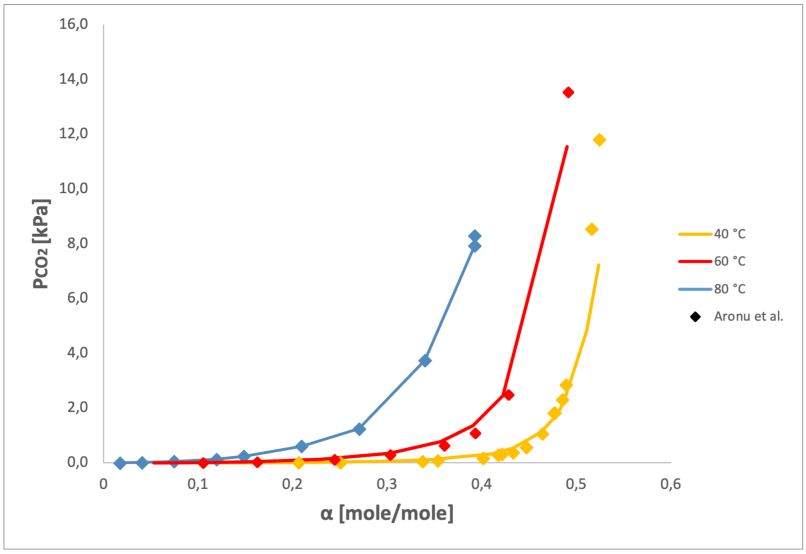

Figure 6: Simulated partial pressure of CO_2 vs. loading with 30 wt% at 40, 60 and 80 °C from Aronu et al. (2011) [2].

The total pressures for the high temperature experiments were provided in the study by Aronu et al. (2011) [2]. However, in the case of experiments with total pressures of 170.2 and 256.6 kPa at 100 °C, the simulated flash unit produced a gas outlet with a vapor fraction of 0. Therefore, the pressure for these experiments was adjusted to 164 and 252 kPa, respectively. Figure 6 shows the CO_2 partial pressure plotted against CO_2 loading for temperatures of 100 and 120 °C, compared with experimental data. For higher temperatures, it can be observed from Figure 7 that the simulated model is under-predicted compared to the experimental data. It should be noted that the deviations increase with increasing loading, particularly for the runs with temperature of 120°C. This observation may indicate that the predicted results for the desorber are overestimated, which suggests that the actual duty required for the desorber could be lower than initially anticipated.

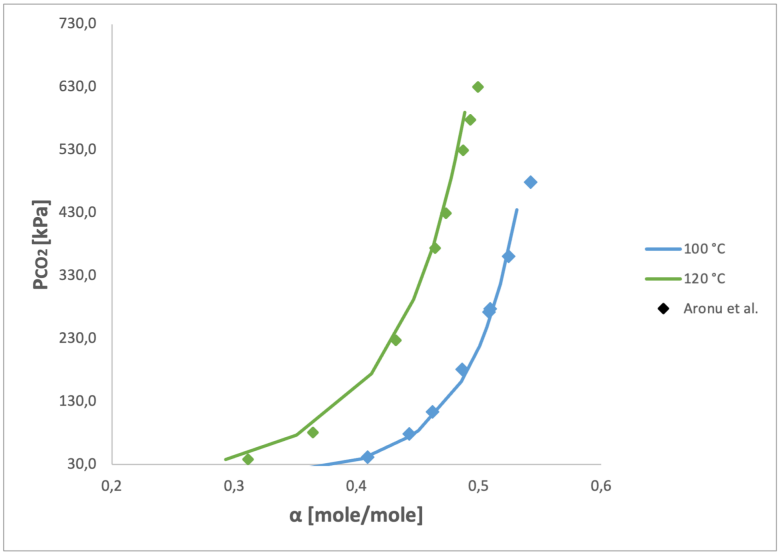

Figure 7: Simulated partial pressure of CO_2 vs. loading with 30 wt% at 100 and 120 °C from Aronu et al. (2011) [2].

The AARDs for the CO_2 partial pressures and total pressures were calculated to be 17.9% and 38.5%, respectively. A comparison with the findings of Aronu et al. (2011) showed that the AARD for CO_2 partial pressures in this validation is notably better at 17.9% compared to Aronu et al's (2011) value of 24.3%. However, when considering the AARDs for total pressures, the contrast becomes more significant. This difference can be due to the unavailability of total pressure data for higher temperatures in the referenced paper, which made it necessary to use Raoult's law for estimation.

5.2 Validation of the Absorber

To validate the absorber model, two experimental campaigns were compared with CO2SIM simulation models. The experimental data used for comparison were obtained from Tobiesen et al. (2007) [54] and Notz et al. (2021) [3]. An overview of the absorber specifications and the flow parameters in the experimental campaigns is presented in Table 10. The following experimental data were used as a basis for the absorber model validation:

- Incoming liquid and gas streams to the absorber: molar flow rate (F), component molar fraction (x_i), temperature (T), and pressure (P).
- The outlet liquid and gas streams from the absorber: molar flow rate (F), component molar fraction (x_i), temperature (T), and pressure (P).
- Temperatures through the absorber packing to generate a temperature profile.

Table 10: Overview of the experimental campaigns used for simulation validation in the absorber simulations.

Experimental Campaign	Tobiesen et al. (2007)	Notz et al. (2012)
Absorber Specifications		
Column Internal Diameter [m]	0.150	0.125
Main Packing Height [m]	4.36	4.2
Packing Type (Experimental)	Sulzer Mellapak 250Y	Sulzer Mellapak 250Y
Packing Type (CO2SIM)	Sulzer Mellapakk 250Y	Sulzer Mellapak 250Y
Flow Parameters		
Fluegas Flow Rate [kg/h]	137.0-165.4	55.5-100.0
Lean Solution Flow [kg/h]	187.9-579.1	75.0-350.3
L/G [mol/mol]	1.3-4.5	1.3-5.4
Lean Solution Loading [mol CO_2/mol MEA]	0.183-0.409	0.111-0.356
Temperature Flue Gas [°C]	36-69	23-49
Temperature Lean Solution [°C]	40-66	30-50
Absorber Pressure [kPa]	99-104	100

The inputs for the absorber simulations were set as the lean amine liquid stream and the flue gas. The outputs were the CO_2-free gas from the top of the absorber and the rich amine liquid stream from the bottom.

To evaluate the model's performance, several parameters from the experimental campaigns were compared with the simulated values for the absorber. Specifically, the outlet flows, temperature profiles and CO_2 absorption rate were investigated. Since liquid measurements are generally considered more accurate than gas measurements in the absorber column, the reported liquid measurements were used for comparison of the CO_2 absorption rate. The percentage deviation between the simulated and experimental absorption rate was calculated using Equation 4, where v_{sim} and v_{exp} represent the CO_2 absorption rate given in kg/h from the simulations and experimental data respectively. Given that the absorption rate is typically a quite small number, even slight deviations between the simulated and experimental data can result in larger percentage deviations.

$$x_i = \frac{v_{sim} - v_{exp}}{v_{exp}} \cdot 100 \tag{4}$$

Further, the percentage deviation was used to find the average deviation (AD) from Equation 5.

$$AD = \frac{1}{n} \sum_{i=1}^{n} |x_i| \tag{5}$$

The percentage deviation was also used to find the absolute average deviation (AAD) from Equation 6.

$$AAD = \frac{1}{n}\sum_{i=1}^{n}|x_i - \bar{x}| = \frac{\sum_{i=1}^{n} x_i}{n} \tag{6}$$

5.2.1 Absorber Simulations - Tobiesen et al. (2007)

The experimental campaign by Tobiesen et al. (2007) [54] involved 20 runs over a period of three months. The absorber specifications and flow parameters used in the experiments are provided in Table 10. Since the reported vol% of CO_2 in the flue gas was based on a dry basis, the wet vol% of CO_2 was calculated with the assumption that the flue gas was fully saturated with water. The amount of H_2O entering the absorber was calculated using Raoult's law, while the remaining gas entering the absorber was assumed to be inert.

Simulation results for the rich loading, absorption rate, and percentage deviation for each of the 20 runs can be found in Table 34 in Appendix C, as well the calculated ratio between simulated and experimental absorption rate. Only comparing the simulated and the experimental outlet loading does not give a precise indication of the model's accuracy due to the sensitivity to errors being low, and the data presented this way may conceal significant inconsistencies [63]. Therefore, the ratio between simulated and experimental absorption rate have been calculated, as this is a more accurate approach. If the calculated ratio is 1, the simulated absorption rate is equal to the experimental. This ratio was used to investigate potential systematic errors by plotting it against variables such as lean solvent loading, volume percentage of CO_2 absorption rate, and inlet stream temperatures.

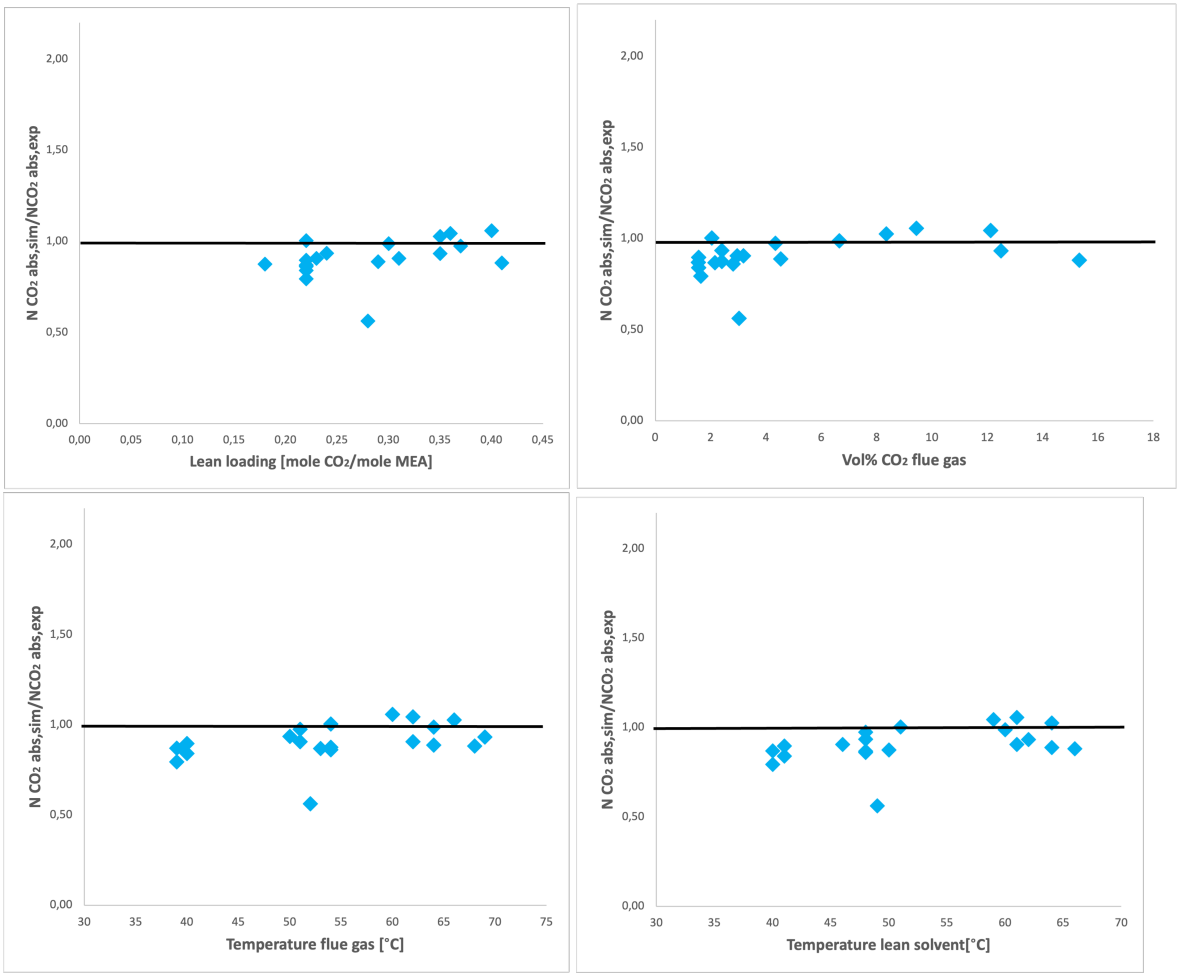

Figure 8: Plots of ratio between simulated and experimental absorption rate plotted against lean loading, volume percentage of CO_2 in the flue gas, temperature in flue gas, and temperature in lean solvent. (Tobiesen et al. (2007))

In Figure 8, the ratio between the simulated and experimental absorption rate is plotted against various parameters for the 20 runs, including lean loading, volume percentage of CO_2 absorption rate, flue gas temperature, and lean solvent temperature. The results show that the simulated model generally agrees well with the experimental model. The results are both over- and under-predicted, but mostly under-predicted. Notably, run 7 had a significantly lower ratio of 0.56, but no clear explanation was found after examining other parameters such as inlet temperatures and flue gas CO_2 volume. It is possible that the observed deviation for run 7 is partly due to experimental deviations. The ratio between the desorption rates was found to be within 0.80 and 1.06, indicating good comparability between the simulated and the experimental data. The AD and AAD for the outlet temperatures, rich loading, and CO_2 absorbed yielded satisfactory results, as shown in Table 11.

Table 11: AD and AAD values for outlet temperatures, rich loading and CO_2 absorbed for absorber. (Tobiesen et al. (2007))

	AD [%]	AAD [%]
Outlet Temperature (Gas)	1.001	0.006
Outlet Temperature (Liquid)	0.479	0.003
Rich Loading	2.424	0.062
CO_2 Absorbed	10.738	0.606

Tobiesen et al. (2007) [54] provided five temperatures throughout the absorber packing for run 7, 10, 12, and 15. These data were plotted against the temperature profile from the simulations provided by CO2SIM, as shown in Figure 9. Overall, the experimental and simulated temperature profiles agreed well, with deviations of less than 2 °C for most runs. For instance, the temperature profile for run 10, shown in Figure 9, exhibits a good agreement. However, larger deviations between the experimental and simulated measurements were observed for runs 7 and 12, particularly at the bulge, where the deviations were approximately 4 °C and 3 °C, respectively. Such deviations were also reported in Tobiesen et al. (2007) [54], indicating that the deviations may stem from errors in the experimental measurements. The small deviations observed in run 15 were consistent with the results reported in Tobiesen et al. (2007) [54].

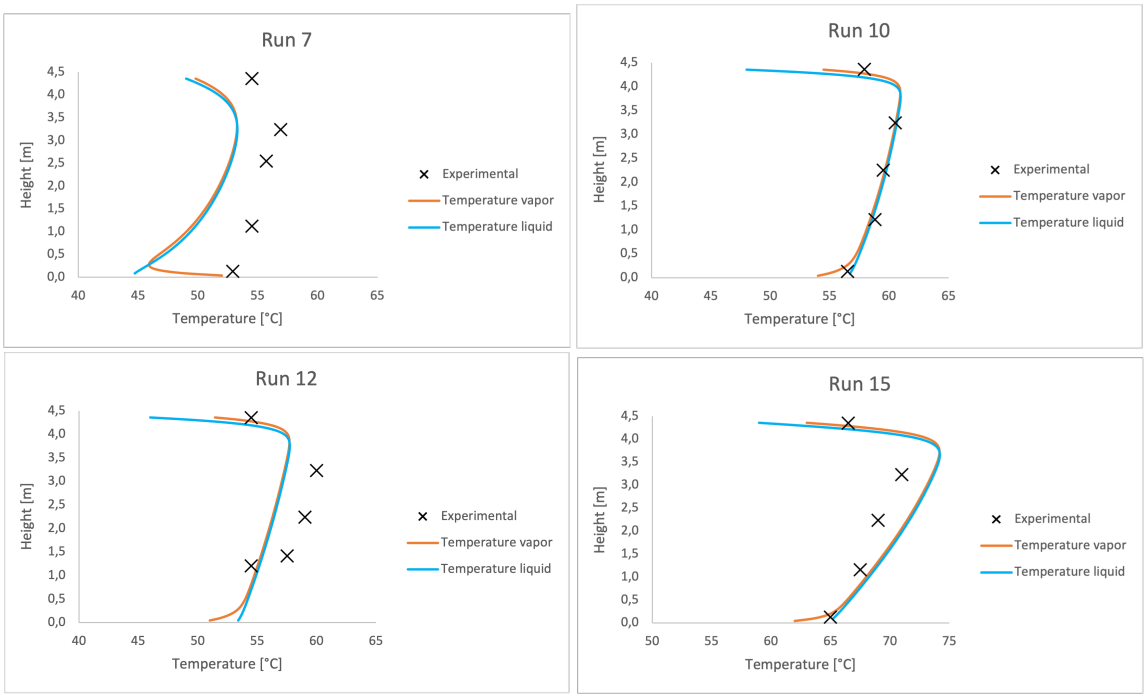

Figure 9: Temperature profile for run 7, 10, 12, and 15. (Tobiesen et al. (2007))

5.2.2 Absorber Simulations - Notz et al. (2012)

Notz et al. (2012) [3] performed 47 experiments, each with their own flow sheet detailing the plant's flow parameters and composition. To validate the model, the absorber and desorber were simulated separately. The flow specifications and parameters for the absorber are presented in Table 10.

The absorber consists of six packing sections, one of which is dedicated to water wash. For the validation of the absorber simulation, the water wash section was excluded. The experimental campaign performed by Notz et al. (2012) [3] provided mass fractions of CO_2, H_2O, N_2, and O_2 in the flue gas composition, but since the version of CO2SIM used in this thesis does not account for O_2, it was added together with N_2 and treated as inert gas. The plant flow sheets included separate compositions and flow parameters for each of the 47 experiments conducted. The simulation was performed by setting the flue gas and lean solvent stream as the two inlets. The parameters for the flue gas can be found in label 8, while the parameters for the lean solvent can be found in label 11 in Figure 31 in Appendix B.

The simulation results for the rich loading, the absorption rate, and the percentage deviation for the 47 runs can be found in Table 35 in Appendix D. The results for the validation of the absorber are presented the same way as previously. The ratio between simulated and experimental absorption rates was plotted against the lean loading, the volume percentage of CO_2 absorption rate, the temperature in flue gas, and the temperature in lean solvent for all 47 runs. These plots are shown in Figure 10. As can be seen from Figure 10, the simulated model closely predicts the experimental model. The results varied between under- and over-predicted. For all runs except run 18, the deviation was less than 20% for the absorption rate. However, there was no apparent reason for the deviation in run 18 when examining other parameters, such as rich loading, temperature of lean solvent, and temperature of flue gas.

Notz et al. (2012) aimed to provide a detailed description and critical evaluation of the plant's operation, as well as to conduct parameter studies. Therefore, the publication does not include simulation results for the CO_2 absorption rate or the temperature profiles, which could be used for comparison with the simulations performed for the validation. The desorption rates ratio for each run, with the exception of run 18, were within 0.93 and 1.03, demonstrating good correlation between the simulated and the experimental data. AD and AAD values for the outlet temperature of the gas and liquid streams, the rich loading, and the CO_2 absorbed are presented in Table 12 and indicate satisfactory results.

Table 12: AD and AAD values for outlet temperatures, rich loading and CO_2 absorbed for absorber. (Notz et al. (2012))

	AD [%]	AAD [%]
Outlet Temperature (Gas)	1.333	0.018
Outlet Temperature (Liquid)	3.707	0.010
Rich Loading	2.223	0.034
CO_2 Absorbed	3.579	0.003

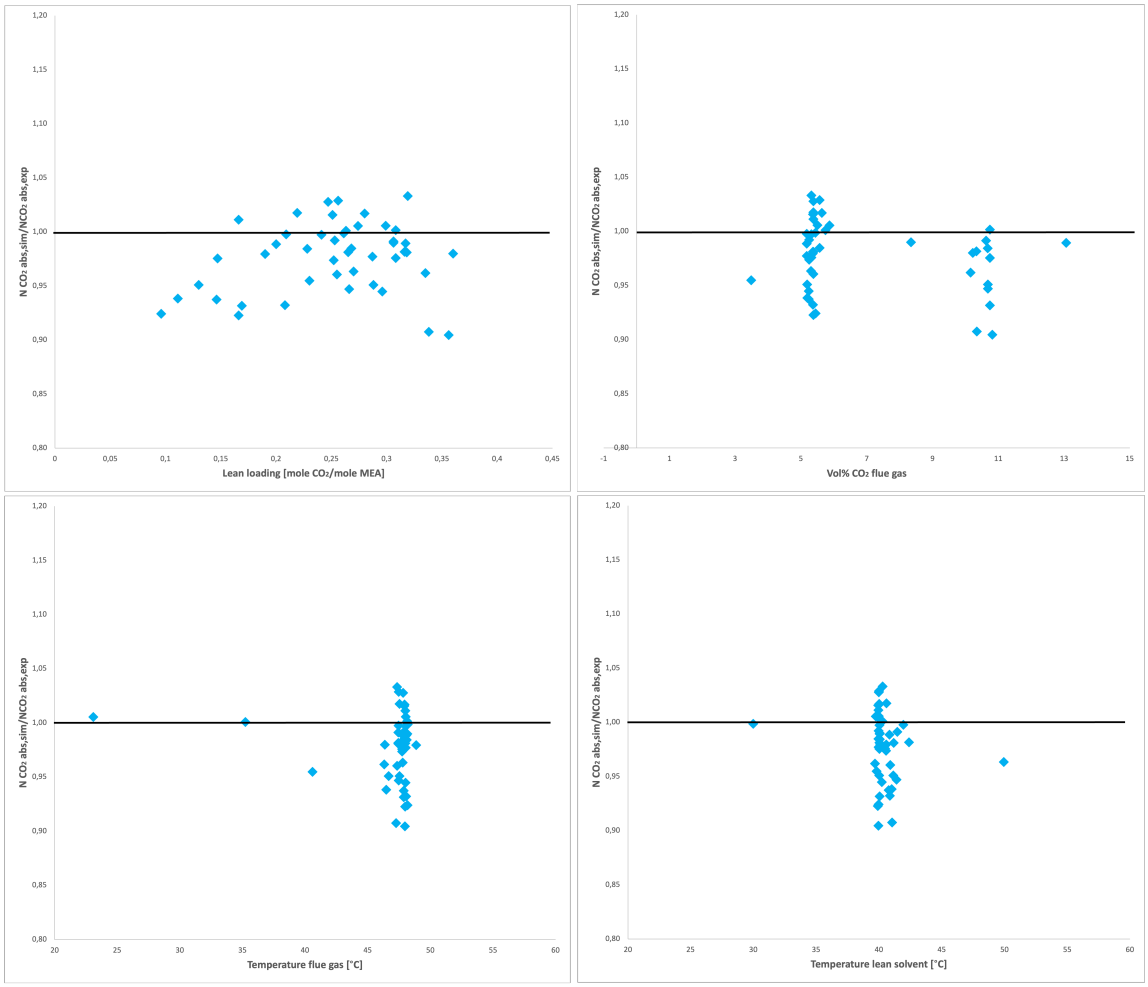

Figure 10: Plots of ratio between simulated and experimental absorption rate plotted against lean loading, volume percentage of CO_2 in the flue gas, temperature in flue gas, and temperature in lean solvent. (Notz et al. (2012))

Notz et al. (2012) [3] provided several temperature measurements through the absorber column. These measurements were plotted against the temperature profile for the liquid phase obtained from the simulations performed in CO2SIM. The liquid phase was chosen because it was assumed, based on the flow sheets, that the measurements were taken from the liquid phase. Figure 11 shows the temperature profiles for runs 4 and 29. These plots illustrates how well the simulated model predicts the experimental model for the temperature measurements. This was the case for the majority of the experiments in this campaign. However, there were a few runs that showed deviations between the simulated and experimental models, specifically run 19, 20, 39, and 45.

The temperature profile for runs 39 and 45 is presented in Figure 12, where run 45 shows an over-prediction of approximately 9 °C, and run 20 shows a significant under-prediction of 14 °C. Runs 19 and 39 also exhibits under-prediction of 5 and 6.5 °C, respectively. By investigating the other parameters for these runs, no apparent cause for the temperature deviation was identified. It is worth noting that all simulations showed a lower temperature at the top of the column compared to the experimental measurements. However, the description provided by Notz et al. (2012) regarding the exact measurement points at the top of the column was inadequate, and the observed variation may be due to dissimilarities in the measurement points utilized in the

simulation and experimental data. The temperature profiles from the remaining experiments with provided temperature measurements can be found in Appendix E.

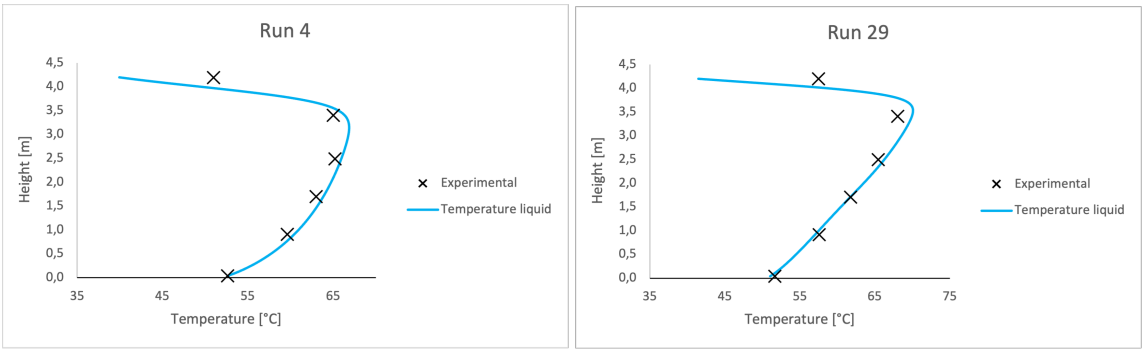

Figure 11: Temperature profile for run 4 and 29. (Notz et al. (2012))

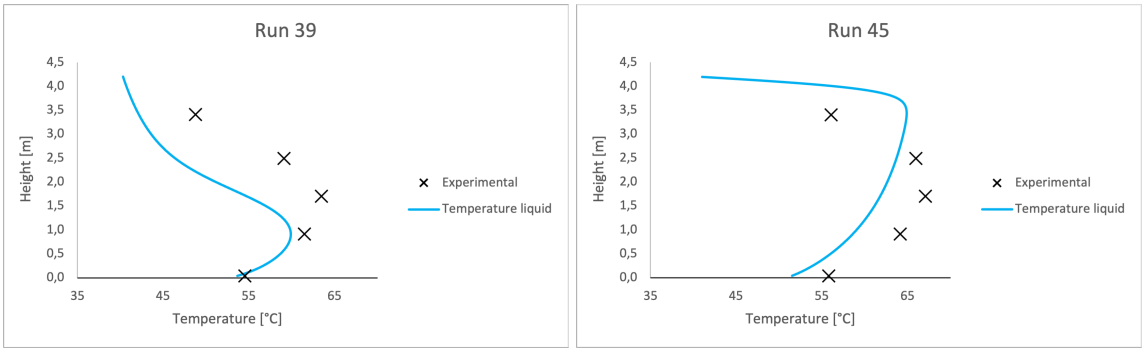

Figure 12: Temperature profile for run 39 and 45. (Notz et al. (2012))

5.3 Validation of the Desorber

For the desorber, the validation was carried out against the experimental campaigns by Tobiesen et al. (2008) [55] and Notz et al. (2012) [3]. Table 13 gives an overview of the desorber specifications and flow parameters in the experimental campaigns used in the validation of the desorber. The following experimental data was used as a basis for the desorber model validation:

- Incoming liquid and gas streams to the desorber: molar flow rate (F), component molar composition (x_i), temperature (T), and pressure (P).
- The outlet liquid and gas streams from the desorber: molar flow rate (F), component molar fraction (x_i), temperature (T), and pressure (P).
- Reboiler heat duty (Q) and pressure (P)
- Condenser temperature (T) and pressure (P)
- Temperatures through the desorber packing to generate a temperature profile where it is possible.

Table 13: Overview of the experimental campaigns used for simulation validation in the desorber simulations.

Experimental campaign	Tobiesen et al.	Notz et al.
Desorber Specifications		
Column Internal Diameter [m]	0.100	0.125
Main Packing Height [m]	3.89	2.52
Packing Type (Experimental)	Mellapak 250Y	Mellapak 250Y
Packing Type (CO2SIM)	Mellapakk 250Y	Mellapak 250Y
Flow Parameters		
Rich Solution Flow Rate [kg/h]	183.5-569.7	79.8-359.0
Rich Solution Loading [mol CO_2/mol MEA]	0.264-0.457	0.297-0.501
Temperature Rich Solution [°C]	103-118	200-230
Desorber Pressure [kPa]	194-216	200-230
Reboiler Duty [kW]	2.9-13.8	5.2-16.7

The input of the desorber was set as the incoming rich amine liquid stream. The outputs were the CO_2 produced and the lean solvent out. For the desorber, the outlet flows, temperature profiles and the CO_2 absorption rate were also investigated. In the desorber, it is unsure whether the gas or the liquid measurements are the most precise, but generally the gas measurements have been used for comparison. To calculate the percentage average, as well as the AD and AAD, the same equations have been used for the desorber as for the absorber, given in Equation 4, Equation 5 and Equation 6 in Section 5.2. The model for CO_2 desorption consists of a desorber packing, reboiler, and condenser. A flow diagram of the pilot plant for the validation of the desorber can be seen in Figure 13.

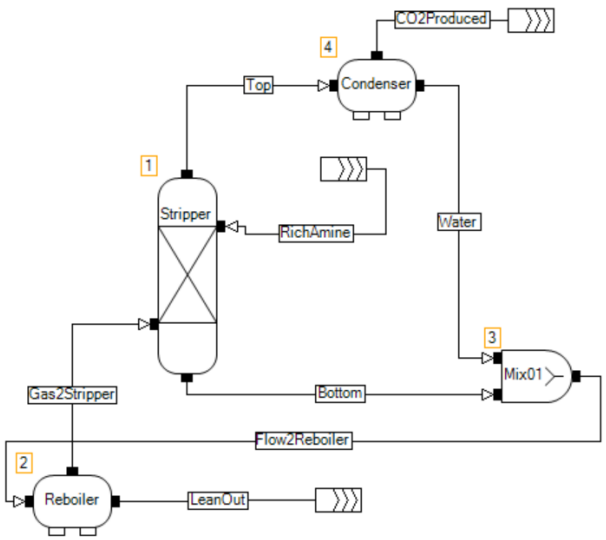

Figure 13: Pilot plant diagram of the desorber part simulated in CO2SIM.

5.3.1 Desorber Simulations - Tobiesen et al. (2008)

The experimental campaign by Tobiesen et al. (2008) [55] consisted of 19 experiments. This work follows a validation study performed on the absorber section, which was described in Tobiesen et al. (2007) [54]. The specifications and flow parameters for the desorber are provided in Table 10. The reported vol% of CO_2 in the flue gas refers to dry basis and had to be calculated to wet vol% of CO_2. This was done by using the same method as described in Section 5.2.1. N_2 was set to be inert gas in this case.

The simulation results for the lean loading, desorption rate, the percentage deviation, and the calculated ratio between simulated and experimental desorption rates for the 19 runs can presented in Table 36 in Appendix F. Additionally, Figure 14 shows how the ratio between the desorption rates varies with rich loading, temperature of the rich solvent, reboiler duty, and rich solvent flow. Although the results exhibit both under- and over- predictions, the ratio between the desorption rates is within the range of 0.83 to 1.19, indicating a good correlation between the simulated and experimental data. Further examination of additional parameters in both inlet streams, including temperature, flow rate, and CO_2 content in the flue gas and lean flow was done to identify any trends that might explain these inconsistencies. However, it was not found any clear factors that could account for the inconsistencies in the results.

During several runs, it was observed a vapor phase in the liquid stream, although it was relatively small in some cases. This included run 6, 12, 13, 14, 15, 16, 17, 18, and 19. However, the vapor phase for several of the runs were quite small. The two runs that had the highest vapor fractions were run 17 and 18 with a vapor fraction of 0.0106 and 0.0119, respectively. These findings are consistent with those reported by a former master student, Witzøe (2015) [63]. In Table 14, the AD and AAD values for lean loading, desorbed CO_2, reboiler temperature, and condenser duty are presented. Although the lean loading has a relatively high AD value, it is still considered adequate, and the other parameters have satisfactory AD and AAD values.

Table 14: AD and AAD values for lean loading, desorbed CO_2, reboiler temperature and condenser duty. (Tobiesen et al. (2008))

	AD [%]	AAD [%]
Lean Loading	15.543	0.266
Desorbed CO_2	10.359	0.417
Reboiler Temperature	0.0046	0.0002
Condenser Duty	0.185	0.001

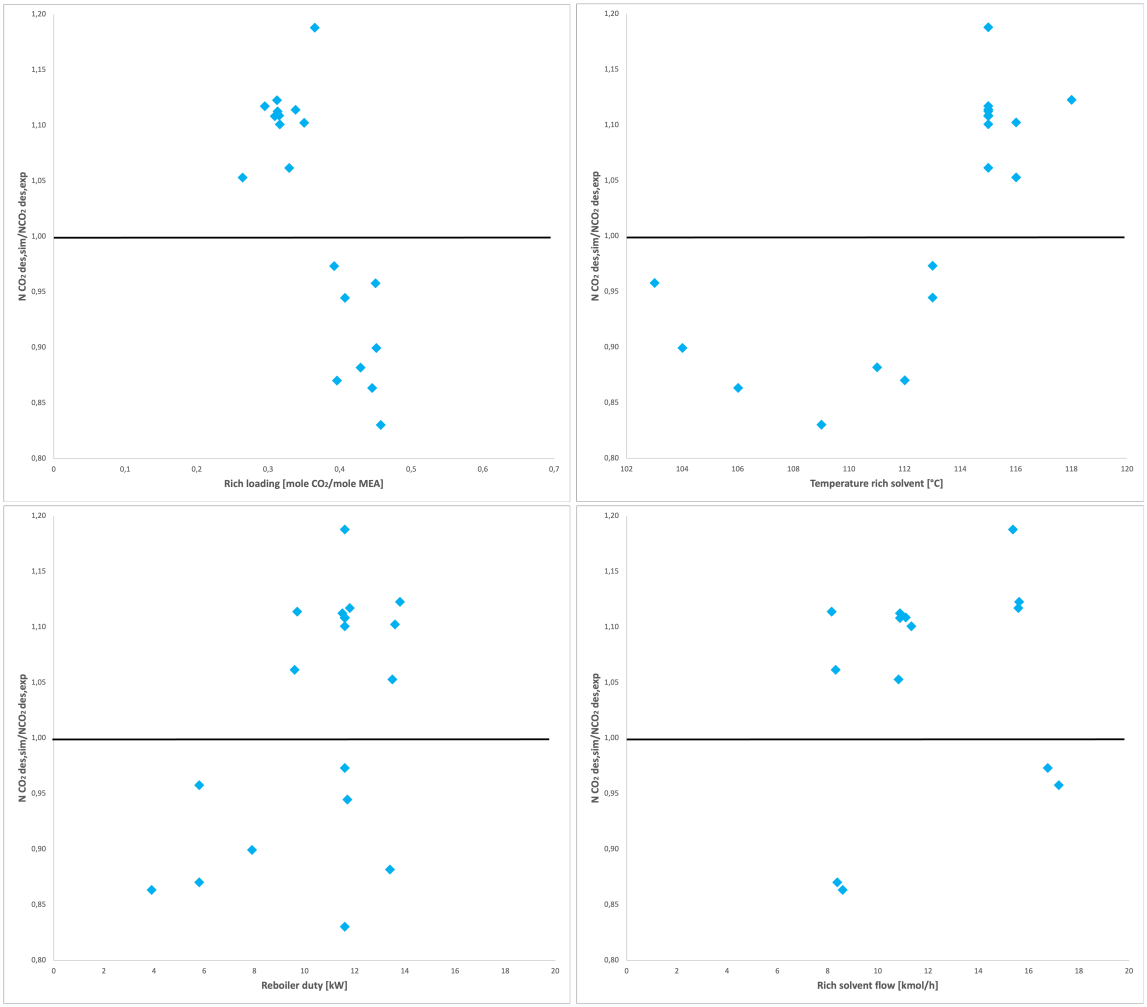

Figure 14: Plots of ratio between simulated and experimental absorption rate plotted against rich loading, temperature in rich solvent, reboiler duty, and rich solvent flow. (Tobiesen et al. (2008))

5.3.2 Desorber Simulations - Notz et al. (2012)

The experimental campaign by Notz et al. [3] was carried out by performing 47 experiments. The desorber specifications and flow parameters for the desorber can be found in Table 13. The composition and mass flow rate of the rich amine stream can be found in label 12 in Figure 31 in Appendix B. In the same flow sheet, the pilot plant for the desorber is shown, where label T42 was decided to be the inlet temperature. Although the flowsheet indicates that label T44 as the inlet temperature for the desorber, label T42 was selected instead because CO2SIM software does not account for heat loss in pipe flow.

The publication by Notz et al. [3] does not provide information on the pressure of the rich solvent. However, it does state that a throttle valve (V57) is installed at the desorber inlet to maintain a sufficiently high pressure (P9) and prevent CO_2 evaporation in the feed line and heat exchanger. The publication also says that the desorber operates within a pressure range of 1-2.3 bar. To ensure that the inlet pressure is higher than the equipment pressure and prevent biphasic flow, a pressure above 2.3 bar is recommended and it is important to check for the absence of a vapor phase.

To avoid a vapor phase in the flow, the pressure for the rich amine was regulated above 2.3 bar for all 47 runs. However, the system failed to converge after 7.5 bar in runs 25 and 27, resulting in the presence of a vapor phase. The deviations between the simulated and experimental data were unacceptably high, with the maximum deviation reaching 76.50%. To address this, 47 new runs were performed where the pressure for the rich amine was set to the same value as the reboiler, which was 1.9 bar. While a vapor phase was present in the liquid stream, the results were better than those obtained previously. Adding a flash unit to the system could potentially eliminate the vapor phase, but this was not implemented in this validation study.

This section will further focus on the 47 runs performed with rich amine pressure of 1.9 bar. Table 37 in Appendix G presents the simulation results for the lean loading, the desorption rate, the percentage deviation, and the calculated ratio between simulated and experimental desorption rates for the 47 runs. Additionally, Figure 15 illustrates the ratio between the simulated and experimental desorption rates against the rich loading, temperature of the rich solvent, reboiler duty, and the rich solvent flow. The results showed both under- and over-predictions, with a deviation ranging from -48.88 and 34.46 between the simulated and experimental desorption rates. While the interval is large, it is noteworthy that only two runs, run 14 and 46, exhibited significantly higher deviations than the other simulations. By examining the data for these runs, nothing stood out as the apparent reason for the discrepancies. Furthermore, Table 15 presents the AD and AAD values for the lean loading, desorbed CO_2, reboiler temperature, and condenser duty. The AD and AAD values indicate that the simulated model's performance was satisfactory.

Table 15: AD and AAD values for lean loading, desorbed CO_2, reboiler temperature and condenser duty. (Notz et al. (2012))

	AD [%]	AAD [%]
Lean Loading	9.610	0.156
Desorbed CO_2	12.191	0.016
Reboiler Temperature	0.519	0.003
Condenser Duty	1.040	0.004

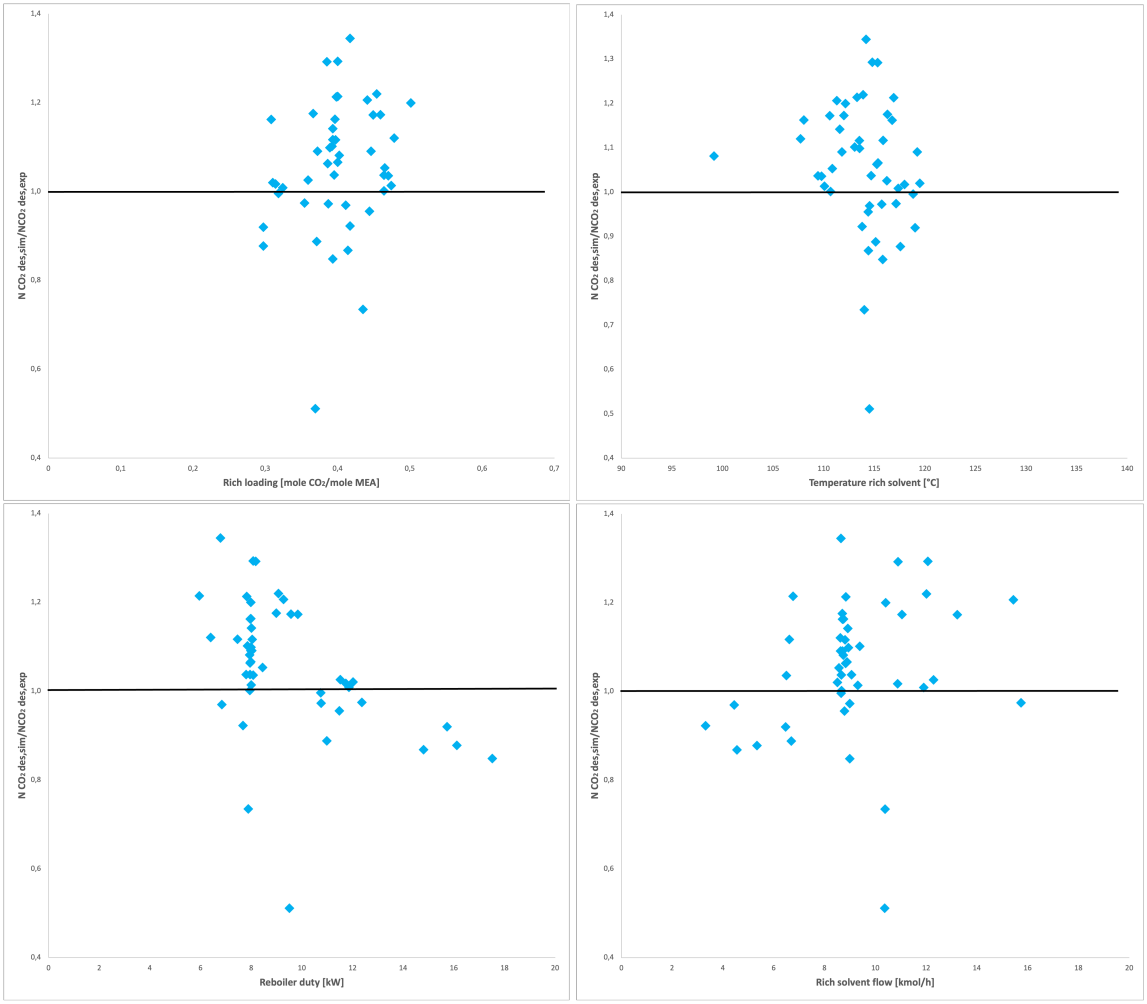

Figure 15: Plots of ratio between simulated and experimental absorption rate plotted against rich loading, temperature in rich solvent, reboiler duty, and rich solvent flow. (Notz et al. (2012))

6 Results and Discussions

This section presents the results for the case studies performed in this thesis. A discussion part is also provided for each case study. Finally, a summary and comparison of the case studies are provided. An overview of the case studies performed can be seen in Table 16. The desired capture rate of CO_2 was set to be 95%.

Table 16: Overview of the simulated cases performed in the case studies.

Coal Flue Gas Case	
Case 1	Total height of WW1 and WW2 decreased to 2 m
Case 2	Total height of WW1 and WW2 decreased to 4 m
Case 3	Total height of WW1 and WW2 increased to 6 m
Case 4	Total height of WW1 and WW2 increased to 8 m
Case 5	Temperature of water in WW1 and WW2 decreased to 20 °C
Case 6	Temperature of water in WW1 and WW2 decreased to 25 °C
Case 7	Temperature of water in WW1 and WW2 increased to 35 °C
Case 8	Temperature of water in WW1 and WW2 increased to 40 °C
Case 9	Temperature of water in WW1 increased to 40 °C and constant at 30 °C in WW2
Case 10	Temperature of water in WW1 increased to 45 °C and constant at 30 °C in WW2
Case 11	Temperature of lean amine decreased to 20 °C
Case 12	Temperature of lean amine decreased to 25 °C
Case 13	Temperature of lean amine decreased to 30 °C
Case 14	Temperature of lean amine decreased to 35 °C
Case 15	Flow rate increased from 20 kmol/h to 40 kmol/h
Case 16	Flow rate decreased from 20 kmol/h to 10 kmol/h
Case 17	1 wt% MEA in the water entering WW2
Case 18	0.5 wt% MEA in the water entering WW2
Remove One Water Wash Section	
Case 19	Case with only one water wash section
Case 20	Water wash with height of 2 m
Case 21	Water wash with height of 4 m
Case 22	Water wash with height of 6 m
Case 23	Water wash with height of 8 m
Case 24	Amine concentration of 1 wt% entering the water wash
Case 25	Amine concentration of 0.5 wt% entering the water wash

6.1 Base Case

To provide a basis for comparison, a base case with constant reboiler duty, gas flow, and lean flow was defined. The height and diameter of the water wash are shown in Table 17, along with the lean loading, rich loading, and MEA emissions before, between, and after the water wash stages. As the focus of this thesis is on emissions, this parameter will be the most important and will be used as a primary point of comparison with the other case studies. The operating conditions and the result for the simulation of the base case can be found in Table 39 in Appendix I.

Table 17: Base Case results.

	Base Case
Water Wash Total Height [m]	4.8
Water Wash Diameter [m]	0.2
L/G absorber [kg/kg]	2.3
L/G WW1 [kg/kg]	2.1
L/G WW2 [kg/kg]	2.3
Reboiler Duty [MJ]	526
Emissions before water washes [ppm]	**480**
Emissions between water washes [ppm]	**3.4**
Emissions after final water wash [ppm]	**0.008**
Lean Loading [mol CO_2/mol MEA]	0.16
Rich Loading [mol CO_2/mol MEA]	0.51

In Figure 16, the vapor temperature profile in the absorber for the base case is presented. From the figure, it can be observed that the temperature bulge is quite close to the top of the column. It can also be observed that the temperature reaches a maximum value of 79 °C. At this temperature, desorption within in the column can happen. This results in unwanted release of CO_2 from the solvent in the absorber. The reason for the temperature increase is the heat generated by the exothermic reaction between the MEA and CO_2.

Figure 17 and Figure 18 shows the vapor temperature profile in the first water wash and the second water wash section, respectively. In the first water wash, the temperature reaches a maximum of 63 °C. The gas temperature entering the first water wash was at 50 °C. It is unclear why these high temperatures are observed. However, similar vapor temperature profiles have been reported previously by former master student, Nesse (2021) [64]. In the second water wash, pinching occurs around 0.25 m, indicating that there is no driving force for further absorption throughout the rest of the column. The temperature in the second water wash is significantly lower than in the first water wash, which result in condensation. The temperature profiles obtained from the base case will be used as a reference for the subsequent case studies. When comparing the MEA emissions in the vapor phase at the top of the absorber with those after the second water wash, it can be observed that the water wash effectively removed 99.9983% of the emissions.

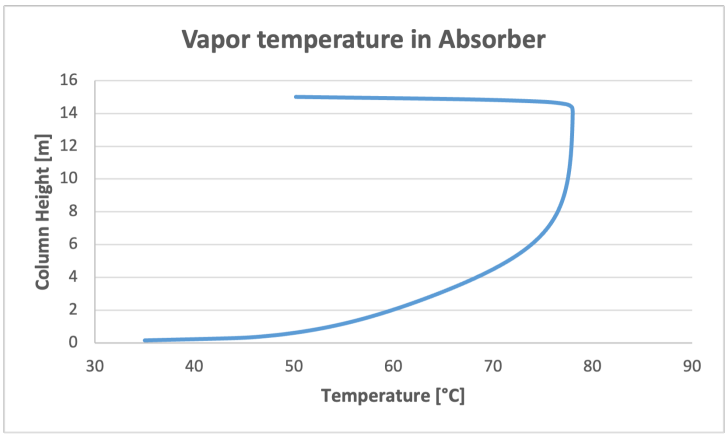

Figure 16: Vapor temperature profile in the absorber.

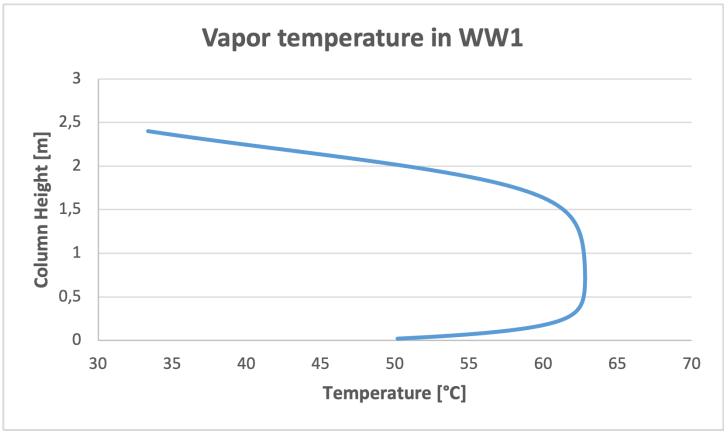

Figure 17: Vapor temperature profile in the first water wash.

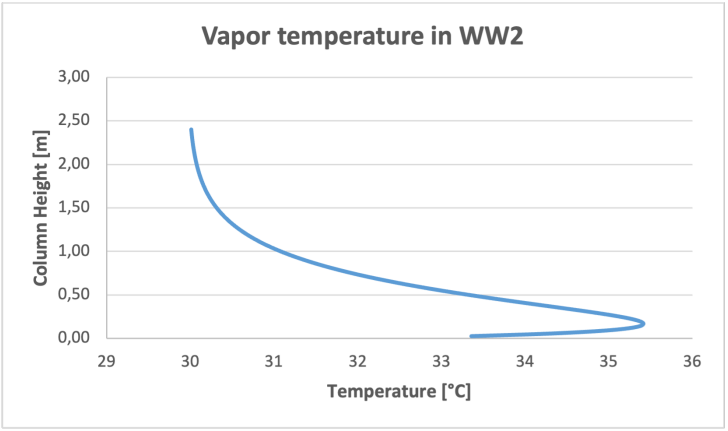

Figure 18: Vapor temperature profile in the second water wash.

The specific reboiler duty (SRD) versus the liquid-to-gas (L/G) ratio for the base case is illustrated in Figure 19. As the liquid flow increases, the SRD initially decreases until it reaches a minimum at the optimal L/G ratio of 4.56 GJ/tonne CO_2. Beyond this point, the SRD starts to increase again.

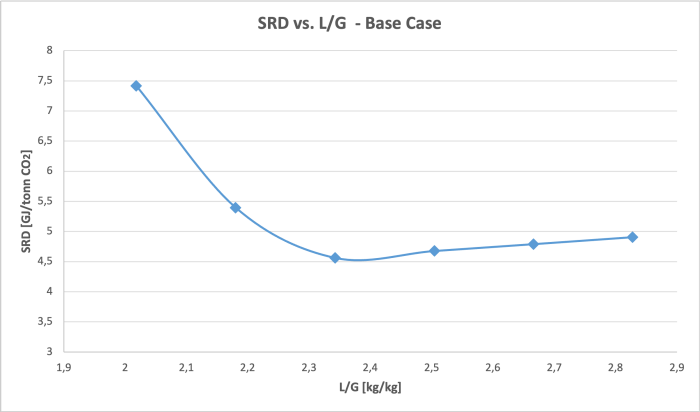

Figure 19: SRD vs. L/G for the base case

6.2 Case Study - Water Wash Height

This section presents the results and discussion of a case study that explores the effect of varying water wash heights. The base case had water wash sections with a packing height of 2.4 each, resulting in a total height of 4.8 m. To investigate the impact of changing the packing height, four cases were set up: Case 1 with a total height of 2 m, Case 2 with a total height of 4 m, Case 3 with a total height of 6 m, and Case 4 with a total height of 8 m. An overview of the case studies performed is provided in Table 16. All cases capture 95% CO_2.

Table 18 summarizes the results of the case study on varying water wash heights, including the total height of the water wash sections and the MEA emissions at different stages for the base case and Cases 1-4 at the optimal point. The MEA emissions before entering the first water wash stage are labeled as "GasAbsTreat", the MEA emissions between the two water wash stages are labeled as "GasWWTreat" and the emissions after the second water wash stage are labeled as "SweetGas". These streams can be seen in Figure 4. The results shows that increasing the water wash height reduces the emissions.

Table 18: The total height of the water wash stages and the emissions before the first water wash, between the water washes and after the final water wash.

	Total height [m]	Emissions [ppm]		
	WW1 & WW2	Before WW1	Between WW	After WW2
Base Case	4.8	480	3.4	0.008
Case 1	2	480	55.0	4.64
Case 2	4	480	6.7	0.04
Case 3	6	480	1.8	$9.2 \cdot 10^{-4}$
Case 4	8	480	1.3	$6.4 \cdot 10^{-5}$

The results presented in Table 18 support the conclusions drawn by Majeed and Svendsen (2018) as discussed in Literature Review (Section 3). Majeed and Svendsen (2018) [56] reported that height of the water wash section does not have a significant impact beyond increasing residence time. When using CO2SIM, only gas phase emissions are considered. Increasing the column height can lead to a reduction in gas phase emissions by enhancing the efficiency of the water wash process in removing emissions. Longer residence times enable more effective removal of emissions by the water wash.

In reality, when all types of emissions are considered, it is important to note that longer residence times can result in larger droplets. This may lead to a decrease in the amount of MEA carried out with the aerosol emissions due to the droplets grow by absorbing water, which can deplete the MEA within the water. Conversely, reducing the water wash height can decrease residence time, resulting in smaller droplet sizes and less MEA carried out with the droplets. Thus, increasing the water wash height may reduce emissions. Moreover, larger droplets are preferable as they are easier for the demister unit to remove [56].

Doubling the water wash height from a total of 2 m to 4 m clearly had a significant effect on the emissions after the first and the second water wash stage, which showed a remarkable reduction of 99.0511% on the emissions after the final water wash stage. However, it is important to consider that increasing the column height leads to increased costs. The goal of this thesis was to keep the volatile emissions under 1 ppm, which was achieved with a total height of 4 m, resulting in a final MEA emission of 0.04 ppm. Further increasing the water wash height to maintain volatile emissions under 1 ppm would not be necessary since it would incur additional costs. These cases demonstrate that increasing water wash height effectively reduces overall MEA emissions from an amine scrubbing system. However, the optimal height remains uncertain, as it is unclear how much more advantage can be achieved by further increasing the height.

The vapor temperature profile for the absorber for Case 1 is shown in Figure 20. The vapor temperature profiles in this case studies were identical for each case and are therefore not provided in this section. However, they can be found in Figure 33 in Appendix J. In every case, the temperature at the top of the absorber column is the same. Due to the remarkably similar temperature profiles observed in all cases, the emissions of vapor MEA at the top of the absorber column remain consistent.

Figure 21 presents the vapor temperature profiles in the first and the second water wash for the base case and the Cases 1-4. It can be observed from the temperature profiles in the first water wash stage that the temperature gradient is more pronounced in the cases with taller columns compared to the cases with shorter columns. This is because taller column provides a larger vertical distance for temperature changes to occur. The increased height also allows for more opportunities for heat transfer and mixing within the column, while the shorter columns exhibit more abrupt changes in temperature of a shorter distance. The temperature variations can affect the mixing patterns and residence time of gases within the column. In taller columns, there may be more opportunities for thorough mixing and longer contact time between the gas and amine, potentially enhancing pollutant removal efficiency and reducing emissions compared to shorter columns. This is consistent with what was observed in Table 18, that increasing height led to a decrease in emissions.

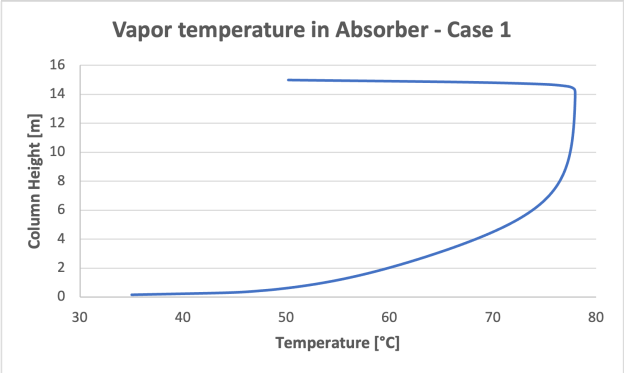

Figure 20: Vapor temperature profile in the absorber for Case 1.

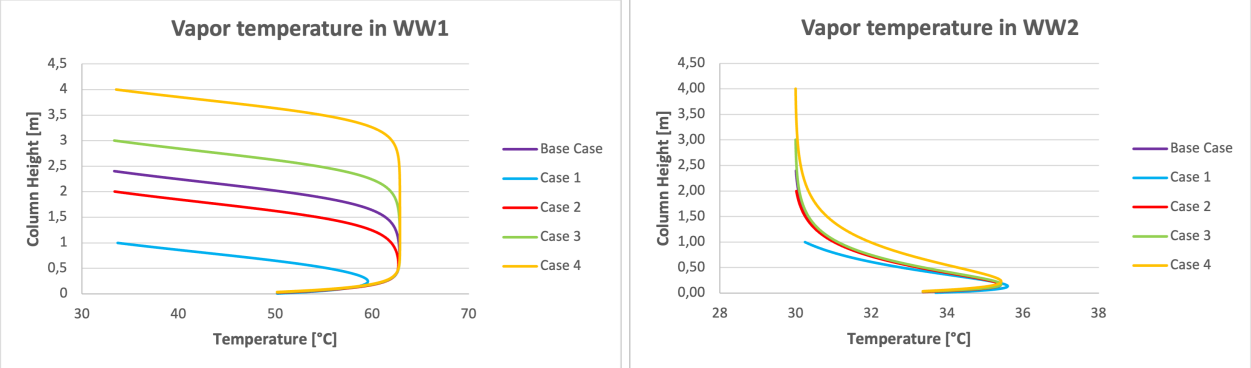

Figure 21: Vapor temperature profiles in the first and the second water wash for the base case and the Cases 1-4.

Table 19 shows the reboiler duty, L/G, lean loading and rich loading for the base case and cases 1-4 at the optimal point. It can be observed that every case provided the same values, despite the varying water wash heights. This indicates that changing the water wash height has no impact on these parameters.

Table 19: The reboiler duty, L/G ratio, lean loading and rich loading for the base case and cases 1-4 at the optimal point.

	Reboiler duty	L/G Absorber	L/G WW1	L/G WW2	Lean loading	Rich loading
	[MJ]	$[\frac{kg}{kg}]$	$[\frac{kg}{kg}]$	$[\frac{kg}{kg}]$	$[\frac{molCO_2}{molMEA}]$	$[\frac{molCO_2}{molMEA}]$
Base Case	526	2.3	2.1	2.3	0.16	0.51
Case 1	526	2.3	2.1	2.3	0.16	0.51
Case 2	526	2.3	2.1	2.3	0.16	0.51
Case 3	526	2.3	2.1	2.3	0.16	0.51
Case 4	526	2.3	2.1	2.3	0.16	0.51

In Figure 22, the SRD is plotted against the L/G for Case 1 and Case 4. It is clear from the figure that the plots are nearly identical. This similarity is because changing the height of the water wash sections has little effect on the VLE or the kinetics of the absorber, and the operating conditions remain mostly the same. For all cases, the SRD reaches a minimum at the optimal L/G, which in this study was found to be 2.3. Beyond this point, the SRD increases again. The behavior of the SRD and L/G is similar for all cases, as can be seen in Figure 36 in Appendix K, which shows the SRD vs. L/G plot for Case 2 and 3.

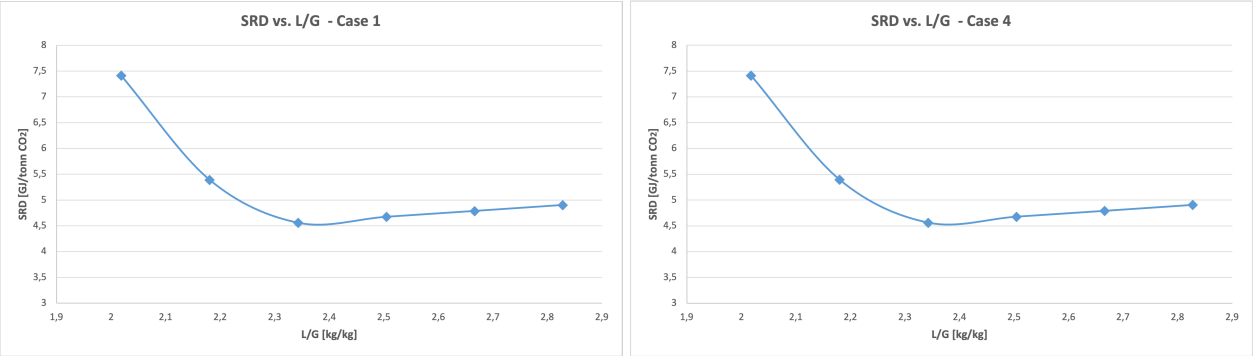

Figure 22: SRD vs. L/G for Case 1 and 4.

6.3 Case Study - Water Temperature in Water Wash Section

This section presents the results and discussion of a case study investigating the effects of varying water temperature on the performance of the water wash sections. A total of six case studies was performed, where the only changing parameter was the temperature of the water entering the water wash sections, labeled as "Water01" and "Water02" in Figure 4. The base case had a temperature of 30 °C in both streams. Case 5-8 had water temperatures varying from 20-40 °C with a 5 °C interval, with an exception of 30 °C as this temperature is the temperature used in the base case. Case 9 and 10 were then performed with a constant temperature of 30 °C in the second water wash, while the first water wash had temperatures of 40 and 45 °C, respectively. All cases capture 95 % CO_2.

In Table 20, the temperature of the water entering the WWI and WW2 and the MEA emissions in the different treatment stages at optimal point, are presented for the base case and the Cases 5-10. As shown in Table 20, increasing the water temperature results in higher MEA emissions. This finding is consistent with the study by Majeed and Svendsen (2018) which is discussed in Section 3 Literature Review [56].

Table 20: The temperature of "Water01" and "Water02", and the emissions before the first water wash, between the water washes and after the final water wash for the base case and case studies 5-10.

	Temperature [°C]		Emissions [ppm]		
	Water01	Water02	Before WW1	Between WW	After WW2
Base Case	30	30	480	3.4	0.008
Case 5	20	20	480	2.7	0.005
Case 6	25	25	455	2.8	0.006
Case 7	35	35	480	3.8	0.011
Case 8	40	40	-	-	-
Case 9	40	30	480	3.9	0.011
Case 10	45	30	480	4.2	0.013

As shown in Table 20 operating with higher water temperatures in the water wash sections still result in MEA emissions below 1 ppm. It is worth noticing that Case 8, which used 40 °C water in both water wash sections, did not yield any emissions values as the simulation failed to converge. This may be due to the high temperature being beyond the optimal range of the process. Operating with water in the range of 20-25 °C offers advantages such as lower emissions and reduced energy demand, as higher temperatures require more energy to achieve. The total load on the reboiler is decreased when the water wash is effective at removing impurities from the amine solution. This means that less energy is required to regenerate the amine solution and bring it back to its desired purity. As a result, the reboiler duty can be reduced when the water wash is optimized. Using lower water temperatures in the water wash is feasible in Norway due to the location of the country as the country is located in a northern latitude, which results in cooler temperatures. The colder ambient temperature in Norway allows for the use of colder water, while countries with warmer climates, such as in central Europe, could encounter difficulties with operating at low temperatures and may prefer to operate at 35-40 °C to avoid incurring additional electricity costs associated with cooling the water.

Case 9 and Case 10 were performed with different temperatures of water entering in WW1 and WW2. These cases were performed to investigate if this modification would give a significant reduction in amine losses. As shown in Table 20, Case 9 with a water temperature of 40 °C in WW1 and 30 °C in WW2 results in emissions that are approximately the same as those in Case 7, where both water washes have a temperature of 35 °C. Case 10 with a water temperature of 45 °C in WW1 and 30 °C in WW2 shows slightly higher emissions, but not significantly so. Therefore, it can be assumed that maintaining the second water wash section at a constant temperature of 30 °C will not have a significant impact on emissions when the temperature is high in the first water wash.

The results in Table 20 reveal an interesting observation regarding Case 6, where the emissions in the stream after the absorber and before entering the first water wash stage are lower compared to the other cases. However, this stream should theoretically be consistent among all cases since it is now influenced by the changing parameter. Therefore, the discrepancy in Case 6 could be attributed to a simulation error.

The temperature of the water used in the water wash section can have both positive and negative impacts on the amine scrubbing process. Firstly, increasing the temperature can improve the efficiency of the amine scrubbing process which can reduce emissions. This is because higher temperatures can enhance the chemical reaction between the amine and the gas, leading to more effective removal of contaminants. Additionally, higher temperatures can result in larger droplet sizes, making it easier for the demister unit to capture these emissions. To optimize the temperature of the water in the water wash section, it is crucial to find a balance between the efficiency of the scrubbing process and the potential for increased emissions.

In Figure 23, the vapor temperature profile in the absorber for Case 5 is shown. Similar to the vapor temperature profiles observed in the other case studies, this study also demonstrates identical temperature profiles for the absorber in each case. The remaining temperature profiles can be found in Figure 34 in Appendix J. It is noteworthy that, in this case as well, the temperature of the top of the absorber column remains unchanged. This consistent temperature observation accounts for the uniform emissions of vapor MEA in all cases at the top of the column.

Figure 24 presents the vapor temperature profile in the first and the second water wash for the base case and Cases 5-7, 9, and 10. The temperature profile for the first water wash shows two different inlet temperatures, even though the only variable being changed is the water temperature. In theory, all inlet temperatures should be the same. However, upon a closer examination of the temperature profile highlights that it is Case 6 that deviates from the other cases. It is worth noting that Case 6 has also exhibited different behavior compared to the other cases in this study earlier. Consequently, it can be concluded that Case 6 is an outlier, and the discrepancy in the inlet temperature compared to the other cases may be attributed to simulation errors. Upon reviewing the simulation and operating conditions, no specific factors were identified as the cause of this inconsistency. Due to time constrains, Case 6 was not rerun, but it would be beneficial to have done this to figure out what causes the discrepancy.

The temperature profile in the second water wash for the different cases performed in this case study shows that the lower temperatures has less variations in temperatures compared to the cases with higher temperatures. Higher temperatures leads to increased heat transfer, which means that heat is transmitted between system components more rapidly. This causes temperature changes to occur faster and with greater intensity. In contrast, the heat transfer rate is slower at lower temperatures, resulting in less abrupt and obvious temperature fluctuations. Another possible explanation for the larger variations in the cases with higher temperatures is that higher temperatures can cause thermal expansion. As the temperature increases, water and the components of the scrubbing system, expand. This expansion can result in changes in the flow pattern, turbulence, and mixing within the system, which again can lead to temperature fluctuations and a less stable temperature profile.

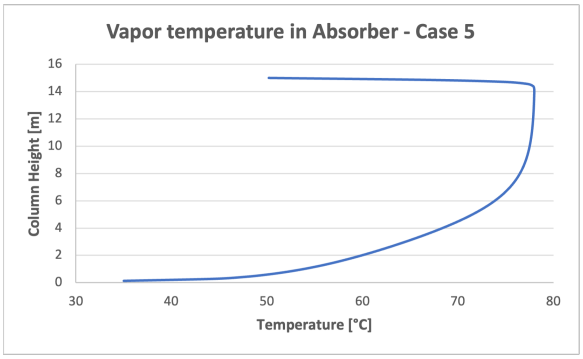

Figure 23: Vapor temperature profiles in the absorber for Case 5

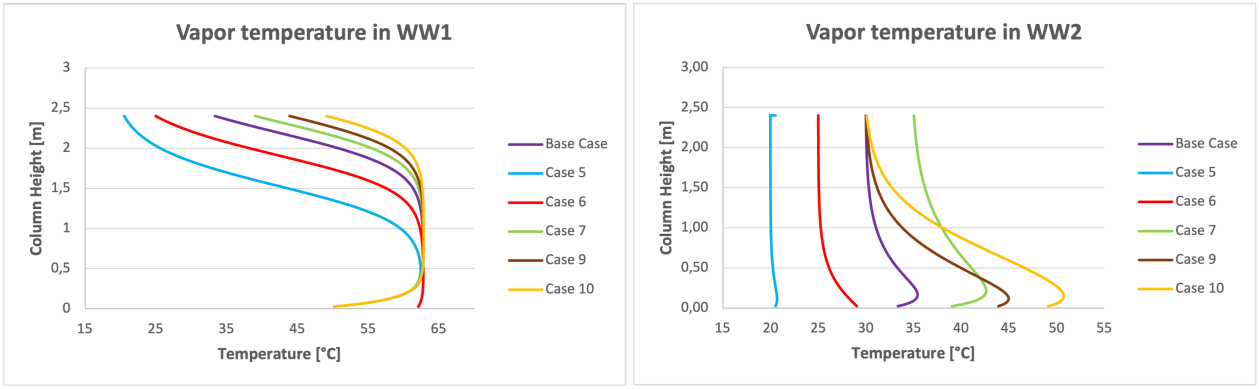

Figure 24: Vapor temperature profile in the first and the second water wash for the base case and the Cases 5-7, 9, and 10.

The reboiler duty, L/G, lean loading, and rich loading for the base case and the case studies performed in this study at the optimal point are presented in Table 21. As observed in Table 21, Case 6 appears to be an outlier, with higher reboiler duty and lean loading than the other cases. Due to the higher lean loading, one would expect the reboiler to reduce and not increase. The amine concentration for every case was checked to see if this might be the reason for the discrepancy, but every case had the same amine concentration. From Table 21, it can be observed that the L/G ratio for the absorber and both water wash sections remains relatively constant for every case that provided results. Since Case 8 did not converge, the case did not provide any information about the parameters presented in Table 21. The SRD vs. L/G plots for the cases performed in this case study can be found in Figure 37 in Appendix K. The cases exhibited similar behavior since the water temperature does not significantly impact the energy numbers in this process.

Table 21: The reboiler duty, L/G ratio, lean loading and rich loading for the base case and cases 5-10 at the optimal point.

	Reboiler duty	L/G Absorber	L/G WW1	L/G WW2	Lean loading	Rich loading
	[MJ]	$[\frac{kg}{kg}]$	$[\frac{kg}{kg}]$	$[\frac{kg}{kg}]$	$[\frac{molCO_2}{molMEA}]$	$[\frac{molCO_2}{molMEA}]$
Base Case	526	2.3	2.1	2.3	0.16	0.51
Case 5	526	2.3	2.0	2.4	0.16	0.51
Case 6	539	2.3	2.1	2.3	0.18	0.51
Case 7	526	2.3	2.1	2.2	0.16	0.51
Case 8	-	-	-	-	-	-
Case 9	526	2.3	2.1	2.2	0.16	0.51
Case 10	526	2.3	2.1	2.2	0.16	0.51

6.4 Case Study - Lean Amine Temperature

This section presents the results and discussion of a case study that explores the impact of varying the temperature of the lean amine on emissions and energy consumption. Four case studies were performed, where the temperature of the lean flow was varied from 20-35 °C with a 5 °C interval. In the base case, the temperature of the lean amine flow was set at 40 °C. The lean amine stream where the temperature was varied is labeled as "LeanAmine" in Figure 4. All cases capture 95% CO_2.

Table 22 shows the temperature of the lean amine and the emissions in the different stages at optimal point for the base case and cases 11-14. Majeed and Svendsen (2018) have previously reported that the lean amine temperature can increase both the droplet size and emissions [56]. Consistent with their findings, the results in Table 22 shows that increasing the lean amine temperature leads to increased emissions. Notably, the emissions after the absorber and before the first water wash stage vary for the different cases. This observation was not made for the case studies in Section 6.2 and Section 6.3. The difference in this case study was that the parameter investigated also affects the absorber, explaining why the emissions vary for this stream in this study and not the other case studies.

Table 22: The temperature of "LeanAmine" and the emissions before the first water wash, between the water washes and after the final water wash for the base case and case studies 11-14.

	Temperature [°C]	Emissions [ppm]		
	Lean Amine	Before WW1	Between WW	After WW2
Base Case	40	480	3.4	0.008
Case 11	20	364	1.1	0.004
Case 12	25	395	1.7	0.004
Case 13	30	425	2.3	0.005
Case 14	35	453	2.8	0.006

As mentioned earlier, the temperature of the lean solvent can have an impact on the absorber, and it was found that increasing the temperature led to higher emissions in the stream before entering the first water wash stage. One possible explanation for this increase could be an increase in the corrosion rate of the absorber. Higher temperatures of the lean solvent can accelerate the corrosion rate and result in increased emissions [65]. To avoid this issue, materials that can withstand the high temperature of the lean amine can be used to reduce the risk of corrosion.

In Figure 25 the vapor temperature profiles in the absorber for the base case and Cases 11-15 are presented. It can be observed that the temperature profiles for the Cases 11 and 12 are almost identical to the base case. However, Case 13 and 14 exhibit lower temperature at the top of the absorber compared to the other cases performed in this case study. The inlet temperature for Case 13 was also significantly lower compared to the other cases.

Figure 26 shows the vapor temperature profiles in the first and the second water wash sections for the case case and Cases 11-15. Notably, Cases 11-13 exhibit similar behavior and values, hence the temperature profiles for Case 11 and 12 are overlapped by Case 13. The occurrence of identical temperature profiles for these cases appear unusual, especially since the cases provided different quantities of emissions in the gas streams before, between and after the water wash sections. This observation might be due to simulation errors. Inaccuracies or limitations in the simulation model used to analyze the case study can be caused by errors or restrictions. The accuracy of the results can be impacted by mistakes in the simulation's assumptions, numerical methodologies, or boundary conditions. To ascertain whether simulation mistakes are contributing to the odd findings, the Cases 11-13 were run again, but gave the same outcome.

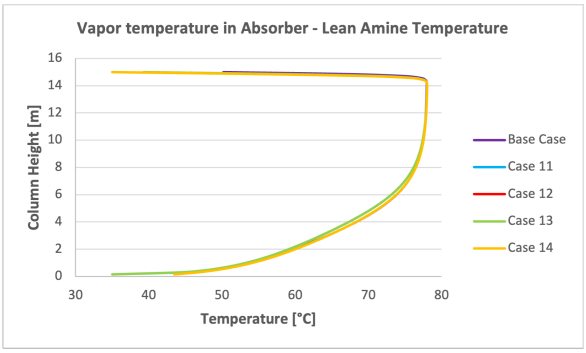

Figure 25: Vapor temperature profiles in the absorber for the base case and Cases 11-15.

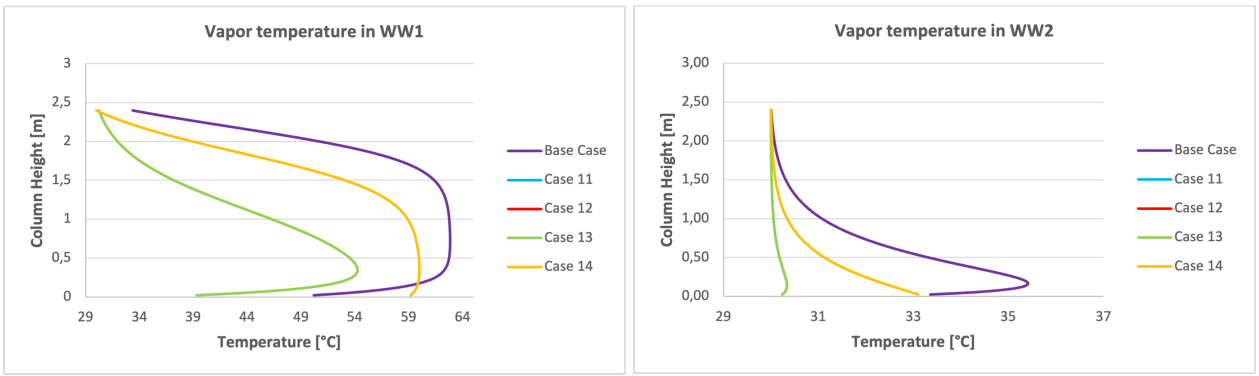

Figure 26: Vapor temperature profiles in the first and the second water wash for the base case and the Cases 11-5.

Table 23: The reboiler duty, L/G ratio, lean loading and rich loading for the base case and cases 1-4 at the optimal point.

	Reboiler duty	L/G Absorber	L/G WW1	L/G WW2	Lean loading	Rich loading
	[MJ]	$[\frac{kg}{kg}]$	$[\frac{kg}{kg}]$	$[\frac{kg}{kg}]$	$[\frac{molCO_2}{molMEA}]$	$[\frac{molCO_2}{molMEA}]$
Base Case	526	2.3	2.1	2.3	0.16	0.51
Case 11	533	2.3	2.2	2.4	0.16	0.51
Case 12	531	2.3	2.2	2.4	0.16	0.51
Case 13	530	2.3	2.1	2.3	0.16	0.51
Case 14	528	2.3	2.1	2.3	0.16	0.51

Table 23 shows the reboiler duty, L/G, lean loading and rich loading for the base case and the cases 11-14 at the optimal point. It can be observed that the reboiler duty is decreasing with increasing temperature. The same observation was made by Eviani et al. [66] that reported that increasing the lean amine temperature decreased the energy consumption. The temperature of the lean amine is an important parameter that affects the reboiler duty, and one explanation to why the reboiler duty decreases with increasing temperature of the lean amine can be due to the heat capacity. The heat capacity of the lean amine solution decreases as the temperature increases. This means that less heat energy is required to raise the temperature of the solution to the boiling point [67]. It can also be seen from Table 23 that the L/G ratio for the absorber and both water wash sections remains relatively constant for every case.

Figure 27 shows a plot of the temperature against the reboiler duty at the optimal point. The plot shows linear behavior, which indicate that as the reboiler duty increases, the temperature decreases in a proportional manner. The SRD vs. L/G plots for the cases in this study can be found in Figure 38 in Appendix K.

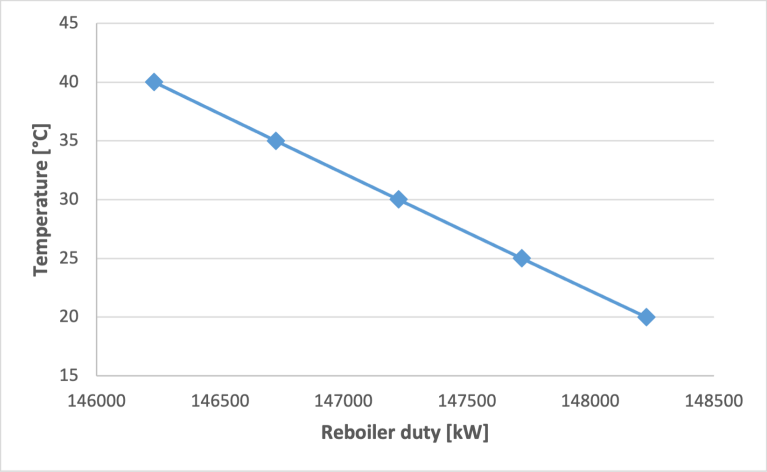

Figure 27: Reboiler duty [kW] for the different temperatures.

6.5 Case Study - Flow Rate

This section presents the results and discussion of a case study where the flow rate was varied to investigate the impact on emissions. The study aimed to determine the optimal water flow rate that still adequately wets the packing, and to assess whether varying the flow rate would significantly affect emissions. It is generally expected that increasing the flow rate will lead to lower emissions, as improved gas-liquid contact enhances mass transfer and pollutant removal efficiency [67].

Three case studies was performed to investigate the effect of varying the flow rate on the emissions. In Case 15, the flow rate was doubled from 20 to 40 kmol/h, while in Case 16 the flow rate was halved from 20 to 10 kmol/h. All cases capture 95% CO_2. Table 24 summarizes the flow rate and emissions in the different stages at optimal point for the base case and Cases 15 and 16. As expected, decreasing the flow rate from 20 to 10 kmol/h resulted in a significant increase in emissions, while increasing the flow rate to 40 kmol/h led to a 50% decrease in the emissions after both water wash sections. While it may seem counterintuitive, a high flow rate is generally not desirable despite resulting in lower emissions. This is due to several reasons. High flow rates requires larger equipment, such as larger columns and pumps, which increases capital and operational costs. The equipment used can also have limitations in terms of maximum flow rates in which the equipment can handle efficiently. Operating beyond these limitations can lead to reduced performance and efficiency, compromising the overall effectiveness of the process. Additionally, high flow rates requires more energy for pumping and circulation, which can increase the overall energy consumption of the process. Higher flow rates are also more challenging to maintain and control. All of these negative impacts may outweigh the benefits of emission reduction achieved by a higher flow rate.

Table 24: The flow rate, L/G and the emissions before the first water wash, between the water washes and after the final water wash for the base case and Case 15 and 16.

	Flow Rate [kmol/h]	Emissions [ppm]		
	-	Before WW1	Between WW	After WW2
Base Case	20	480	3.4	0.008
Case 15	40	479	0.2	0.004
Case 16	10	413	9.6	0.180

Linear behavior is commonly expected in the relationship between flow rate and system performance. Assuming constant operating parameters, the system's behavior should remain consistent across a range of flow rates. Thus, the emission removal efficiency or energy consumption may increase or decrease proportionally to the flow rate. However, an optimal point was not found in the simulations performed in Matlab, and it was not expected to be found either. The SRD vs. L/G plots for Case 15 and Case 16 in Figure 28 align with the anticipated behavior. Notably, Case 16's simulation stopped converging after only three data points were obtained. It can be observed that the expectations mentioned are consistent with the results.

The plots demonstrate a linear relationship between flow rate and system performance, but this may not always be the case in practice. In reality, the relationship between flow rate and system performance can be more complex, with an optimal point or a threshold where increasing the flow rate no longer results in a noticeable improvement in the system's ability to remove emissions. At

this point, further increasing the flow rate may not enhance the system's performance and can even lead to negative effects such as increased energy consumption [67]. Therefore, it is important to evaluate the system's performance at various flow rates while considering all relevant factors to determine the optimal operating conditions for achieving the desired level of emissions removal and energy efficiency. This evaluation may involve conducting a more detailed analysis, such as a sensitivity analysis or optimization study, to identify the most effective flow rate for the specific application.

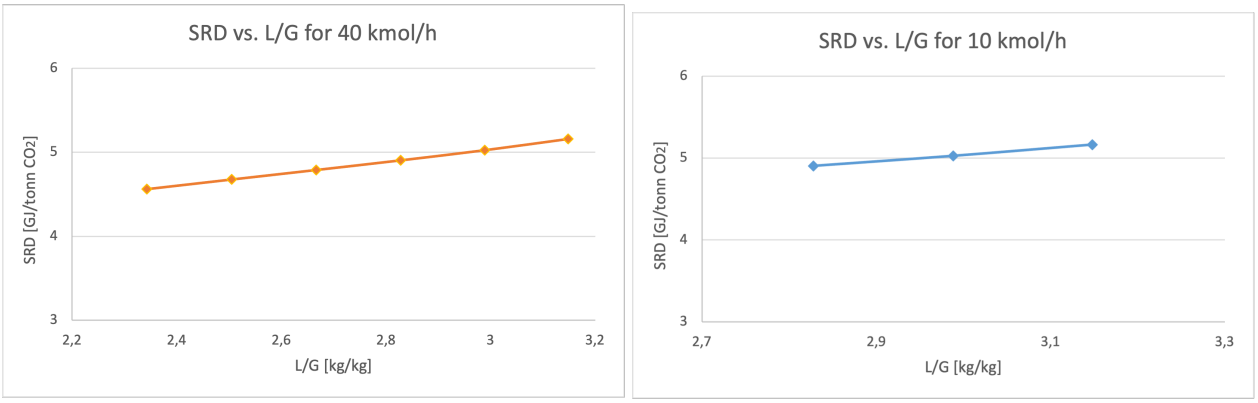

Figure 28: SRD vs. L/G for the case studies with a flow rate of 40 kmol/h and 10 kmol/h.

In Table 25, the reboiler duty, L/G, lean loading, and rich loading are presented for the base case and Case 15 and 16. It can be observed that Case 16 has higher reboiler duty and lean loading compared to Case 15 and the base case. Increasing the flow rate can improve heat and mass transfer between the gas and the solvent, which can enhance the process efficiency and reduce the overall reboiler duty [67], as seen in is Table 25. In contrast, Case 15 shows only a slight difference in reboiler duty compared to the base case. Additionally, the lean and rich loading are the same for both of these cases. By increasing the flow rate, the L/G ratio for the water wash sections increases significantly as well. Conversely, decreasing the flow rate gives lower L/G values.

Table 25: The reboiler duty, L/G ratio, lean loading and rich loading for the base case and Case 15 and 16

	Reboiler duty	L/G Absorber	L/G WW1	L/G WW2	Lean loading	Rich loading
	[MJ]	$[\frac{kg}{kg}]$	$[\frac{kg}{kg}]$	$[\frac{kg}{kg}]$	$[\frac{molCO_2}{molMEA}]$	$[\frac{molCO_2}{molMEA}]$
Base Case	526	2.3	2.1	2.3	0.16	0.51
Case 15	526	2.3	4.0	4.8	0.16	0.51
Case 16	566	2.8	1.1	1.1	0.21	0.50

6.6 Case Study - Amine Concentration in Water in Water Wash Section

This section presents the results and discussion for the case study that examines the effect of initial amine concentration in the water entering the water wash stage. In the base case, the water entering the water wash stage only contain a small amount of MEA. This case study investigates whether the emissions are concentration dependent, in addition to being temperature-dependent. While it is expected that higher amine concentration in water will lead to higher emissions, the study is still valuable in identifying any trends.

Two case studies, labeled as Case 18 and Case 19, were performed to evaluate the effect of different concentrations of MEA in the water entering the second water wash stage, which is represented as "Water02" in Figure 4. Specifically, Case 18 had 0.5 wt% MEA in the mentioned stream, while Case 19 had 1 wt% MEA. All cases capture 95% CO_2. The simulations were carried out using CO2SIM as issues arose when running the models in Matlab. The Matlab simulations yielded unexpected results, which could be attributed to the software's attempt to recalculate the streams to equilibrium while identifying the optimal point. In this case study, the results were obtained using CO2SIM instead of Matlab, which may have affected the accuracy of the results. To ensure a more accurate comparison, the results for the base case were also obtained using CO2SIM. The results for the base case presented in this section will therefore differ from the other case studies. Table 26 shows the amine concentration in the water entering the second water wash stage and the emissions for the base case, Case 17, and Case 18.

Table 26: The amine concentration in "Water02" and the emissions before the first water wash, between the water washes and after the final water wash for the base case and case studies 5-10.

	Concentration [wt%]	Emissions [ppm]		
	Water02	Before WW1	Between WW	After WW2
Base Case	0.1	378	2.3	0.01
Case 17	0.5	377	2.3	0.03
Case 18	1	376	2.4	0.05

The results of the case study demonstrate that the emissions increase with higher amine concentration. Increasing the amine concentration from 0.5 wt% to 1 wt% results in an almost 90% increase in emissions in stream after the final water wash. However, even at 1 wt% MEA in the water, the volatile emissions remain below 1 ppm. Figure 29 shows the MEA concentration in the water entering the second water wash stage plotted against the emissions in the stream after the final water wash, labeled as "SweetGas" in Figure 4. The increase in emissions appears to be approximately linear, indicating a concentration dependent effect on emissions in addition to the temperature dependence. To further observe the impact of amine concentration on emissions, higher amine concentrations in the water could be investigated.

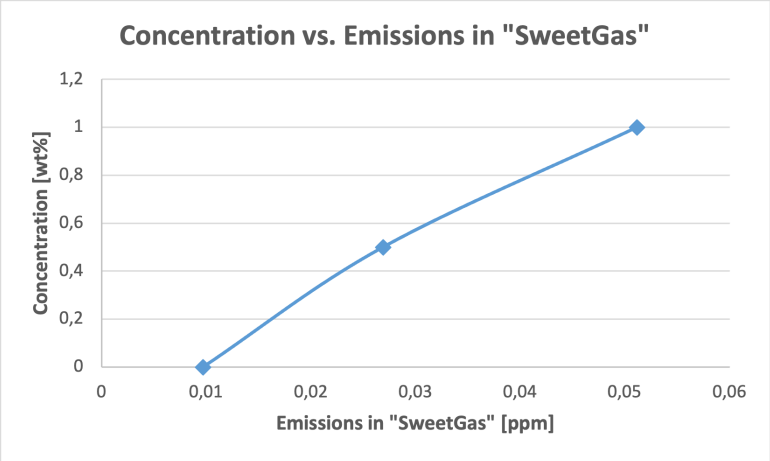

Figure 29: Concentration of MEA in water entering the second water wash stage vs. the emissions in the gas leaving the final water wash stage, labeled as "SweetGas" in Figure 4.

6.7 Case Study - Remove one Water Wash Stage

This section presents the results of the case study with a single water wash stage. A comparison with the case studies featuring two water wash stages will follow in a subsequent discussion. Since the temperature and height of the water wash sections are set to be the same for this case as the cases with two water wash sections, this case is expected to be quite similar to the two-section water wash case. Nonetheless, it is important to verify this assumption.

Seven case studies were performed for this study. Case 19 is referred to as the base case in this study, with a water wash height of 4.8 m and water entering the water wash with a small amount of MEA to make the system converge. All cases capture 95% CO_2. Case 20 to 23 focus on varying the water wash height, while Cases 24 and 25 involve different amine concentrations in the water entering the water wash section. The aim of these case studies is to explore whether having one or two water wash sections makes a significant difference in emissions. Previous studies have shown that two water wash stages are commonly used, but it is unclear why this is the case. One possible reason for this could be that having two stages allows for an assessment of the amine emissions between the different stages, providing a clearer overview of the situation. Conducting a case study with only one water wash stage can help determine whether two water wash sections are necessary.

6.7.1 Case 19, 20, 21, 22 and 23

Table 27 presents the results for cases 19-23. The table consist of the total height of the water wash and the emissions before and after the water wash. These streams are illustrated in Figure 5. The emissions before the water wash are labeled as "GasAbsTreat" and the emissions after the water wash are labeled as "SweetGas". It can be observed that the final emissions in the stream "SweetGas" are relatively high, with each case showing final emission levels above 1 ppm. Notably, Case 20 stands out with MEA emissions of 5.8 ppm, which is significantly reduced when doubling the height from 2 m to 4 m. Further increases in water wash height do not appear to substantially affect the emission levels, as the emissions remain constant even as the height varies between 4 to 8 m.

Table 27: The total height of the water wash and the emissions before and after the water wash for cases 19-23.

	Total height [m]	Emissions [ppm]	
	WW1	Before WW	After WW
Case 19	4.8	414	1.2
Case 20	2	414	5.8
Case 21	4	414	1.2
Case 22	6	414	1.2
Case 23	8	414	1.2

The vapor temperature profile for the absorber in this particular case study resembles that of the case study featuring two water wash sections. The reason behind this similarity is that the process modifications implemented in this case study only affects the water wash section, thereby leaving the temperature unaffected. Consequently, the temperature profiles leading up to the water wash section exhibit similar behavior. However, the temperature profiles for the absorber for this case study can be found in Figure 35 in Appendix J. In Figure 30 the vapor temperature profiles in the water wash section for Cases 19-23 is shown. In every case, the temperature at the top of the water wash column is the same with the exception of Case 23. Case 23 also stands out in regards to the inlet temperature, which differs from the other cases performed in this case study. Interestingly, despite this discrepancy, there seems to be no apparent reason or correlation between the observed temperature variation and the emissions data.

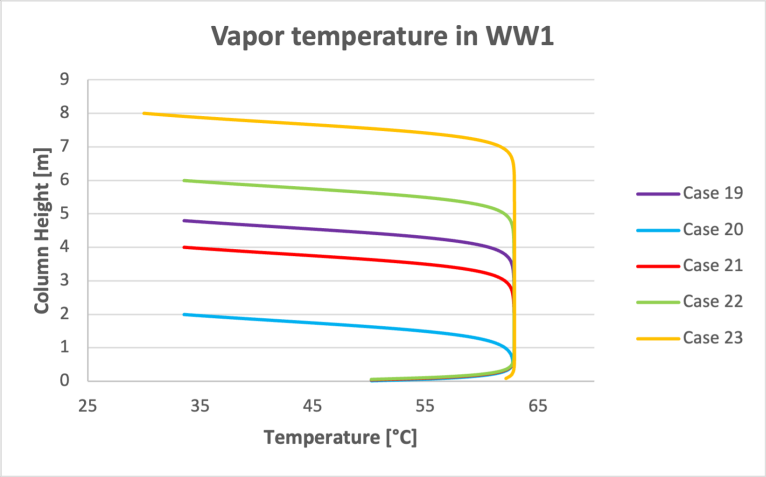

Figure 30: Vapor temperature profiles in the water wash section for Cases 19-23.

6.7.2 Case 24 and 25

The results for Case 19, 24, and 25 are presented in Table 28. The table shows the total height of the water wash, the emissions before the water wash, labeled as "GasAbsTreat", and the emissions after the water wash labeled as "SweetGas". These streams can be seen in Figure 5. The simulations for Cases 24 and 25 were done using CO2SIM due to issues with running the simulations on Matlab. The same issues were observed in the same case study with two water wash stages. As a result, the accuracy of the results may not be as good as those obtained from the other case studies. Therefore, the results for Case 19 were obtained from CO2SIM are included to provide a more precise comparison. In Case 24 the water entering the water wash section contains 0.5 wt% MEA, while in Case 25 the water contains 1 wt% MEA. This water stream is labeled as "Water" in Figure 5.

As shown in Table 28, increasing the amine concentration in the water entering the water wash results in higher emissions. This behavior is consistent with the observations from the case study with two water wash sections, and were expected since more MEA in the process leads to higher MEA emissions.

Table 28: The flow rate and the emissions before and after the water wash for Case 19, 24 and 25.

	Concentration [wt%]	Emissions [ppm]	
	Water	Before WW	After WW
Case 19	0.1	376	0.8
Case 24	0.5	375	2.0
Case 25	1	374	3.4

6.8 Comparison of using one and two WW sections

This section will discuss and compare the use of two versus one water wash stage in the process. In the case study with one water wash section, two parameters were investigated; the height of the water wash and the amine concentration in water entering the water wash section. These cases will therefore be compared with the cases investigating the same parameters but for the process with two water wash sections.

Table 29 presents the results for the case studies performed with one and two water wash sections. The results given are the MEA emissions in the stream labeled as "SweetGas" in both cases. It can be observed from the Table 29 that having only one water wash section in the process gives significantly higher emissions than having two water wash sections. In this thesis, the objective was to keep the volatile emissions under 1 ppm. By using one water wash section, the objective was not achieved despite how high the packing height was. By using two water wash section, the objective was achieved when using two water wash sections with a height higher than 2 m each. For the case with MEA emissions in the water entering the water wash sections, the volatile emissions was under 1 ppm for the case with only a small MEA present in the water. When the MEA was increased to 0.5 wt% MEA, the case with one water wash had a significant increase in emissions. The case with two water wash sections also showed an increase, but not nearly as high as the case with one water wash. The same observation was made for the case with 1 wt% MEA.

The results were expected to be the same for a case with one water wash section and a case with two water wash sections, provided that the temperature and total packing height were the same. The additional water wash section would mainly provide redundancy and extra capacity, but was not expected to significantly affect the overall performance of the system as long as the operating conditions were similar. In theory, the number of water wash sections would not be the determining factor in the performance of the system, but rather the other variables such as temperature and packing height would have a greater impact. Although the second water wash section would serve as a backup and add extra capacity, it should not substantially change the expected outcome as observed.

One of the reasons to why having two water wash sections reduces emissions more than one water wash can for instance be that two water wash sections are more effective. Two water wash sections can allow for better removal of impurities from the gas stream, as the first water wash section removes the majority of the impurities, while the second section ensures that any remaining impurities are removed. As mentioned, having two water wash sections provide higher capacity. Even though the capacity was not expected to affect the outcome, it may have had an impact on the results.

Table 29: Comparison of the results for the case study with one water wash section and the case studies with two water wash sections.

	1 WW	2 WW
Total height [m]	Emissions [ppm]	Emissions [ppm]
2	5.8	4.64
4	1.2	0.04
4.8	1.2	0.008
6	1.2	$9.2 \cdot 10^{-4}$
8	1.2	$6.4 \cdot 10^{-5}$
MEA concentration in water [wt%]	Emissions [ppm]	Emissions [ppm]
0.1	0.8	0.010
0.5	2.0	0.027
1	3.4	0.051

6.9 Final Case

This section presents the findings from the case studies performed, concluding in a final study. The final case study combines all the relevant information regarding emissions, focusing on identifying the optimal water wash configuration and the corresponding operating parameters that resulted in the lowest MEA emissions.

Regarding the water wash geometry, it was observed that a higher water wash height resulted in significantly reduced emissions. However, it is important to consider the associated increase in cost with higher columns. Since the Tiller plant used as a reference in this study is relatively small, a water wash height of 8 m would be impractical. Therefore, a water wash height of 6 m was chosen for the final case study. This configuration yielded a 88% reduction in emissions compared to the base case, which utilized a water wash height of 4.8 m. While the initial objective was to maintain the volatile emissions below 1 ppm, this target has was met by using water wash sections with a total height of 4 m. However, it is advantageous to strive for further reduction in emissions if possible. It was also found that using two water washes worked more effectively than only using one water wash.

The water entering the water wash stage had a temperature of 30°C in the base case. By varying this temperature from 20-40°C, it was found that the lower temperatures gave less emissions. However, operating at water temperatures of 20-25°C is not feasible in warmer climates, such as in central Europe. Therefore, it was chosen to keep the water temperature at 30 °C. The same observation was made for the lean amine temperature, that increasing the temperature would give higher amount of emissions. In the base case, the lean amine temperature was set to 40 °C. By decreasing this temperature to 30 °C, the emissions had a reduction of 37.5%. At 35 °C, the emissions had a reduction of 25%. Although a temperature of 30°C gave less emissions than 35 °C, the temperature chosen for the lean amine was set to be 35 °C in the final case study. This was because it was observed that at 35 °C the simulation converged better than at 30 °C.

In the base case, the water entering the water wash stage had a temperature of 30 °C. By varying this temperature within the range of 20-40 °C, it was discovered that lower temperatures resulted in reduced emissions. It was decided to maintain the water temperature at 30 °C, due to the complications that low temperatures entail in relation to countries with warmer climates. Similar observations were made for the lean amine temperature, where increasing the temperature led to higher emissions. Initially, the lean amine temperature in the base case was set at 40 °C. By lowering this temperature to 30 °C, emissions were reduced by 37.5%. At 35 °C, a reduction of 25% was achieved. Although a temperature of 30°C resulted in lower emissions than 35 °C, 35 °C was chosen for the lean amine temperature in the final case study. This decision was based on the observation that the simulation converged more effectively at 35 °C compared to 30 °C.

The flow rate in this final case study was decided to be kept at 20 kmol/h. The reason for this is because it is desired to use the lowest flow rate that still wets the packing. By doubling the flow rate to 40 kmol/h it was observed that an emissions reduction of 50% was achieved. However, high flow rate is generally not desirable despite resulting in lower emissions. This was discussed in Section 6.5.

The amine concentration was kept constant compared to the base case. While the case study with increased amine concentration in the water entering the water wash was performed to investigate if the emissions were concentration dependent and not only temperature dependent, it was determ-

ined that these results were not relevant for the final case study. It was anticipated that higher concentrations of MEA would lead to increased emissions. Therefore, in the final case study, only a small amount of MEA was added to facilitate system convergence. The capture rate was set to be 95%. To achieve this, the reboiler duty was adjusted to 45 kJ/s and the lean flow rate was 24 kmol/h. The other operating conditions were the same as for the base case.

Table 30: Final Case results.

	Final Case
Water Wash Total Height [m]	6
Water Wash Diameter [m]	0.2
L/G [kg/kg]	2.3
Reboiler Duty [MJ]	526
Emissions before water washes [ppm]	**480**
Emissions between water washes [ppm]	**1.8**
Emissions after final water wash [ppm]	$\mathbf{9.2 \cdot 10^{-4}}$
Lean Loading [mol CO_2/mol MEA]	0.16
Rich Loading [mol CO_2/mol MEA]	0.51

Table 30 present the results obtained for the final case. It can be observed that the results for the final case are identical as those of Case 3. This shows that a mere reduction of 5 °C in the lean amine temperature had a minimal impact on the emissions, whereas modifying the water wash height proved to be significantly more effective. In Case 14, only one parameter was modified, namely the lean amine temperature set at 35 °C. The results showed a 25% reduction in MEA within the stream after the final water wash stage. Therefore, it was anticipated that the emissions would be further diminished in the final case when combining the lower lean amine temperature with the increased water wash height.

By discussing the various parameters and findings to determine the optimal final case, it was noticed that the initial base case worked well in regards to the emissions. In the final case, several parameters were deliberately maintained at constant values based on the base case. This was because in the base case, these parameters already represented a balanced compromise between minimizing emissions and ensuring smooth process operations.

6.10 Summary of the Case Studies

This section will present a summary of the case studies performed in this thesis. The first case study focused on examining the impact of water wash height on emissions. The result of this case study clearly showed that higher water wash sections led to lower emissions. By doubling the water wash height from 2 m to 4 m, a reduction of 99.0511% was achieved in the final stream leaving the water wash section. Nevertheless, it is important to note that increasing the column height involves an associated increase in cost. To determine the optimal water wash, it is important to consider the entire amine scrubbing process comprehensively. Investigating the process as a whole allows for a thorough evaluation of various factors that may influence the selection of water wash height, such as the desired emission reduction targets, the cost associated with increasing column height, and any potential trade-offs between emission reduction and operational efficiency.

Two case studies were performed exploring the effects of temperature variations in different aspects of the process. One focused on water temperature, while the other investigated lean amine temperature. It was observed in both cases that as the temperature increased, the emissions also increased. However, even at the highest temperatures examined, the volatile emissions remained below 1 ppm. These results are deemed satisfactory, given that the objective of this thesis was to maintain volatile emissions below the 1 ppm threshold.

The flow rate was investigated to see if varying the flow rate would significantly affect the emissions. The findings indicated a notable decrease in emissions with an increase in flow rate. However, it is important to consider that a high flow rate will lead to higher costs and challenges in terms of maintenance and control. Conversely, a low flow rate not only leads to increased emissions, but also hinders the smooth operation of the process, as it is important for the packing to be adequately wetted by a sufficiently high flow rate. Therefore, it is desired to find the balance between high and low flow rate to optimize the process effectively.

The case study performed with an increased amount of MEA in the water entering the water wash section was conducted to investigate whether the emissions were dependent on the concentration. It was anticipated that a higher initial amount of MEA in the water would result in increased emissions, and the findings confirmed this expectation. A linear relationship between MEA concentration and emissions was observed when plotting the two variables, which indicates that the emissions are concentration dependent.

The last case study involved removing one water wash stage. The results showed a substantial increase in emissions when only one water wash stage was used, where every study performed resulted in volatile emissions exceeding 1 ppm. In contrast, using two water wash stages consistently yielded volatile emissions below 1 ppm, except for Case 1.

A final case was provided based on the information gathered throughout this thesis. In the final case, the only parameters modified from the base case were the water wash height and the lean amine temperature. The results obtained from the final case showed that the emissions in this case were the same as for Case 3, where the sole parameter changed was the water wash height. Surprisingly, adjusting the lean amine temperature from 40 to 35 °C did not appear to have any noticeable effect on the emissions. However, in Case 14, where the sole parameter changed was the lean amine temperature set at 35 °C, a reduction of 25% in emissions was observed compared to the base case with a temperature of 40 °C. Consequently, it was anticipated that combining a lower lean amine temperature with Case 3's higher water wash height would result in even lower emissions.

The expected results did not align with the observed results. Another notable observation is that some of the parameters studied in this thesis kept the same value as the ones used in the base case. This indicates that the water wash sections in the base case were initially well-optimized and required minimal modifications. The decision to maintain these values was because the parameters used in the base case achieved both low emissions and smooth process operations.

A consistent trend noted throughout almost every case study performed in this thesis was the lack of change in energy requirements despite modifications made to the process. This recurring pattern strengthens the understanding that the emission regulation methods implemented do not have a significant impact on the energy numbers. It suggests that adjustments in the water wash, despite their potential influence on emissions, do not significantly alter the energy requirements of the process.

7 Conclusion and Further Work

The main objective of this thesis was to investigate how the water wash design and operating conditions affected the amine emissions in an amine scrubbing process, and optimize the water wash to minimize these emissions. By exploring the effects of various parameters, including water wash height, water temperature, lean amine temperature, flow rate, increased amine concentration in the water, and the removal of a water wash stage, valuable insights were gained. The work involved performing several case studies, in which the parameters mentioned were varied. The simulation tool used in this thesis was CO2SIM, an in-house process simulation program developed at SINTEF.

Increasing the height of the water wash was discovered to have a significant impact on reducing emissions. However, it is important to consider the overall amine scrubbing process when determining the optimal water wash height, as increasing column height incurs additional costs. Additionally, increasing the flow rate contributed to a decrease in emissions. Similar to the water wash height, it is crucial to strike a balance between high and low flow rates to optimize the process effectively and minimize amine emissions, taking into account the associated cost implications.

The findings also unveiled the impact of lean amine temperature and water temperature on emissions. It was observed that higher temperatures resulted in increased emissions, whereas lower temperatures exhibited a reduction in emissions. However, it is important to consider practical constraints, especially in countries with warmer climates, where operating with low water temperatures may not be feasible. Furthermore, excessively low lean amine temperature can compromise the effectiveness of the process. These insights highlights the importance of precise control over these parameters to effectively mitigate amine emissions while taking into account operational limitations and maintaining process efficiency.

Another observation made was that increasing the amine concentration in the water entering the second water wash stage led to increased emissions. While this outcome was anticipated, it remains noteworthy that emissions are not only dependent on temperature but also on the concentration. In the last case study performed, one water wash section was removed to investigate the impact of using one versus two water wash stages. The results showed a substantial increase in emissions when using a single water wash stage in comparison to the use of two water wash stages. This finding implies that using two water wash stages are more effective in mitigating emissions and achieving optimal emission reduction.

In the final study, considering all the information gathered throughout the thesis, modifications were made to the water wash height and lean amine temperature. Notably, it was found that the lean amine temperature had a limited impact on emissions reduction compared to the water wash height. Therefore, focusing on optimizing the water wash height can be a more effective approach for minimizing amine emissions in the process. Furthermore, the base case used in this study was found to be a favorable initial process in regards to the emissions. This indicates that the existing system already had a relatively efficient design, which serves as a valuable reference for future optimization efforts.

It is worth noting that the energy consumption remained unaffected by the modifications made to the water wash. This implies that the suggested optimizations can be implemented without compromising energy efficiency, which is a crucial consideration for sustainable and cost-effective operations.

In summary, this thesis provides valuable insights into optimizing the water wash section of the amine scrubbing process to reduce amine emissions. The findings highlight the importance of controlling parameters such as water wash height, water temperature, lean amine temperature, flow rate, amine concentration, and the number of water wash stages. These findings contribute to advancing the understanding of amine scrubbing processes and provide practical guidance for future work seeking to minimize amine emissions effectively.

7.1 Further work

This section will provide some suggestions for future work to further advance the optimization of the water wash section in the amine scrubbing process and continue the efforts in reducing amine emissions.

One suggestion for further work is the optimization of other process parameters. Investigating the effects of additional variables, such as different solvents or additives, variations in amine types or concentrations, changes in the L/G ratio, or modifications to the absorber column design, can provide valuable insights into further optimizing the amine scrubbing process and reducing emissions. Understanding the impact of these parameters will enhance the overall efficiency of the process.

To assess the cost-effectiveness and sustainability of the proposed optimizations, a economic and environmental analysis can be performed. Evaluating factors such as capital and operating costs, energy consumption, greenhouse gas emissions, and potential environmental impacts associated with the optimized water wash section will provide important insights for decision-making.

It could also be beneficial to investigate the robustness of the proposed modifications by examining their efficacy with different types of flue gas. The case studies performed in this thesis focused on flue gas derived from a coal-fired power plant. However, exploring the effects of the implemented modifications done in this thesis with for instance natural gas can provide valuable insights. These investigations would determine if the changes have similar effects in different flue gas compositions, making the findings more useful and widely applicable.

By pursuing these research directions, a comprehensive understanding of the optimization of the water wash section in the amine scrubbing process can be achieved. These studies will contribute to the ongoing efforts in reducing amine emissions and advancing the field of emission control technologies such as water wash sections.

References

[1] Hallvard F. Svendsen, Erik T. Hessen, and Thor Mejdell. Carbon dioxide capture by absorption, challenges and possibilities. *Chemical Engineering Journal*, 171:718–724, 2011. URL: https://www.sciencedirect.com/science/article/pii/S1385894711000416.

[2] Ugochukwu E. Aronu, Shahla Gondal, Erik T. Hessen, Tore Haug-Warberg, Ardi Hartono, Karl A. Hoff, and Hallvard F. Svendsen. Solubility of co2 in 15, 30, 45 and 60 mass% mea from 40 to 120c and model representation using the extended uniquac framework. *Chemical Engineering Science*, 66:6393–6406, 2011. URL: https://www.sciencedirect.com/science/article/pii/S0009250911006117.

[3] Ralf Notz, Hari Prasad Mangalapally, and Hans Hasse. Post combustion co2 capture by reactive absorption: Pilot plant description and results of systematic studies with mea. *International Journal of Greenhouse Gas Control*, 6:84–112, 2008. URL: https://www.sciencedirect.com/science/article/pii/S1750583611002143.

[4] Kangkang Li, Ashleigh Cousins, Hai Yu, Paul Feron, Moses Tade, Weiliang Luo, and Jian Chen. Systematic study of aqueous monoethanolamine-based co2 capture process: model development and process improvement. *Energy Science & Engineering*, 4:23–39, 2016. URL: https://www.sciencedirect.com/science/article/pii/S1750583611000387.

[5] E. David, V. Stanciu, C. Sandru, A. Armeanu, and V. Niculescu. Exhaust gas treatment technologies for pollutant emission abatement from fossil fuel power plants. *National Research Institute of Cryogenics and Isotopic Technologies*, pages 1–10, 2007. URL: https://www.witpress.com/Secure/elibrary/papers/SDP07/SDP07088FU2.pdf.

[6] I.P.C.C. Climate change 2014 synthesis report summary for policymakers, 2014. URL: https://www.ipcc.ch/site/assets/uploads/2018/02/AR5_SYR_FINAL_SPM.pdf.

[7] Stephen Montzka. The noaa annual greenhouse gas index, 2022. URL: https://gml.noaa.gov/aggi/aggi.html.

[8] National Grid. What are greenhouse gases? URL: https://www.nationalgrid.com/stories/energy-explained/what-are-greenhouse-gases.

[9] UNFCCC. The paris agreement, 2015. URL: https://unfccc.int/process-and-meetings/the-paris-agreement/the-paris-agreement.

[10] Bert Metz, Ogunlade Davidson, Heleen Coninck, Manuela Loos, and Leo Meyer. Ipcc special report on carbon dioxide capture and storage. *IPCC*, 2005. URL: https://www.ipcc.ch/report/carbon-dioxide-capture-and-storage/.

[11] Paul H. M. Feron. *1 - Introduction*. Woodhead Publishing, 2016. URL: https://www.sciencedirect.com/book/9780081005149/absorption-based-post-combustion-capture-of-carbon-dioxide.

[12] Tabbi Wilberforce, Ahmad Baroutaji, Bassel Soudan, Abdul Hai Al-Alami, and Abdul Ghani Olabi. Outlook of carbon capture technology and challenges. *Science of the Total Environment*, 657:56–72, 2019. URL: https://www.sciencedirect.com/science/article/pii/S004896971834779X.

[13] Neda Razi, Hallvard F. Svendsen, and Olav Bolland. The impact of design correlations on rate-based modeling of a large scale co_2 capture with mea. *Energy Procedia*, 37:1977–1986, 2013. URL: https://www.sciencedirect.com/science/article/pii/S1876610213003214.

[14] Renjie Shao and Aage Stangeland. Amines used in co_2 capture - health and environmental impacts. *The Bellona Foundation*, pages 1–49, 2009. URL: https://bellona.org/assets/sites/3/2015/06/fil_Bellona_report_September__2009_-_Amines_used_in_CO2_capture-11.pdf.

[15] Hammad Majeed and Hallvard F. Svendsen. Effect of water wash on mist and aerosol formation in absorption column. *Chemical Engineering Journal*, 333:636–648, 2017. URL: https://www.sciencedirect.com/science/article/pii/S1385894717316236.

[16] Mai Bui, Claire S. Adjiman, André Bardow, Edward J. Anthony, Andy Boston, Solomon Brown, Paul S. Fennell, Sabine Fuss, Amparo Galindo, Leigh A. Hackett, Jason P. Hallett, Howard J. Herzog, George Jackson, Jasmin Kemper, Samuel Krevor, Geoffrey C. Maitland, Michael Matuszewski, Ian S. Metcalfe, Camille Petit, Graeme Puxty, Jeffrey Reimer, David M. Reiner, Edward S. Rubin, Stuart A. Scott, Nilay Shah, Berend Smit, J.P. Martin Trusler, Paul Webley, Jennifer Wilcox, and Niall Mac Dowell. Carbon capture and storage (ccs): the way forward. *Energy Environ. Sci.*, 11:1062–1176, 2018. URL: https://pubs.rsc.org/en/content/articlehtml/2018/ee/c7ee02342a.

[17] Jon Gibbins and Chalmers Hannah. Carbon capture and storage. *Energy Policy*, 36:4317–4322, 2008. URL: https://www.sciencedirect.com/science/article/pii/S0301421508004436.

[18] Global CCS Institute. Global status of ccs. URL: https://status22.globalccsinstitute.com/2022-status-report/global-status-of-ccs/.

[19] Mohamed Kanniche, René Gros-Bonnivard, Philippe Jaud, Jose Valle-Marcos, Jean-Marc Amann, and Chakib Bouallou. Pre-combustion, post-combustion and oxy-combustion in thermal power plant for co2 capture. *Applied Thermal Engineering*, 30:53–62, 2010. URL: https://www.sciencedirect.com/science/article/pii/S1359431109001471.

[20] Office of Fossil Energy and Carbon Management. Pre-combustion carbon capture research. URL: https://www.energy.gov/fecm/science-innovation/carbon-capture-and-storage-research/carbon-capture-rd/pre-combustion-carbon.

[21] Cong Chao, Yimin Deng, Jan Baeyens, and Xianfeng Fan. Post-combustion carbon capture. *Renewable and Sustainable Energy Reviews*, 138, 2021. URL: https://www.sciencedirect.com/science/article/pii/S1364032120307760.

[22] DXP. Pre-combustion vs. post-combustion carbon capture technologies. URL: https://ifsolutions.com/pre-combustion-vs-post-combustion-carbon-capture/.

[23] Bryce Dutcher, Maohong Fan, and Armistead G. Russell. Amine-based co2 capture technology development from the beginning of 2013 - a review. *Appl. Mater. Interfaces*, 7:2137–2148, 2015. URL: https://pubs.acs.org/doi/10.1021/am507465f.

[24] Eirik F Da Silva. Formation of nitrosamines and alkyldiazohydroxides in the gas phase: the ch3nh + no reaction revisited. *Environmental Science & Technology*, 47:7766–7772, 2013. URL: https://pubs.acs.org/doi/full/10.1021/es401591n.

[25] James G. Speight. 3 - unconventional gas. *Natural Gas (Second Edition)*, pages 59–98, 2019. URL: https://www.sciencedirect.com/topics/earth-and-planetary-sciences/flue-gas.

[26] G. Puxty and M. Maeder. 2 - the fundamentals of post-combustion capture. *Absorption-Based Post-Combustion Capture of Carbon Dioxide*, pages 13–33, 2016. URL: https://www.sciencedirect.com/book/9780081005149/absorption-based-post-combustion-capture-of-carbon-dioxide.

[27] Andrew J. Sexton. Amine oxidation in co_2 capture process. pages 1–286, 2008.

[28] Udara S. P. R. Arachchige and Morten C. Melaaen. Selection of packing material for gas absorption. *European Journal of Scientific Research*, pages 117–126, 2012. URL: https://openarchive.usn.no/usn-xmlui/bitstream/handle/11250/2438548/ArachchigeEJSR87_1.pdf?sequence=1&isAllowed=y.

[29] H. Kolderup, E. da Silva, T. Mejdell, A. Tobiesen, K. Haugen, K. A. Hoff, K. Josefsen, T. Strøm, O. Furuseth, K. F. Hanssen, H. Wirsching, T. Myhrvold, and K. Johnsen. Emission reducing technologies. *SINTEF Materials and Chemistry*, pages 1–123, 2011. URL: https://gassnova.no/app/uploads/sites/6/2019/10/emissionredtechnologies_sintef.pdf.

[30] Barath Baburao and Michael W. Pontbriand. Water wash method and system for a carbon dioxide capture process. *Canadian Intellectual Property Office*, pages 1–25, 2012. URL: https://patents.google.com/patent/CA2786997C/en.

[31] Mohammed Isah Yakub, Mohamed Samah, and Sule Umar Danladi. Technical and economic considerations of post-combustion carbon capture in a coal fired power plant. *International Journal of Advances in Engineering & Technology*, 7:1549–1581, 2014. URL: https://www.researchgate.net/publication/274075209_Technical_and_economic_considerations_of_post-combustion_carbon_capture_in_a_coal_fired_power_plant.

[32] Hidetaka Yamada. Amine-based capture of co2 for utilization and storage. *Polymer Journal*, 53:93–102, 2021. URL: https://www.nature.com/articles/s41428-020-00400-y.

[33] A. B. Rao and E. S. Rubin. A technical, economic, and environmental assessment of amine-based co2 capture technology for power plant greenhouse gas control. *Environmental Science Technology*, 36:4467–4475, 2002. URL: https://pubs.acs.org/doi/10.1021/es0158861.

[34] Xiaomei Wu, Yunsong Yu, Zhen Qin, Zhang, and Zaoxiao. The advances of post-combustion co2 capture with chemical solvents: Review and guidelines. *Energy Procedia*, 63:1339–1346, 2014. URL: https://www.sciencedirect.com/science/article/pii/S1876610214019584.

[35] Bryce Dutcher, Maohong Fan, and Armistead G. Russell. Amine-based co2 capture technology development from the beginning of 2013 - a review. *ACS Appl Mater Interfaces*, 7:48–2137, 2015. URL: https://pubmed.ncbi.nlm.nih.gov/25607244/.

[36] Y. S. Yu, Y. Li, H. F. Lu, Yan. L. W., and Z. X. Zhang. Performance improvement for chemical absorption of co2 by global field synergy optimization. *International Journal of Greenhouse Gas Control*, 5:649–658, 2011. URL: https://www.sciencedirect.com/science/article/pii/S1750583611000387.

[37] Paul H. M. Feron, Ashleigh Cousns, Kaigi Jiang, Rongrong Zhai, and Monica Garcia. An update of the benchmark post-combustion co2-capture technology. *Fuel*, 273, 2020. URL: https://www.sciencedirect.com/science/article/pii/S0016236120307717f.

[38] Global Cement and Concrete Association. Amine-based post-combustion capture. URL: https://gccassociation.org/cement-and-concrete-innovation/carbon-capture-and-utilisation/amine-based-post-combustion-capture/.

[39] M. Azzi and S. White. 20 - emissions from amine-based post-combustion co_2 capture plants. *Absorption-Based Post-combustion Capture of Carbon Dioxide*, pages 487–504, 2016. URL: https://www.sciencedirect.com/science/article/pii/B9780081005149000202.

[40] Hammad Majeed, Hanna Knuutila, Magne Hillestad, and Hallvard F. Svendsen. Effect of amine volatility on aerosol droplet development in absorption columns. *Energy Procedia*, 114:977–986, 2017. URL: https://www.sciencedirect.com/science/article/pii/S1876610217314194.

[41] Abhoyjit S. Bhown and Brice C. Freeman. Analysis and status of post-combustion carbon dioxide capture technologies. *Environ. Sci. Technol.*, 45:8624–8632, 2011. URL: https://pubs.acs.org/doi/full/10.1021/es104291d.

[42] Ida M. Bernhardsen and Hanna K. Knuutila. A review of potential amine solvents for co2 absorption process: Absorption capacity, cyclic capacity and pka. URL: https://ntnuopen.ntnu.no/ntnu-xmlui/bitstream/handle/11250/2469408/Manuscript_InPress.pdf?sequence=2.

[43] Susanna S. Uhre. The effect of the aborber design and operating conditions on the mea emissions and energy consumption in an absorption-based carbon capture plant. *Master Thesis*, pages 1–145, 2021.

[44] Shaukat A. Mazari, Brahim Si Ali, Badrul M. Jan, Idris Mohamed Saeed, and S. Nizamuddin. An overview of solvent management and emissions of amine-based co2 capture technology. *International Journal of Greenhouse Gas Control*, 34:129–140, 2015. URL: https://www.sciencedirect.com/science/article/pii/S175058361400396X.

[45] Fatemah Yazdipour, Mehdi A. Torkmahalleh, Mohammahmahdi Kamyabi, and Rahmat Sotudeh-Gharebagh. On solvent losses in amine absorption columns. *ACS Sustainable Chem. Eng.*, 10:11154–11164, 2022. URL: https://pubs.acs.org/doi/full/10.1021/acssuschemeng.2c02179.

[46] Purvil Khakharia, Jan Mertens, Thijs J. H. Vlugt, and Earl Goetheer. Predicting aerosol based emissions in a post combustion co2 capture process using an aspen plus model. *Energy Procedia*, 63:911–925, 2014. URL: https://www.sciencedirect.com/science/article/pii/S187661021401916X.

[47] Thu Nguyen, Marcus Hilliard, and Gary T. Rochelle. Amine volatility in co2 capture. *International Journal of Greenhouse Gas Control*, 4:707–715, 2010. URL: https://www.sciencedirect.com/science/article/pii/S1750583610001003.

[48] Ningtong Yi, Mengxiang Fang, Wentao Di, Zhixiang Xia, Tao Wang, and Qinhui Wang. Aerosol emissions of amine-based co2 absorption system: Effects of condensation nuclei and operating conditions. *Environ. Sci. Technol.*, 55:5152–5160, 2021. URL: https://pubs.acs.org/doi/10.1021/acs.est.0c04630.

[49] Eirik F. da Silva, Herman Kolderup, Earl Goetheer, Kai W. Hjarbo, Arjen Huizinga, Purvil Khakaria, Ilse Tuinman, Thor Mejdell, Kolbjørn Zahlsen, Kai Vernstad, Astrid Hyldbakk, Torunn Holten, Hanne M. Kvamsdal, Peter van Os, and Aslak Einbu. Emission studies from a

co2 capture pilot plant. *Energy Procedia*, 37:778–783, 2013. URL: https://www.sciencedirect.com/science/article/pii/S187661021300177X.

[50] David Hosansky. Flue gas treatment, 2014. URL: https://www.britannica.com/technology/flue-gas-treatment.

[51] Gas Vessel. Natural gas vs. coal - a positive impact on the environment, 2020. URL: https://www.gasvessel.eu/news/natural-gas-vs-coal-impact-on-the-environment/.

[52] Zhichao Li, Yang Wang, Yongqi Lu, and Pratim Biswas. Investigation of aerosol and gas emissions from a coal-fired power plant under various operating conditions. *Journal of the Air & Waste Management Association*, 69:34–46, 2018. URL: https://www.tandfonline.com/doi/full/10.1080/10962247.2018.1503981.

[53] Purvil Khakharia, Leonie Brachert, Jan Mertens, Christopher Anderlohr, Arhen Huizinga, Eva Sanchez Fernandez, Bernd Schallert, Karlheinz Schaber, Thijs J. H. Vlugt, and Earl Goetheer. Understanding aerosol based emissions in a post combustion co2 capture process: Parameter testing and mechanisms. *International Journal of Greenhouse Gas Control*, 34:63–74, 2015. URL: https://www.sciencedirect.com/science/article/pii/S1750583615000080.

[54] Finn Andrew Tobiesen, Hallvard F. Svendsen, and Olav Juliussen. Experimental validation of a rigorous absorber model for co2 postcombustion capture. *Dept. of Chemical Engineering, NTNU and SINTEF*, 53:846–865, 2007. URL: https://aiche.onlinelibrary.wiley.com/doi/full/10.1002/aic.11133.

[55] Finn Andrew Tobiesen, Olav Juliussen, and Hallvard F. Svendsen. Experimental validation of a rigorous desorber model for co2 post-combustion capture. *Chemical Engineering Science*, 63:2641–2656, 2008. URL: https://www.sciencedirect.com/science/article/pii/S0009250908000754.

[56] Hammad Majeed and Hallvard F. Svendsen. Characterization of aerosol emissions from co2 capture plants treating various power plant and industrial flue gases. *International Journal of Greenhouse Gas Control*, 74:282–295, 2018. URL: https://www.sciencedirect.com/science/article/pii/S1750583617309751.

[57] Marcin Stec, Adam Tatarczuk, Lucyna Więcław-Solny, Aleksander Krótki, Tomasz Spietz, Andrzej Wilk, and Dariusz Śpiewak. Demonstration of a post-combustion carbon capture pilot plant using amine-based solvents at the Łaziska power plant in poland. *Clean Technologies and Environmental Policy*, 18:151–160, 2016. URL: https://link.springer.com/article/10.1007/s10098-015-1001-2.

[58] Jia-Lin Kang, Yue Zhang, Steven Fulk, and Gary T. Rochelle. Modeling amine aerosol growth in the absorber and water wash. *Energy Procedia*, 114:959–976, 2017. URL: https://www.sciencedirect.com/science/article/pii/S1876610217314170.

[59] Steven M. Fulk and Gary T. Rochelle. Modeling aerosols in amine-based co_2 capture. *Energy Procedia*, 37:1706–1719, 2013. URL: https://www.sciencedirect.com/science/article/pii/S1876610213002890.

[60] Claudio Madeddu, Maddimiliano Errico, Davide Porcu, and Roberto Baratti. Solvent recovery system for a co_2-mea reactive absorption-stripping plant. *Chemical Engineering Transactions*, 74, 2019. URL: https://www.aidic.it/cet/19/74/135.pdf.

[61] Aslak Einbu. Co2sim (flytskjema simulator for co2 absorptions prosesser). URL: https://www.sintef.no/programvare/co2sim-flytskjema-simulator-for-co2-absorpsjons-pr/.

[62] H. F Svendsen, H. Majeed, H. Knuutila, M. Hillestad, S. Evjen, T. Mejdell, A. Einbu, K. W. Hjarbo, G. Haugen, and K. A. Hoff. Aerosol growth in co2 absorption with mea, modelling and comparison with experimental results. *International Journal of Greenhouse Gas Control*, 109, 2021. URL: https://www.sciencedirect.com/science/article/pii/S1750583621001420.

[63] Trine Witzøe. Simulation of pilot data with aspen plus. *Master Thesis*, pages 1–178, 2015.

[64] Ingeborg H. H. Nesse. Researching the behaviour of aerosol emissions in an amine scrubbing system. *Master Thesis*, pages 1–156, 2021.

[65] Fanzhi Meng, Yuan Meng, Tongyao Ju, Siyu Han, Li Lin, and Jianguo Jiang. Research progress of aqueous amine solution for co2 capture: A review. *Renewable and Sustainable Energy*, 168, 2022. URL: https://www.sciencedirect.com/science/article/pii/S1364032122007845.

[66] M Eviani, Hary Deviantio, P. Widiatmoko, I. Sukmana, Husna Fitri, and F. Yusupandi. Simulation of co_2 capture process for coal based power plant in south sumatra indonesia. *Materials Science and Engineering*, 1143, 2021. URL: 012047.10.1088/1757-899X/1143/1/012047.

[67] Arthur L. Kohl and Richard B. Nielsen. *Gas Purification*. Gulf Professional Publishing, 1997.

Appendix

A Data used for VLE validation

Table 31: The total pressure calculated and the total pressure used in the VLE validation for 40 °C.

P_{tot} calculated	P_{tot} used in CO2SIM
6.49	6.49
6.42	6.42
6.39	6.39
6.33	6.33
6.33	6.33
6.31	6.31
6.31	6.90
6.32	6.90
6.32	6.90
6.34	7.10
6.40	7.70
6.52	8.10
6.52	8.20
6.59	8.40
6.67	8.90
7.58	11.40
8.10	13.80

Table 32: The total pressure calculated and the total pressure used in the VLE validation for 60 °C.

P_{tot} calculated	P_{tot} used in CO2SIM
17.61	17.61
17.51	17.51
17.41	17.41
17.26	17.26
17.18	18.10
17.12	18.50
17.13	19.10
17.29	20.20
18.94	29.30

Table 33: The total pressure calculated and the total pressure used in the VLE validation for 80 °C.

P_{tot} calculated	P_{tot} used in CO2SIM
42.02	42.02
41.91	41.91
41.76	41.76
41.55	41.55
41.41	41.41
41.19	42.50
41.03	43.50
41.07	45.50
41.49	49.50
41.55	49.50

B Flowsheet of the pilot plant in Notz et al. (2012)

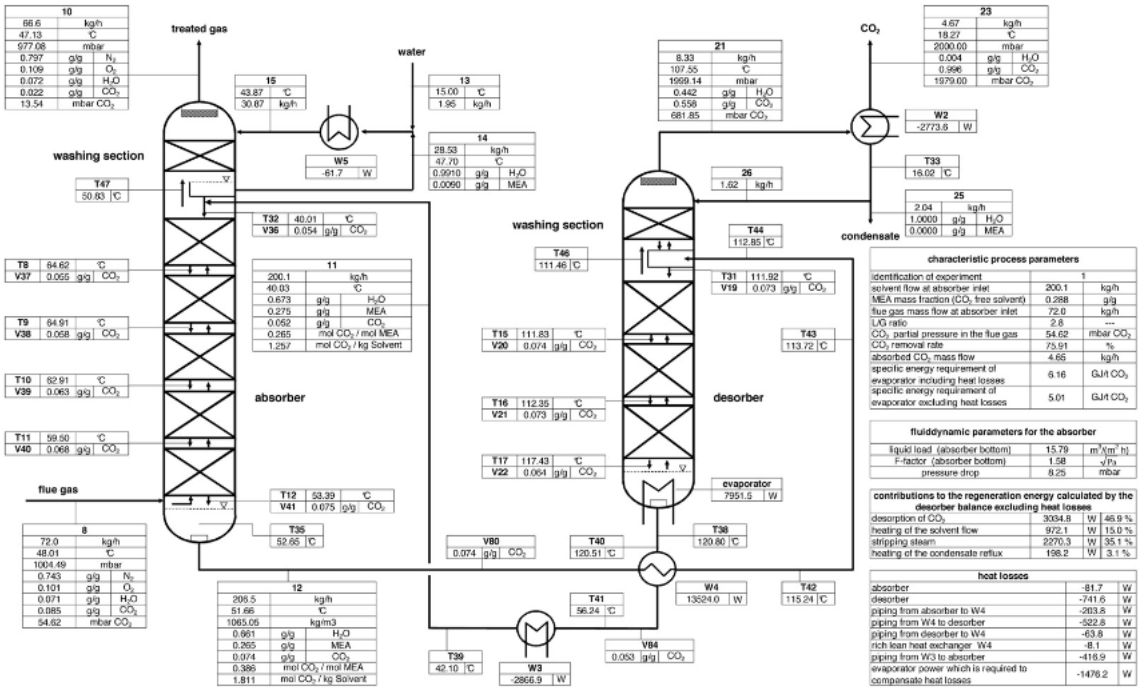

Figure 31: Flow sheet of the pilot plant data of Notz et al. (2012) [3]

C Validation of Absorber - Tobiesen et al. (2007)

Table 34: Lean loading. rich loading. absorbed CO_2. percentage deviation and ratio between simulated and experimental absorption rate for validation of absorber. (Tobiesen et al.)

	Lean Loading [molCO$_2$/molMEA]	Rich Loading [molCO$_2$/molMEA]		Absorbed CO$_2$ [kg/h]		Xi.CO$_2$abs [%]	NCO$_2$abs.sim/NCO$_2$abs.exp -
Run	Exp	Exp	Sim	Exp	Sim	-	-
1	0.22	0.28	0.27	3.42	2.72	-20.49	0.80
2	0.22	0.28	0.27	2.85	2.56	-10.30	0.90
3	0.22	0.27	0.26	2.96	2.57	-13.04	0.87
4	0.22	0.28	0.27	3.06	2.57	-15.88	0.84
5	0.22	0.27	0.27	3.01	3.02	0.43	1.00
6	0.18	0.27	0.26	4.37	3.83	-12.40	0.88
7	0.28	0.35	0.32	4.47	2.52	-43.70	0.56
8	0.24	0.3	0.29	4.13	3.86	-6.46	0.94
9	0.23	0.3	0.29	4.92	4.46	-9.41	0.91
10	0.22	0.33	0.32	4.57	3.94	-13.83	0.86
11	0.22	0.31	0.30	3.51	3.05	-13.13	0.87
12	0.31	0.4	0.39	3.71	3.36	-9.39	0.91
13	0.30	0.39	0.39	7.44	7.35	-1.18	0.99
14	0.37	0.44	0.44	2.93	2.86	-2.54	0.97
15	0.36	0.44	0.44	9.45	9.87	4.44	1.04
16	0.40	0.45	0.45	3.76	3.98	5.79	1.06
17	0.41	0.45	0.45	5.08	4.48	-11.83	0.88
18	0.35	0.43	0.42	10.12	9.44	-6.70	0.93
19	0.35	0.4	0.40	6.51	6.68	2.67	1.03
20	0.29	0.34	0.33	5.83	5.18	-11.17	0.89

D Validation of Absorber - Notz et al. (2012)

Table 35: Lean loading. rich loading. absorbed CO_2. percentage deviation and ratio between simulated and experimental absorption rate for validation of absorber. (Notz et al.)

	Lean Loading [molCO$_2$/molMEA]	Rich Loading [molCO$_2$/molMEA]		Absorbed CO$_2$ [kg/h]		Xi.CO$_2$abs [%]	NCO$_2$abs.sim/NCO$_2$abs.exp
Run	Exp	Exp	Sim	Exp	SIm		
1	0.27	0.39	0.38	4.65	4.56	-1.88	0.98
2	0.31	0.46	0.46	6.11	6.12	0.17	1.00
3	0.23	0.31	0.31	3.35	3.20	-4.51	0.96
4	0.27	0.40	0.39	4.83	4.76	-1.52	0.99
5	0.31	0.45	0.44	5.64	5.58	-1.00	0.99
6	0.32	0.46	0.47	6.24	6.17	-1.07	0.99
7	0.36	0.48	0.46	4.82	4.36	-9.54	0.91
8	0.23	0.44	0.44	9.06	8.92	-1.56	0.98
9	0.15	0.39	0.39	10.56	10.30	-2.46	0.98
10	0.30	0.40	0.41	4.34	4.36	0.57	1.01
11	0.28	0.40	0.40	4.59	4.67	1.71	1.02
12	0.26	0.37	0.38	4.76	4.90	2.88	1.03
13	0.29	0.40	0.40	3.53	3.45	-2.28	0.98
14	0.25	0.37	0.37	5.41	5.37	-0.78	0.99
15	0.24	0.36	0.36	6.34	6.32	-0.27	1.00
16	0.10	0.41	0.37	6.37	5.89	-7.58	0.92
17	0.17	0.37	0.37	6.38	5.89	-7.72	0.92
18	0.22	0.39	0.44	6.43	8.17	27.00	1.27
19	0.25	0.35	0.35	6.43	6.61	2.78	1.03
20	0.26	0.40	0.39	4.71	4.70	-0.14	1.00
21	0.27	0.40	0.39	4.64	4.47	-3.66	0.96
22	0.26	0.39	0.40	4.8	4.80	0.10	1.00
23	0.27	0.39	0.40	4.73	4.76	0.56	1.01
24	0.25	0.39	0.40	4.57	4.64	1.58	1.02
25	0.17	0.44	0.44	4.19	4.24	1.13	1.01
26	0.29	0.47	0.47	5.89	5.60	-4.90	0.95
27	0.17	0.50	0.49	5.03	4.69	-6.84	0.93
28	0.27	0.47	0.46	6.63	6.28	-5.30	0.95
29	0.31	0.47	0.45	6.64	6.58	-0.87	0.99
30	0.32	0.46	0.45	6.67	6.55	-1.84	0.98
31	0.34	0.45	0.45	6.71	6.09	-9.25	0.91
32	0.34	0.45	0.45	6.61	6.36	-3.81	0.96
33	0.36	0.44	0.46	6.6	6.47	-2.00	0.98
34	0.15	0.42	0.41	4.44	4.16	-6.25	0.94
35	0.21	0.41	0.41	4.55	4.24	-6.78	0.93
36	0.25	0.39	0.40	4.46	4.34	-2.63	0.97
37	0.30	0.40	0.41	4.41	4.17	-5.51	0.95
38	0.31	0.39	0.40	4.5	4.39	-2.42	0.98
39	0.32	0.40	0.40	4.48	4.63	3.32	1.03
40	0.11	0.30	0.28	5.27	4.95	-6.16	0.94
41	0.13	0.30	0.28	5.27	5.01	-4.90	0.95
42	0.19	0.31	0.30	5.26	5.15	-2.05	0.98
43	0.20	0.32	0.31	4.98	4.92	-1.13	0.99
44	0.21	0.31	0.31	5.01	5.00	-0.23	1.00
45	0.22	0.32	0.31	5.18	5.27	1.76	1.02
46	0.32	0.42	0.42	4.01	3.93	-1.91	0.98
47	0.26	0.37	0.37	4.86	4.67	-3.94	0.96

E Temperature profiles - Notz et al. (2012)

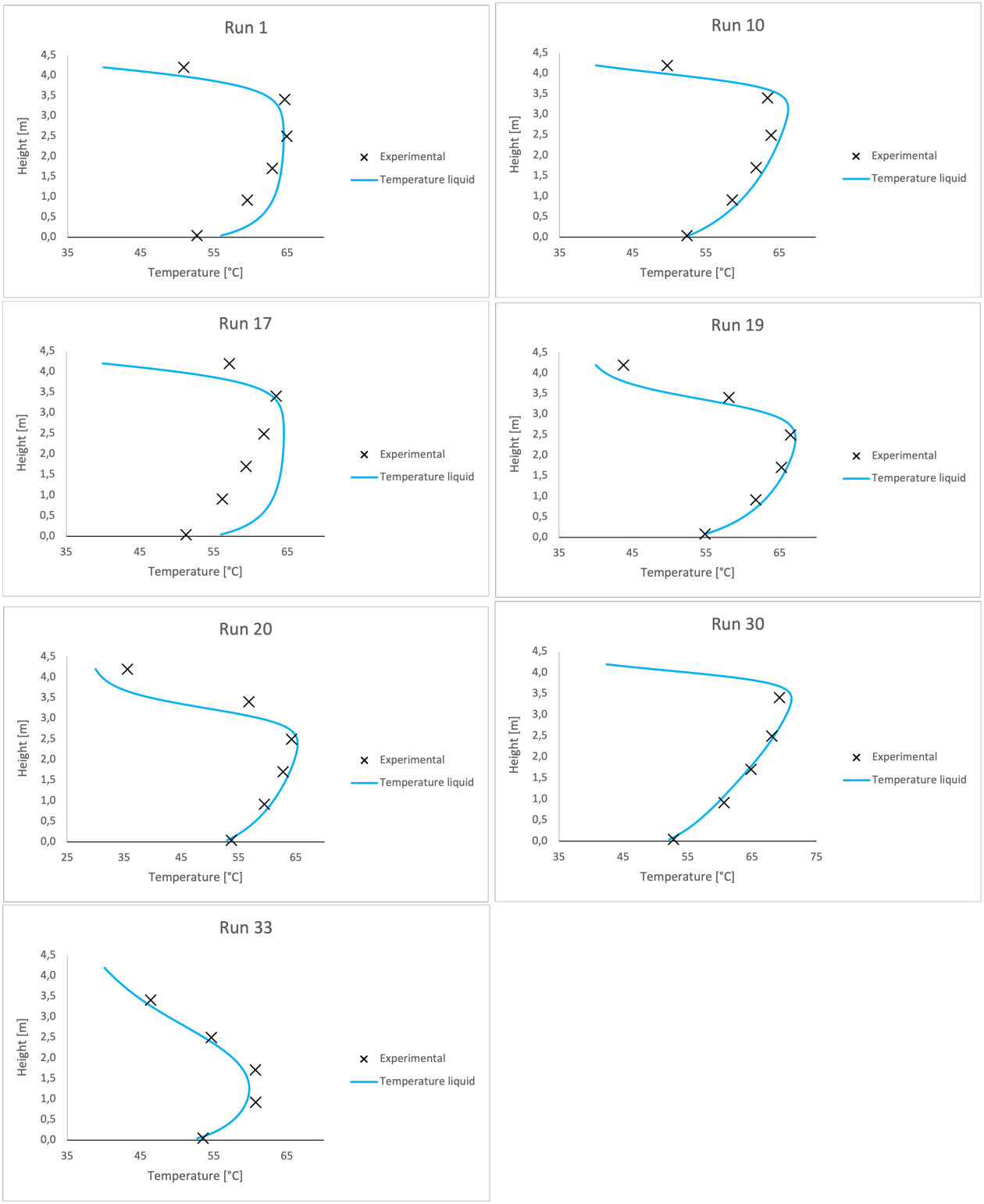

Figure 32: Temperature profiles for run 1, 10, 17, 19, 20, 30 and 33. (Notz et al. (2012))

F Validation of Desorber - Tobiesen et al. (2008)

Table 36: Lean loading. rich loading. desorbed CO_2. percentage deviation and ratio between simulated and experimental desorption rate for validation of desorber. (Tobiesen et al.)

	Lean Loading [molCO$_2$/molMEA]		Rich Loading [molCO$_2$/molMEA]	Desorbed CO_2 [kg/h]		Xi.CO$_2$des [%]	NCO$_2$des.sim/NCO$_2$des.exp -
Run	Exp	Sim	Exp	Exp	Sim	-	-
1	0.27	0.21	0.32	5.10	5.61	10.09	1.10
2	0.25	0.21	0.32	5.00	5.54	10.88	1.11
3	0.26	0.21	0.31	4.90	5.45	11.26	1.11
4	0.27	0.21	0.31	4.80	5.32	10.83	1.11
5	0.21	0.18	0.26	4.40	4.63	5.30	1.05
6	0.33	0.26	0.37	6.20	7.37	18.80	1.19
7	0.28	0.23	0.30	4.60	5.14	11.72	1.12
8	0.27	0.22	0.31	6.20	6.96	12.27	1.12
9	0.25	0.20	0.33	4.70	4.99	6.16	1.06
10	0.26	0.20	0.34	4.70	5.24	11.40	1.11
11	0.36	0.26	0.40	3.60	3.13	-12.98	0.87
12	0.34	0.29	0.39	8.30	8.08	-2.67	0.97
13	0.41	0.38	0.45	3.20	2.76	-13.65	0.86
14	0.40	0.38	0.46	11.50	9.55	-16.97	0.83
15	0.44	0.40	0.45	3.90	3.74	-4.22	0.96
16	0.44	0.41	0.45	6.10	5.49	-10.05	0.90
17	0.39	0.34	0.43	11.70	10.32	-11.81	0.88
18	0.37	0.34	0.41	9.10	8.60	-5.52	0.95
19	0.32	0.28	0.35	7.40	8.16	10.24	1.10

G Validation of Desorber - Notz et al. (2012)

Table 37: Lean loading. rich loading. desorbed CO_2. percentage deviation and ratio between simulated and experimental desorption rate for validation of desorber. (Notz et al.)

	Lean Loading [molCO$_2$/molMEA]		Rich Loading [molCO$_2$/molMEA]	Desorbed CO$_2$ [kg/h]		Xi.CO$_2$des [%]	NCO$_2$des.sim/NCO$_2$des.exp -
Run	Exp	Sim	Exp	Exp	Sim	-	-
1	0.27	0.26	0.39	4.88	5.19	6.30	1.06
2	0.31	0.34	0.46	6.48	6.49	0.15	1.00
3	0.23	0.22	0.31	3.07	3.57	16.23	1.16
4	0.27	0.26	0.40	4.88	5.45	11.62	1.12
5	0.31	0.33	0.45	5.76	6.28	9.08	1.09
6	0.32	0.35	0.46	6.08	6.31	3.70	1.04
7	0.36	0.37	0.48	4.74	5.31	12.04	1.12
8	0.23	0.24	0.44	9.15	8.74	-4.45	0.96
9	0.15	0.18	0.39	10.67	9.05	-15.18	0.85
10	0.30	0.33	0.40	4.28	4.63	8.15	1.08
11	0.28	0.27	0.40	4.65	5.41	16.29	1.16
12	0.26	0.25	0.37	4.63	5.05	9.10	1.09
13	0.29	0.27	0.40	3.41	4.14	21.42	1.21
14	0.25	0.19	0.37	5.19	2.65	-48.88	0.51
15	0.24	0.24	0.36	6.34	6.50	2.57	1.03
16	0.10	0.14	0.41	6.57	5.70	-13.21	0.87
17	0.17	0.19	0.37	6.2	5.50	-11.22	0.89
18	0.22	0.22	0.39	6.32	6.15	-2.74	0.97
19	0.25	0.25	0.35	6.86	6.68	-2.57	0.97
20	0.26	0.26	0.40	4.98	5.17	3.73	1.04
21	0.27	0.26	0.40	4.99	5.32	6.61	1.07
22	0.26	0.25	0.39	4.59	5.04	9.86	1.10
23	0.27	0.26	0.39	4.42	5.05	14.18	1.14
24	0.25	0.25	0.39	3.95	4.35	10.17	1.10
25	0.17	0.23	0.44	4.18	3.07	-26.53	0.73
26	0.29	0.28	0.47	5.93	6.01	1.36	1.01
27	0.17	0.28	0.50	5.01	6.01	19.97	1.20
28	0.27	0.26	0.47	6.75	6.99	3.58	1.04
29	0.31	0.30	0.47	6.94	7.31	5.31	1.05
30	0.32	0.34	0.46	6.29	7.38	17.31	1.17
31	0.34	0.34	0.45	6.05	7.38	21.96	1.22
32	0.34	0.35	0.45	6.33	7.42	17.26	1.17
33	0.36	0.33	0.44	5.96	7.19	20.63	1.21
34	0.15	0.17	0.42	4.46	4.11	-7.76	0.92
35	0.21	0.23	0.41	4.68	4.54	-3.07	0.97
36	0.25	0.23	0.39	4.31	4.81	11.68	1.12
37	0.30	0.26	0.40	4.44	5.39	21.30	1.21
38	0.31	0.28	0.39	4.27	5.52	29.22	1.29
39	0.32	0.30	0.40	4.39	5.68	29.29	1.29
40	0.11	0.13	0.30	5.44	4.77	-12.24	0.88
41	0.13	0.15	0.30	5.42	4.99	-8.02	0.92
42	0.19	0.19	0.31	5.18	5.28	2.02	1.02
43	0.20	0.20	0.32	5.09	5.07	-0.42	1.00
44	0.21	0.21	0.31	5.13	5.22	1.72	1.02
45	0.22	0.22	0.32	5.65	5.70	0.85	1.01
46	0.32	0.29	0.42	3.75	5.04	34.46	1.34
47	0.26	0.24	0.37	4.57	5.37	17.56	1.18

H Data for Base Case with Coal Flue Gas

Table 38: In-house data of the operating conditions at the Tiller plant for coal-fire flue gas.

Variable [unit]	Value
Absorber	
Height [m]	15
Diameter [m]	0.2
Gas Inlet [m^3/h]	160
CO_2 Inlet [vol% dry]	13
CO_2 Outlet [vol % dry]	2.44
Liquid Inlet [kg/min]	7.03
L/G Ratio [kg/kg]	2.3
Lean Amine [mole/kg]	5.19
Lean Loading [mole/mole]	0.17
Rich Loading [mole/mole]	0.47
Temperature Gas Inlet [°C]	35
Temperature Lean Inlet [°C]	39.4
Desorber & Reboiler	
Height [m]	12
Diameter [m]	0.12
Desorber Pressure [kPa]	179.5
Reboiler Pressure [kPa]	192.0
Reboiler Duty [kJ/s]	36.5
Temperature Liquid Reboiler [°C]	121.2
SRD [MJ/kg CO_2]	4.79
CO_2 Recovery [%]	83
Water wash	
Height [m]	2.4
Diameter [m]	0.2
Temperature Inlet [°C]	31.79
Flowrate Liquid Inlet [kmole/h]	23.22
Loading Liquid Bottom [mole/mole]	0.68

I Base Case Results for Coal Flue Gas Case

Table 39: Conditions for the streams in the coal flue gas case. The stream names corresponds to the labels in Figure 4.

Stream	Temperature	Pressure	Flow Rate	Mole Fraction	Mole Fraction	Mole Fraction	Mole Fra
-	[°C]	[kPa]	[kmol/h]	CO_2	H_2O	MEA	N_2
Stream	Temperature	Pressure	Flow rate	Mole fraction	Mole fraction	Mole fraction	Mole frac
-	[°C]	[kPa]	[kmol/h]	CO2	H2O	MEA	N2
FlueGas	35.00	100	6.25	0.1227	0.0560	0	0.821
GasAbsTreat	39.16	100	6.71	0.0051	0.2301	0.0004	0.764
RichAmine	45.66	100	24.01	0.0573	0.8257	0.1170	0
GasWWTreat	40.00	100	5.62	0.0059	0.0806	0	0.913
P06	49.53	100	21.32	0.0007	0.9973	0.0019	0
Water01	33.08	100	20.22	0.0007	0.9973	0.0019	0
SweetGas	30.00	100	5.39	0.0062	0.0425	0	0.951
Water02	49.53	100	20.00	0.0003	0.9993	0.0004	0
P10	30.27	100	20.22	0.0003	0.9993	0.0004	0
P11	30.00	400	20.22	0.0003	0.9993	0.0004	0
P12	37.10	400	21.32	0.0007	0.9973	0.0019	0
P13	37.10	400	24.01	0.0573	0.8257	0.1170	0
P14	30.00	100	0	0	0	0	0
P15	30.00	100	21.32	0.0007	0.9973	0.0019	0
P16	30.00	100	0	0	0	0	0
P17	30.00	100	20.22	0.0003	0.9993	0.0004	0
P18	30.00	100	0.22	0.0003	0.9993	0.0004	0
P19	30.00	100	1.32	0.0007	0.9973	0.0019	0
P21	30.00	100	20.00	0.0007	0.9973	0.0019	0
P22	39.16	190	23.22	0.0277	0.8513	0.1210	0
P23	49.16	400	24.01	0.0573	0.8257	0.1170	0
P24	113.50	100	1.67	0.439	0.5608	0.0002	0
P25	101.97	190	26.81	0.0324	0.8623	0.1053	0
P26	117.73	190	3.59	0.0629	0.9334	0.0037	0
P27	120.52	190	23.22	0.0277	0.8513	0.1210	0
P28	120.52	100	0	0	0.8878	0.1122	0
P29	0	100	0.06	0	0.9997	0.0003	0
P30	0	100	24.48	0.0263	0.8588	0.1149	0
P31	48.37	100	24.54	0.0262	0.8592	0.1146	0
P32	48.37	100	0	0	0.0000	0.0000	0
LeanAmine	40.00	100	24.48	0.0263	0.8588	0.1149	0
P33	40.00	100	0.79	0.9264	0.0736	0	0
P34	40.00	100	0.88	0.0008	0.9989	0.0004	0
P38	108.55	100	24.90	0.0553	0.8318	0.1129	0

J Vapor Temperature Profiles

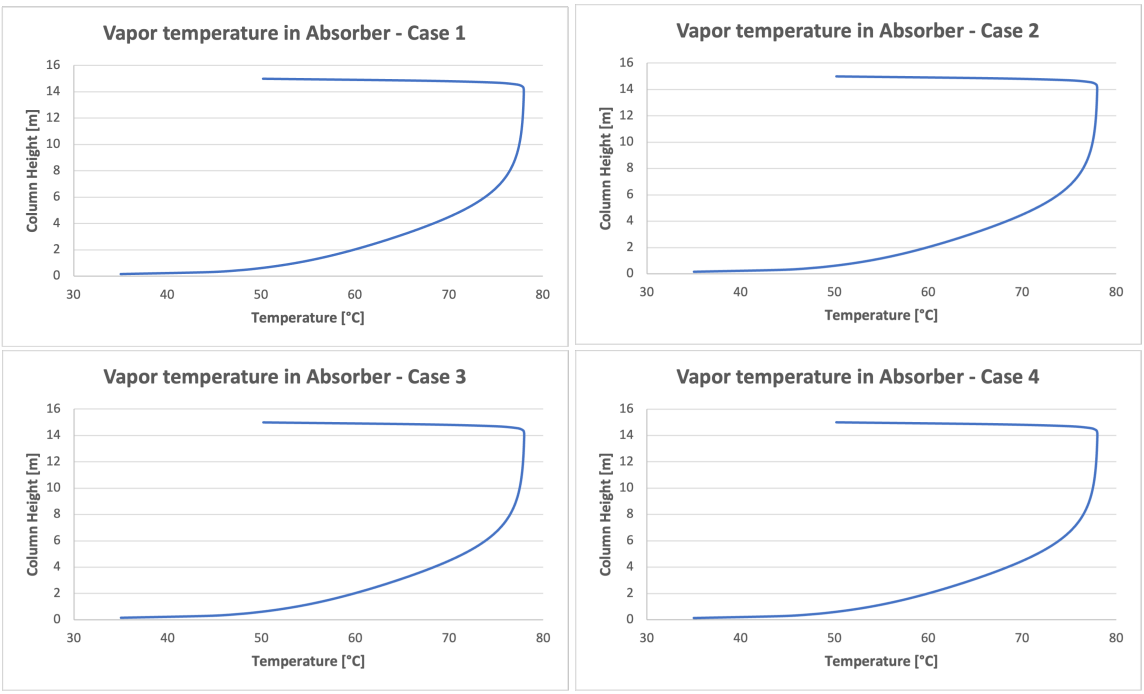

Figure 33: Vapor temperature profile for Cases 1-4.

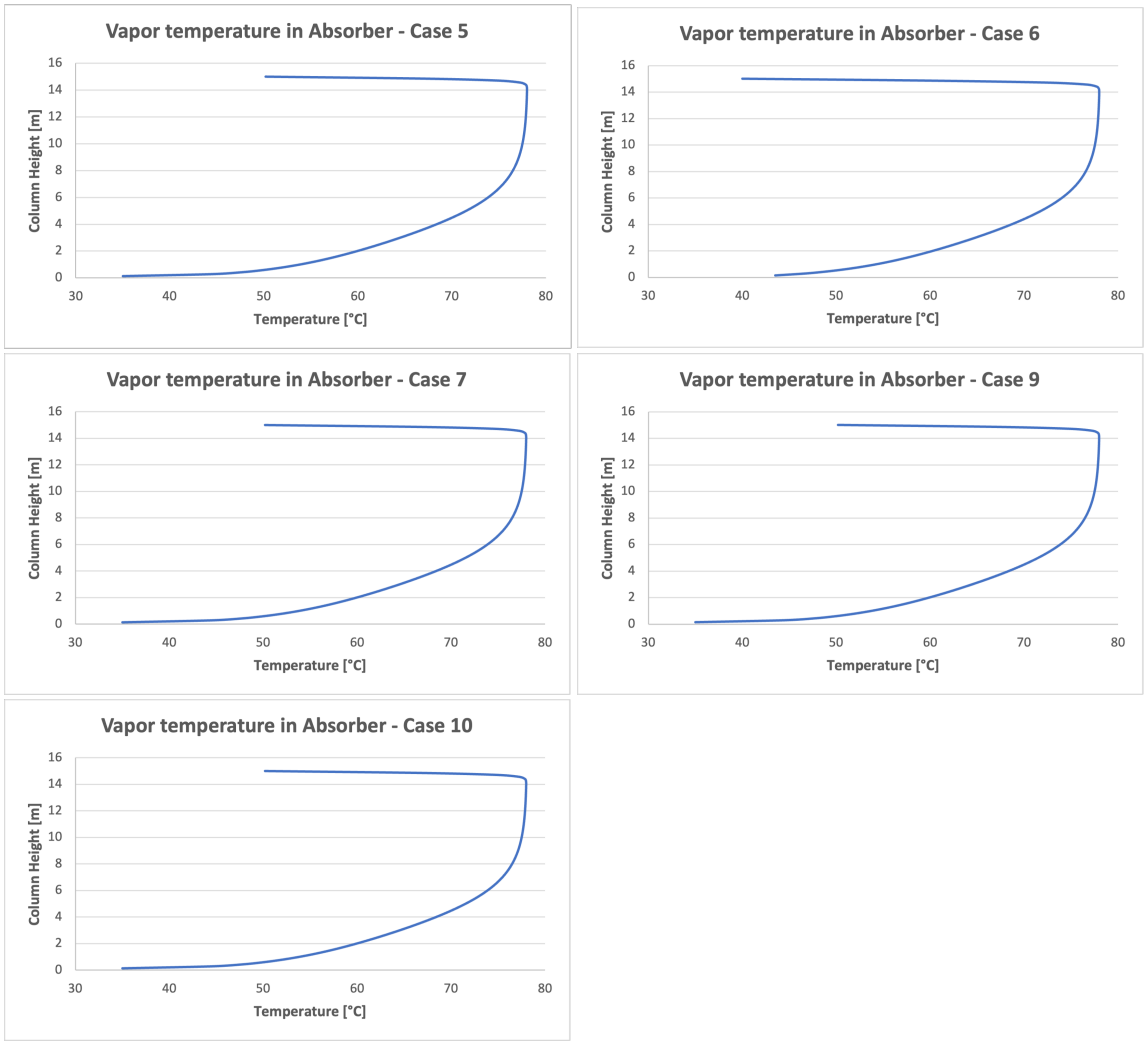

Figure 34: Vapor temperature profile for Cases 5-7, 9 and 10.

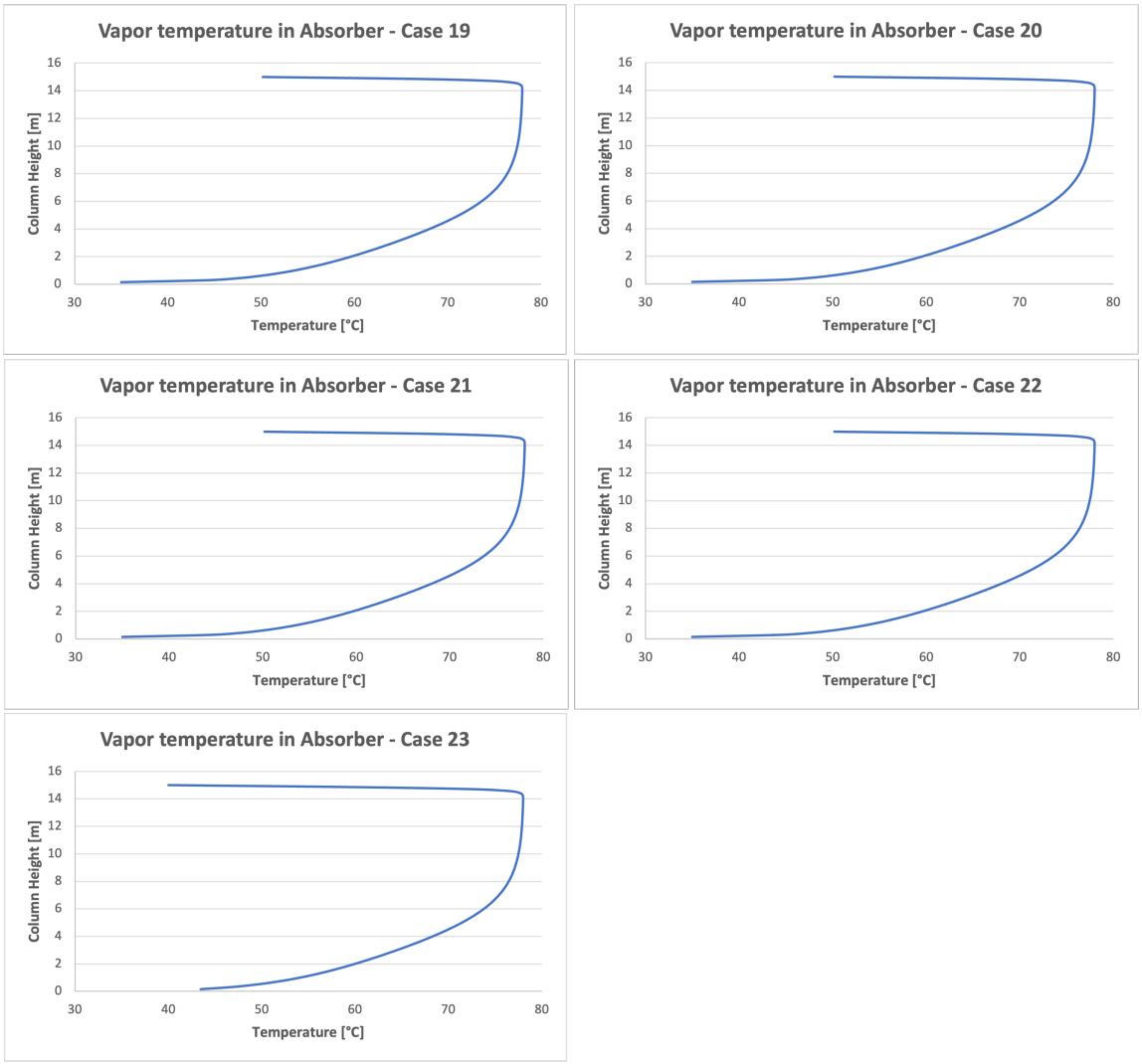

Figure 35: Vapor temperature profile for 19-23

K SRD vs. L/G plots

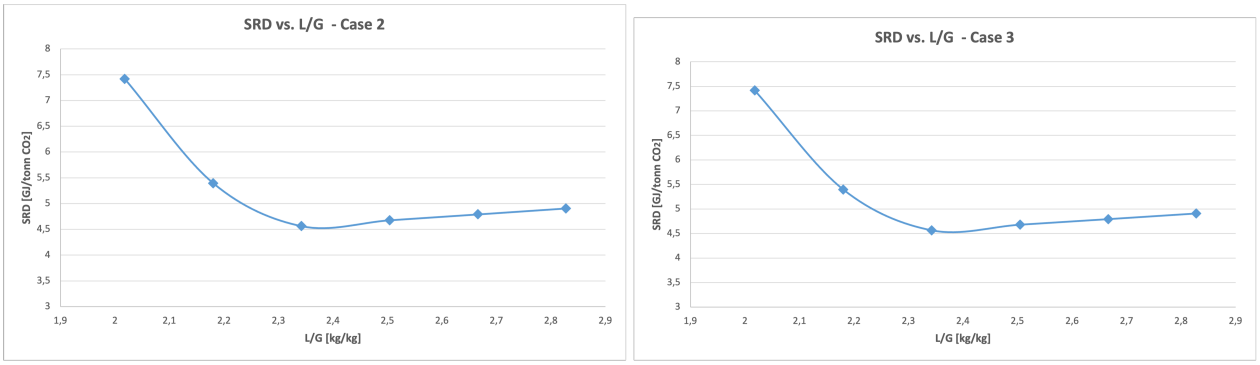

Figure 36: SRD vs. L/G for Case 2 and 3.

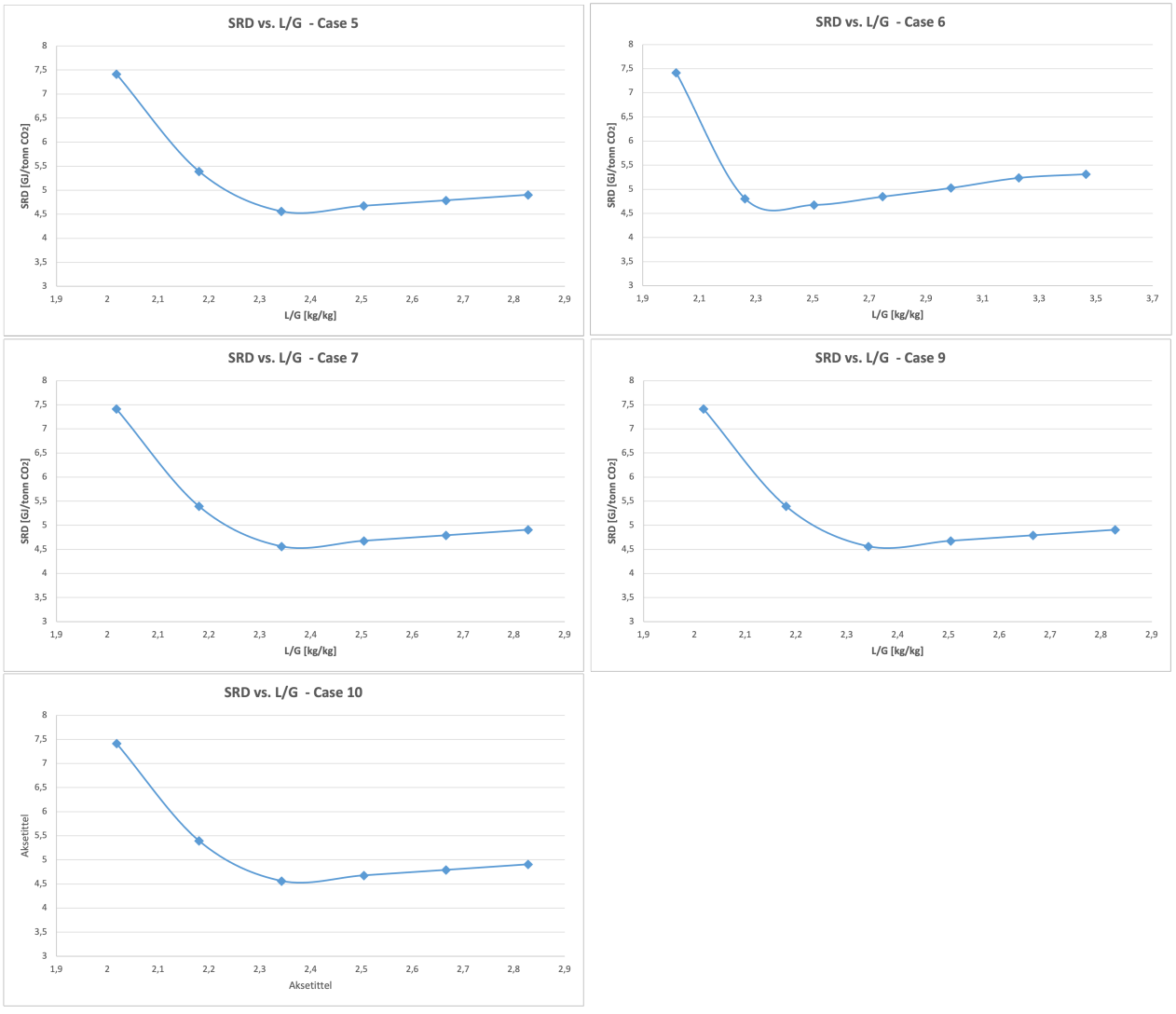

Figure 37: SRD vs. L/G for Case 5, 6, 7, 9 and 10.

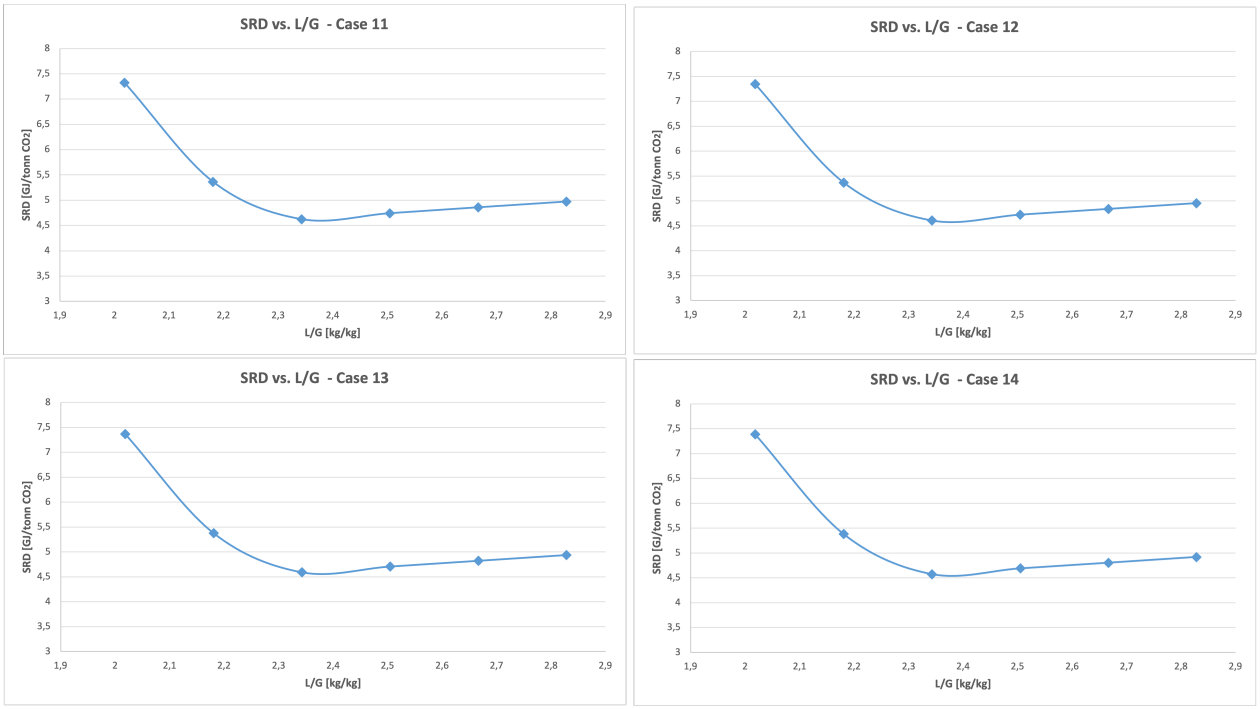

Figure 38: SRD vs. L/G for Case 11, 12, 13 and 14.

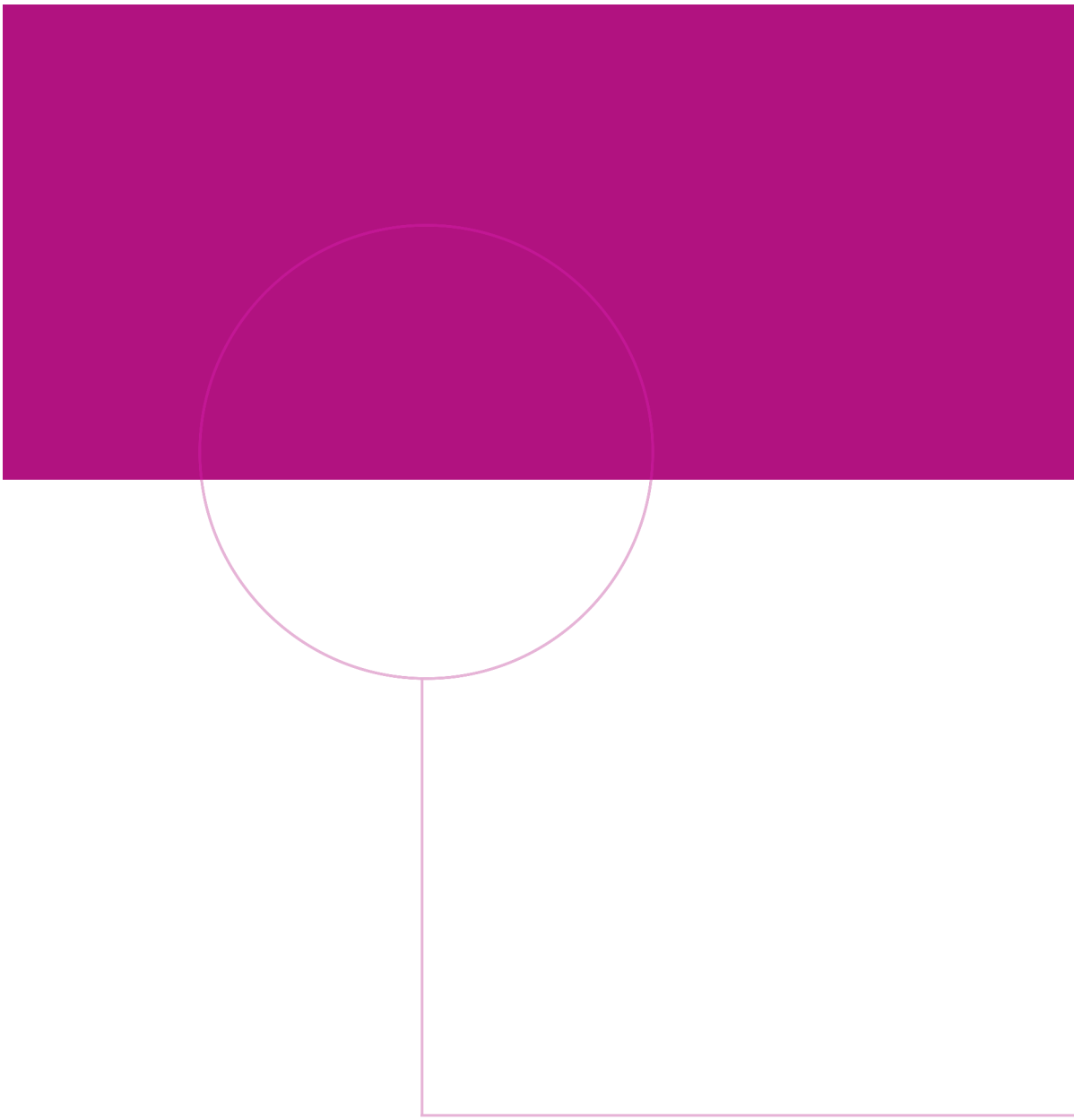

NTNU

Norwegian University of
Science and Technology